

University of Alabama in Huntsville

**LOUIS**

---

Theses

UAH Electronic Theses and Dissertations

---

2012

**Surface modification of poly(dimethylsiloxane) with 254 NM irradiation : a comparative study of hydroxyl, carboxylic, and fluoro-terminated groups**

Kenya M. Wallace

Follow this and additional works at: <https://louis.uah.edu/uah-theses>

---

**Recommended Citation**

Wallace, Kenya M., "Surface modification of poly(dimethylsiloxane) with 254 NM irradiation : a comparative study of hydroxyl, carboxylic, and fluoro-terminated groups" (2012). *Theses*. 538.  
<https://louis.uah.edu/uah-theses/538>

This Thesis is brought to you for free and open access by the UAH Electronic Theses and Dissertations at LOUIS. It has been accepted for inclusion in Theses by an authorized administrator of LOUIS.

**SURFACE MODIFICATION OF POLY(DIMETHYLSILOXANE) WITH 254 NM  
IRRADIATION: A COMPARATIVE STUDY OF HYDROXYL, CARBOXYLIC,  
AND FLUORO-TERMINATED GROUPS**

**by**

**KENYA M. WALLACE**

**A THESIS**


**Submitted in partial fulfillment of the requirements  
for the degree of Master of Science  
in  
The Department of Chemistry  
to  
The School of Graduate Studies  
of  
The University of Alabama in Huntsville**

**HUNTSVILLE, ALABAMA**

**2012**

**Copyright by**  
**Kenya M. Wallace**  
**All Rights Reserved**  
**2012**

In presenting this thesis in partial fulfillment of the requirements for a master's degree from The University of Alabama in Huntsville, I agree that the Library of this University shall make it freely available for inspection. I further agree that permission for extensive copying for scholarly purposes may be granted by my advisor or, in his absence, by the Chair of the Department or the Dean of the School of Graduate Studies. It is also understood that due recognition shall be given to me and to The University of Alabama in Huntsville in any scholarly use which may be made of any material in this thesis.

  
(Student Signature)

10.30.2012  
(Date)

## THESIS APPROVAL FORM

Submitted by Kenya M. Wallace in partial fulfillment of the requirements for the degree of Master of Science in Chemistry and accepted on behalf of the Faculty of the School of Graduate Studies by the thesis committee.

We, the undersigned members of the Graduate Faculty of The University of Alabama in Huntsville, certify that we have advised and/or supervised the candidate on the work described in this thesis. We further certify that we have reviewed the thesis manuscript and approve it in partial fulfillment of the requirements for the degree of Master of Science in Chemistry.

Emanuel G. Wallace 10/29/2012 Committee Chair  
(Date)

G. Plaf 10/29/12

W. H. H. H. 10/30/2012

William M. H. H. 10-29-12 Department Chair

J. J. J. J. 10/29/12 College Dean

Rhonda Kay Haede 10/31/12 Graduate Dean

## ACKNOWLEDGEMENTS

I am extremely grateful to have achieved another level in my academic career. This journey has been long, thought-provoking, and demanding, but there have been many people along the way to help me get to this point. It is my pleasure to thank those who made this thesis possible. First I would like to give all honors and thanks to God for leading, protecting, and blessing me while I progressed through this master's program. His word and his promise gave me the strength to continue on even during the toughest times.

It is my genuine pleasure to give thanks to my advisor, Dr. Emanuel Waddell. From the beginning he has provided encouragement, guidance, and support. His faith in my capabilities gave me the drive and push I need to fully understand and conceptualize the work presented in this thesis. His custom of asking mind stimulating questions led me to think beyond the normal and has in turn strengthened my academic abilities. His moral support has made this thesis and master's degree an attainable reality. I look forward to any and all future endeavors with Dr. Waddell as a mentor, advisor, and friend.

I owe my deepest appreciation to my family (Mom, Granny, Shamea, Nicole, and Ethan) for all of their unconditional love, support, prayers, blessings, and so much more. They continuously believe in me and push me toward my goals. They have been my stability and rationality along this journey. To them I am forever indebted. I would like to express thanks to my church family (Shekinah Glory House of Praise) for all of their encouragement and prayers as well. Special thanks to my friends and extended family for listening and inspiring me through the difficult times.

**ABSTRACT**  
The School of Graduate Studies  
The University of Alabama in Huntsville

Degree: Master of Science College/Dept.: Science/Chemistry

Name of Candidate: Kenya M. Wallace

Title: Surface Modification of Poly(dimethylsiloxane) by 254 nm Irradiation: A Comparative Study of Hydroxyl, Carboxylic, and Fluoro-terminated Groups

This work serves as a comparison between hydroxyl, carboxylic, and fluoro-terminated groups formed on the surface of poly(dimethylsiloxane) (PDMS). PDMS is a silicone-based polymer with repeat units of  $[\text{SiO}(\text{CH}_3)_2]$  that allows for ease of reorientation and substitution of other functional groups. Air-oxygen plasma and a NaOH solution are used to generate hydroxyl groups and 254 nm narrow band ultraviolet radiation generates carboxylic groups on the surface of PDMS. Pentafluorophenol (PFP) is a fluorine-terminated coupling agent and it is linked to the surface of irradiated PDMS via 1-ethyl-3-[3-dimethylaminopropyl] carbodiimide hydrochloride (EDC). Each functional group forms a bond to PDMS. The bond formed between the three functional groups and PDMS is characterized by contact angle goniometry, ATR-Infrared spectral analysis, UV-Vis spectroscopy, and by a contact angle titration curve.

Abstract Approval: Committee Chair

Emmanuel G. Wallace

Department Chair

William D. Allen

Graduate Dean

Rhonda Kay Gaede 10/31/12

## ACKNOWLEDGEMENTS

I am extremely grateful to have achieved another level in my academic career. This journey has been long, thought-provoking, and demanding, but there have been many people along the way to help me get to this point. It is my pleasure to thank those who made this thesis possible. First I would like to give all honors and thanks to God for leading, protecting, and blessing me while I progressed through this master's program. His word and his promise gave me the strength to continue on even during the toughest times.

It is my genuine pleasure to give thanks to my advisor, Dr. Emanuel Waddell. From the beginning he has provided encouragement, guidance, and support. His faith in my capabilities gave me the drive and push I need to fully understand and conceptualize the work presented in this thesis. His custom of asking mind stimulating questions led me to think beyond the normal and has in turn strengthened my academic abilities. His moral support has made this thesis and master's degree an attainable reality. I look forward to any and all future endeavors with Dr. Waddell as a mentor, advisor, and friend.

I owe my deepest appreciation to my family (Mom, Granny, Shamea, Nicole, and Ethan) for all of their unconditional love, support, prayers, blessings, and so much more. They continuously believe in me and push me toward my goals. They have been my stability and rationality along this journey. To them I am forever indebted. I would like to express thanks to my church family (Shekinah Glory House of Praise) for all of their encouragement and prayers as well. Special thanks to my friends and extended family for listening and inspiring me through the difficult times.

I would like to thank the members of my committee, Dr. Carmen Scholz and Dr. Michael George for their guidance, suggestions, and comments. A special thanks goes to Dr. Scholz for her recommendations pertaining to thesis work as well as letters for scholarships and fellowships. I also wish to acknowledge the UAHuntsville Alliance for Minority Participation (AMP) Program and the Office of Graduate Studies as my funding source. Lastly, I offer my best regards and blessings to the members Minority Graduate Student Association (MGSA) for their friendship, academic insight and enrichment, and never-ending support.

## TABLE OF CONTENTS

	Page
List of Figures.....	xi
List of Schemes.....	xiv
List of Tables.....	xv
List of Symbols.....	xvi
<b>CHAPTER</b>	
<b>ONE INTRODUCTION.....</b>	<b>1</b>
1.1 Surface Science.....	1
1.2 Use of Poly(dimethylsiloxane) in Surface Chemistry.....	2
1.3 Hypothesis and Objective.....	4
1.4 Thesis Outline.....	5
<b>TWO BACKGROUND.....</b>	<b>7</b>
2.1 Sylgard® 184.....	7
2.2 Contact Angle: Wettability and Adhesion.....	8
2.3 Hydrophobicity Loss and Recovery of PDMS.....	10
2.4 Literature Review Hydroxyl Group Formation.....	12
2.4.1 Effect of Plasma Discharges of PDM.....	13
2.4.2 NaOH Wet Chemical Solution.....	15
2.5 Literature Review: Carboxylic Group Formation.....	18
2.6 Pentafluorophenol.....	23
<b>THREE MODIFICATION AND CHARACTERIZATION TECHNIQUES OF PDMS.....</b>	<b>25</b>
3.1 Plasma Treatment.....	25

3.2 Wet Chemistry.....	28
3.3 Ultraviolet Surface Modification.....	28
3.4 Contact Angle Goniometry.....	29
3.4.1 Contact Angle Measuring: Static Sessile Drop Method.....	30
3.4.2 Hysteresis and Young's equation.....	31
3.4.3 Surface Free Energy.....	33
3.5 Ultraviolet-Visible Spectroscopy.....	37
3.6 Attenuated Total Reflectance Infrared Spectroscopy.....	39
3.7 Contact Angle Titration Curve.....	45
<b>FOUR EXPERIMENTAL.....</b>	<b>47</b>
4.1 Chemical, Reagents, and Sample Preparation.....	47
4.2 Plasma Discharge.....	48
4.3 NaOH Solution.....	49
4.4 Excimer Radiation Set-up.....	49
4.5 PFP Bond Formation.....	50
4.6 Contact Angle Measurements.....	50
4.7 Absorbance Measurements.....	51
4.8 Infrared Spectroscopy.....	53
<b>FIVE RESULTS AND DISCUSSION.....</b>	<b>54</b>
5.1 Hydroxyl Groups.....	54
5.1.1 Plasma Treatment.....	54
5.1.2 NaOH Treatment.....	55
5.1.3 Surface Tension.....	58

5.1.4	Recovery of Hydroxyl Group.....	58
5.2	Carboxylic Groups.....	62
5.2.1	Contact Angle Measurements.....	62
5.2.2	ATR-IR spectra Results.....	64
5.2.3	UV-Vis Methylene Blue Experiment.....	66
5.2.4	Surface Tension of Irradiated PDMS.....	70
5.2.5	Recovery of Carboxylic Group.....	71
5.3	Fluoro-terminated Groups.....	73
5.3.1	Contact Angle Measurements.....	73
5.3.2	ATR-IR spectra Analysis.....	74
5.3.3	UV-Vis Anti-Methylene Blue Experiment.....	79
5.3.4	Recovery of Fluoro-terminated Group.....	81
5.3.5	Contact Angle Titration Curve.....	84
<b>SIX</b>	<b>SUMMARY, CONCLUSION, AND FUTURE WORK.....</b>	<b>87</b>
6.1	Summary.....	87
6.2	Conclusion and Future Work.....	90
	<b>REFERENCES.....</b>	<b>92</b>

## LIST OF FIGURES

Figure	Page
2.1 Representation of a contact angle on a sample surface.....	8
2.2 Interaction between cohesive and adhesive forces.....	9
2.3 Characteristics of a hydrophobic surface vs. a hydrophilic surface.....	10
2.4 Contact angle measurements of PDMS and water as a function of Exposure to plasma discharges for 25s. (The plot is of a microwave plasma treated surface, the inlet is of a plasma cleaner treated surface).....	14
2.5 Reorientation of hydroxyl groups back into the polymer bulk as a function of contact angles versus recovery time after 25s plasma exposure.....	15
2.6 ATR-FTIR spectra of native, plasma treated, and NaOH treated PDMS at (A) high wavenumbers ( $3500\text{-}2750\text{ cm}^{-1}$ ) and (B) low wavenumbers ( $1500\text{-}600\text{ cm}^{-1}$ ). The insets show the maximum absorbance peak associated with the $\text{-CH}_3$ groups.....	17
2.7 Change in contact angle with respect to irradiation time. The contact angle progressively decreases until the formation of cracks occurs at 90 minutes.....	19
2.8 IR spectra of native and irradiated PDMS. Carboxylic groups can be detected by the formation of $\text{-OH}$ stretch and the carbonyl stretch.....	20
2.9 Quantification of carboxylic groups on irradiated PDMS surface.....	21
2.10 Rotation of the carboxylic bond of a 45 minute irradiated PDMS sample stored in air over a ten day period.....	22
2.11 Structure of Pentafluorophenol.....	23
3.1 Plasma is the fourth state of matter.....	26
3.2 Concept of plasma processing. Energy is supplied to plasma discharges and produces reactive molecules and ions. The molecules and ions are transported to the polymer surface.....	27
3.3 Tangent line that measures the contact angle.....	31
3.4 Representation of how contact angles are observed.....	32

3.5	Diagram of the interfacial forces that forms the contact angle.....	33
3.6	Relationship between surface energy of the solid and surface tension of the liquid.....	34
3.7	Representation of the Zisman plot.....	36
3.8	Chemical structure of methylene blue.....	37
3.9	Diagram of a single beam spectrophotometer.....	39
3.10	Schematic of an attenuated total reflectance system.....	41
4.1	Harrick Plasma PDC-32G Plasma Cleaner.....	48
4.2	USHIO excimer lamp and irradiation set-up.....	50
4.3	Rame' Hart Contact Angle Goniometer.....	51
4.4	HP 8452A Diode Array Spectrophotometer.....	52
4.5	Perkin Elmer Spectrum One Infrared Spectrometer with ATR accessory....	53
5.1	ATR-IR spectra of PDMS treated with NaOH.....	57
5.2	Zisman Plot of plasma treated PDMS.....	58
5.3	Contact angle test drops on Air-oxygen plasma treated PDMS at (a) initial, (b) after one hour, (c) after two hours, (d) after three hours, (e) after four hours, (f) after five hours, and (g) after six hours.....	59
5.4	Contact angle as a function of elapsed recovery time after exposure to air-oxygen plasma.....	60
5.5	Observation of hydroxyl group rotation by area under the curve analysis of IR spectra taken during NaOH ambient air experiment.....	61
5.6	Contact angle versus increased irradiation time.....	63
5.7	Contact angle drops on PDMS after COOH formation on (a) 30 minutes, (b) 45 minutes, (c) 60 minutes, (d) 75 minutes, (e) 90 minutes, and (f) 120 minutes irradiated samples.....	64
5.8	ATR-IR spectra of PDMS after UV exposure to form –COOH group.....	65

5.9	Difference in absorbance of PDMS samples stained with methylene blue with respect to exposure time.....	67
5.10	Calibration graph used to determine concentration of carboxylic groups....	67
5.11	Number of carboxylic groups per $\text{cm}^2$ with respect to exposure time.....	69
5.12	Methylene blue experiment used to measure absorbance.....	69
5.13	Contact angle variations of test liquids on PDMS surfaces of varying irradiation times.....	70
5.14	Zisman plots of irradiated PDM.....	71
5.15	Rotation of carboxylic groups back into the PDMS bulk.....	72
5.16	Contact angle droplets for PDMS-PFP in varying solutions.....	74
5.17	Pentafluorophenol IR spectrum.....	75
5.18	30 minutes irradiated samples in varying solutions containing PFP.....	77
5.19	75 minutes irradiated samples in varying solutions containing PFP.....	78
5.20	Methylene blue treatment to determine concentration carboxylic acids remaining on the surface PDMS after immersion in an acetic-acid/water PFP solution.....	80
5.21	Methylene blue experiment indicates no change in color of the PFP based solution.....	80
5.22	Recovery of Acetic acid-water solution.....	82
5.23	Recovery of Acetone solution.....	82
5.24	Recovery of Ethanol solution.....	83
5.25	Recovery of PBS solution.....	83
5.26	Contact angle titration curve of native, PDMS-COOH, and PDMS-PFP....	84
5.27	Extent of ionization a function of pH.....	85
5.28	Variation in the effective $\text{pK}_a$ .....	86

## LIST OF SCHEMES

Scheme		Page
1	Proposed reaction for the formation of hydroxyl groups on a PDMS surface.....	3
2	Cross-linking reaction of Sylgard® 184.....	7
3	Development of [Si-CH <sub>2</sub> -OH] structure.....	13
4	Formation of carboxylic groups by UV irradiation.....	18
5	Reaction mechanism for the coupling of PFP to PDMS induced by EDC...	24

## LIST OF TABLES

Table	Page
1.1 Properties of PDMS.....	2
3.1 Physical properties of commonly used ATR crystals.....	43
5.1 Assignment of spectral peaks with –OH presence.....	54
5.2 Assignment of spectral peaks with –COOH presence.....	64
5.3 Contact angle measurements of native and irradiated PDMS samples after immersion in PFP solutions.....	74
5.4 Spectral assignment of Pentafluorophenol.....	75
6.1 Comparison of Hydroxyl, Carboxylic, and Pentafluoropheonl groups.....	90

## LIST OF SYMBOLS

<u>Symbol</u>	<u>Definition</u>
$\theta$	Contact angle
$\lambda$	Wavelength
$\text{cm}^{-1}$	Wavenumber
$\gamma$	Surface tension
$\gamma_{LV}$	Liquid-vapor interfacial tension
$\gamma_{SL}$	Solid-liquid interfacial tension
$\gamma_{SV}$	Solid-vapor interfacial tension
D	Dispersive component
P	Polar component
S	Solid surface
L	Liquid drop
(+)	Surface tension contributed by acid
(-)	Surface tension contributed by base
$\gamma_c$	Critical surface tension
A	Absorbance
$\varepsilon$	Molar absorptivity
b	Path length
c	Concentration
$I_0$	Incident light intensity
I	Intensity of light within the cell

$d_p$	Depth of penetration
$n_1$	Refractive index of the sample
$n_2$	Refractive index of the crystal
$d_e$	Effective thickness
$\alpha_i$	Extent of ionization
$\text{pK}_a^{\text{eff}}$	Effective (apparent) $\text{pK}_a$

# **CHAPTER ONE**

## **INTRODUCTION**

### **1.1. Surface Science**

Surface science is the study of physical and chemical phenomena that occur at the surface. Surface science includes the fields of surface chemistry and surface physics. Surface science covers concepts such as heterogeneous catalysis, self-assembled monolayers, and corrosion and adhesion. A surface is defined as the boundary layer between a solid and a vacuum, gas, or liquid [1]. Many chemical reactions involve interactions between different kinds of atoms across a surface or interface [2]. A surface or interface exists in a system in any case where there is an abrupt change in the system properties [3]. The surface differs substantially from the interior of the solid both in chemical composition and physical properties [1].

Surface chemistry can be defined as the study of chemical reactions at interfaces, aimed at modifying the chemical composition of a surface by incorporation of selected elements or functional groups that produce various desired effects or improvements in the properties of the surface or interface. Surface chemistry is of particular importance to the field of heterogeneous catalysis, particularly adsorption, which is the adhesion of gas or liquid molecules to the surface. In chemistry, heterogeneous catalysis refers to the form of catalysis where the phase of the catalyst differs from that of the reactants. Surface

analysis is crucial for explaining many surface phenomena and improving the properties of many solid materials and devices [1]

## 1.2. Use of Poly(dimethylsiloxane) in Surface Chemistry

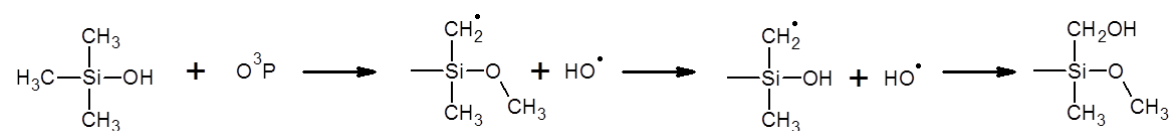
For many polymer applications the surface needs to be modified in order to improve properties such as wettability or adhesion. Consequently, the modification of technically relevant polymers like poly(dimethylsiloxane) (PDMS) is a growing research field [4]. The use of silicone elastomers based on PDMS has been documented in the chemical, biomedical, physical, and electronics literature [5]. PDMS is a silicone-based rubber polymer. It is used in many research laboratories for building of chip-based microfluidic device fabrication [6].

PDMS is a bulk polymer that consists of an inorganic back bone of alternating silicon and oxygen atoms. It has repeat units of  $[\text{Si}(\text{CH}_3)_2\text{O}]_n$ , and methyl groups are attached to the silicon atoms, forming the repeat unit in the polymer [5], [7]. Four structural characteristics of PDMS account for the surface properties: (1) the low intermolecular force between methyl groups, (2) the unique flexibility of the siloxane backbone, (3) the high strength of the siloxane bond, and (4) the partial ionic nature of the siloxane bond [8]. Table 1.1 summarizes other favorable properties of PDMS.

Table 1.1: Favorable properties of PDMS [5–8]

Properties of PDMS		
1. Low molecular weight (6,800-30,000 g/mol)	4. Self-releasing leaving little residue on molds	6. Non-toxic
2. Chemically inert	5. Seals readily with glass, PDMS, and other polymers	7. Relatively inexpensive
3. Optically transparent		8. Low glass transition temperature

A review of the literature shows that PDMS is widely utilized for surface modification as well as in microfluidics and microfabrication. Carlson and Hollahan studied the reaction of radiofrequency-excited oxygen plasma and corona discharges on the surfaces of cured and uncured PDMS to achieve hydroxylation of the surface region[9]. Through experimentation and analysis of infrared spectra, they found that the radio-frequency oxygen plasma and corona treated PDMS materials have a high density of hydroxyl groups and extensive hydrogen bonding [9]. Scheme 1 gives the Hollahan and Carlson's proposed reaction for the development of SiCH<sub>2</sub>OH structures.



Scheme 1. Proposed reaction for the formation of hydroxyl groups on a PDMS surface [9]

Schnyder et al. used UV-irradiation to modify PDMS films by a 172 nm Xe<sup>\*</sup><sub>2</sub> excimer lamp [4]. The excimer UV source was driven at frequencies of 225-280 kHz and voltage amplitude of 10 kV. The PDMS films were irradiated with intensity of approximately 30 mW/cm<sup>2</sup>. Through the use of X-ray photoelectron spectroscopy and spectroscopic ellipsometry, the researchers were able to conclude that the carbon content of the PDMS surface decreases with irradiation time and that the binding energies of the Si and O increase due to the UV-irradiation the carbon content [4]. Lahann et al. reported on the fabrication, characterization, and use of microfluidic analysis devices containing surface-immobilized cell-capturing molecules to develop a procedure for protein immobilization within a lab-on-a-chip device [10]. A submicrometer thin reactive coating of poly(*p*-xylylene carboxylic acid pentafluorophenolester-co-*p*-xylylene) (PPX-PFP) was

homogeneously deposited on the interior surface of the device allowing for self-assembly of biological ligands, proteins, and cells. The thickness of the PPX-PFP films were determined to be between 90 and 150 nm using spectroscopic ellipsometry and the chemical composition of PPX-PFP was in good accordance with reported values [10]. Patrito et al. patterned the surface of PDMS by grafting poly(acrylic acid) (PAA) and poly(methacrylic acid) (PMMA) onto the surface by combining ultraviolet-initiated graft polymerization and photolithography. Contact angle measurements found that at the PAA graft regions the water contact angle measured 58° and at the PMAA grafted regions the water contact angle measured 46°. The decrease in the contact angle from that of the native PDMS contact angle of 104° confirmed the presence of the grafted acrylates on the surface. To further confirm the presence of the grafted acrylates, toluidine blue staining was employed. The positively charged toluidine blue interacted with the negatively charged carboxyl groups of the acrylates and stained only the hydrophilic regions of the PDMS surface [11]

### 1.3. Hypothesis and Objective

Modification of PDMS has been carried out by a plasma treatment, a wet chemical solution of sodium hydroxide (NaOH), and through UV-irradiation by a narrow band 254 nm mercury lamp. The purpose of this research is to complete a comparative study of the functional groups attached to the bond formed on the PDMS surface once it has been modified. Plasma treatment and NaOH form hydroxyl groups on the surface, whereas UV-irradiation forms carboxylic groups on the surface. Previous research has shown that these bonds are not retained and ultimately rotate back into the polymer bulk.

It is hypothesized that the carboxylate group with a fluoro-terminated group such as pentafluorophenol (PFP) should retain the bond formed through UV-irradiation.

Researchers believe that the low molecular mass of PDMS, is heavily contributing to this bond reorientation. We have hypothesized that increasing the molecular weight of the attached functional group will retain the bond formed. In comparison, the hydroxyl group has a molecular weight of 17.02 g/mol, the carboxyl group has a molecular weight of 45.02 g/mol, and PFP has a molecular weight of 184.07 g/mol. The surface modification techniques of PDMS presented in this thesis have been characterized by contact angle goniometry, contact angle titration, Attenuated Total Reflectance Infrared spectroscopy, and UV/Vis spectroscopy.

#### 1.4. Thesis Outline

Chapter two provides background information on the previous work that has been carried out on the surface modification of PDMS. It also gives an overview of the experimentation performed and results found on hydroxyl groups and carboxylic groups. In addition, it details the experimental results obtained by previous researchers and explains the methodology they employed in their respective research projects. This chapter also introduces pentafluorophenol (PFP), the fluor-terminated functional group that is used within the scope of this research to characterize a UV modified surface of PDMS.

Chapter three explains in detail the characterization and modification techniques that are used to study the surface of PDMS. It contains information on the design of a plasma treatment process; the definition of wet chemistry and how it has been used in

previous research; the components of contact angle goniometry including the sessile drop technique, surface free energy, and Young's equation; the measurement of absorbance by a spectrophotometer; the principles of infrared spectroscopy and attenuated total reflectance spectroscopy.

Chapter four lays out the experimental design for this thesis project. It provides details about the preparation of PDMS, the chemical and reagents used. It also gives the make, model, and instrumental parameters of the equipment used. In addition, it explains the idea of radiation by an excimer lamp.

Chapter five contains the experimental results and discussion for all experiments performed. This chapter focuses on the contact angle results and the infrared spectra results to provide an answer to the hypothesis of this research. UV-Vis spectroscopy was used to determine absorbance measurements and to quantify the concentration of carboxylic groups on UV modified PDMS. A contact angle titration curve compared the surface functionalization of native, irradiated, and PPF bound PDMS surface. The recovery-rotation of the hydroxyl, carboxylic, and fluoro-terminated bonds formed are reported on to further answer the theorized hypothesis.

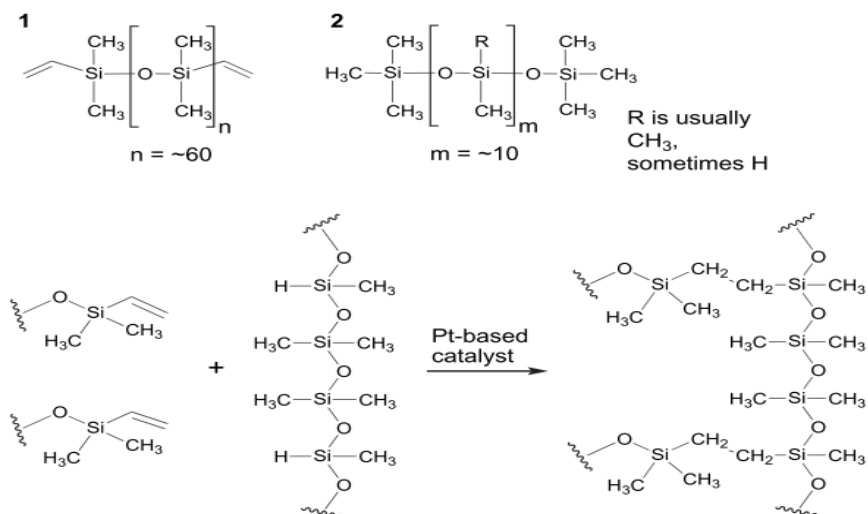
Chapter six contains a summary of the research conducted for the thesis work presented. The conclusion sums up the hypothesis and gives the advantage of the characterization work performed. Finally, recommendations for future work are given.

## CHAPTER TWO

### BACKGROUND

#### 2.1 Sylgard® 184

Silicones are entirely synthetic polymers that contain Si-O repeating backbones and organic groups attached directly to the silicon via silicon-carbon bonds [12]. Poly(dimethylsiloxane) is the most common example of a silicone polymer. The PDMS used in this research is a product produced by Dow Corning and is known as Sylgard® 184. This particular form of PDMS is sold as a kit that consists of a base and a curing agent. Scheme 1 shows the reaction that occurs between the two parts. Both the base and the curing agent contain dimethyl-vinyl terminated dimethyl siloxane (<60%) as well as dimethylvinylated and trimethylated silica (>40%) [5], [13]. A platinum-based catalyst included in the base cures the elastomer by an organometallic cross-linking reaction. When Part 1, Part 2, and the catalyst are combined, Si-CH<sub>2</sub>-CH<sub>2</sub>-Si linkages are formed.



Scheme 2: Cross-linking reaction of Sylgard® 184 [13]

## 2.2 Contact Angle: Wettability and Adhesion

Contact angle (CA,  $\theta$ ) is a quantitative measure of the wetting of a solid by a liquid. CA determines surface energy indirectly by examination of the surface. Three interfacial forces between the drop, the vapor, and the test surface balance at the edge of a drop. Two of the forces, the force of the drop and the test surface and the force of the test surface and the vapor, are in opposite directions and the third force, the force of the drop and the vapor, forms a tangent angle to the surface. The tangent angle is called the contact angle [14]. Geometrically, it is defined as the angle formed by a liquid at the three phase boundary where a liquid, gas, and solid intersect. Figure 2.1 shows a pictorial representation of contact angles.

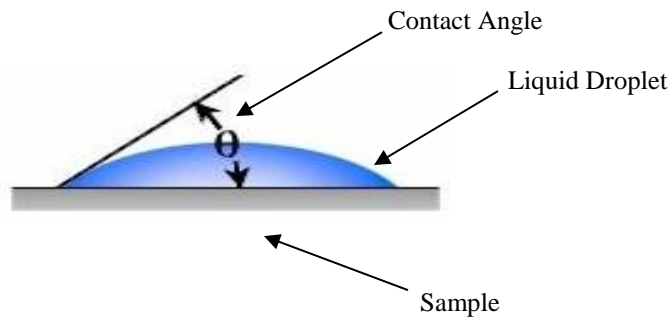


Figure 2.1: Representation of a contact angle on a sample surface

The ability of a liquid to spread on a solid surface and maintain its contact with that surface is known as wettability. Wettability is a manifestation of the physical aspects of the solid-liquid interface. Measurements of surface free energies and contact angles give clearer insight into the nature and effect of the forces that act at the interface [15], [16]. A drop of liquid, free in space, is drawn into a spherical shape by the tensile forces of its surface tension. When a drop of liquid is brought into contact with a flat solid surface, the final shape taken by the drop depends on the relative magnitudes of the

molecular forces that exist within the liquid (a cohesive force) and the solid (an adhesive force). Figure 2.2 gives a pictorial representation of the interaction that occurs between the two forces. Adhesive forces cause a liquid drop to spread. Cohesive forces cause the drop to ball up. The contact angle is determined by competition between these two forces [16].

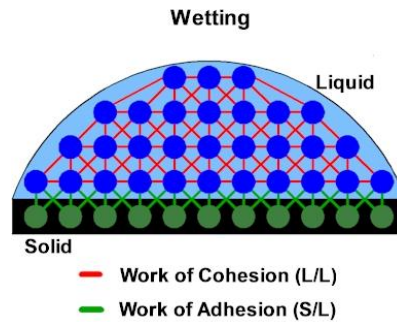


Figure 2.2: Interaction between cohesive and adhesive forces

Wetting and dewetting along with hydrophilic and hydrophobic are two sets of terms used to describe the liquid drop placed on the solid surface. Wettable or hydrophilic surfaces produce a contact angle where  $\theta \leq 90^\circ$ . Dewettable or hydrophobic surfaces produce a contact angle where  $\theta \geq 90^\circ$ . Within this research, water is mostly used as the test liquid. When describing water droplets placed on the modified PDMS surface, the latter terms of hydrophilic and hydrophobic are used.

Native PDMS is very hydrophobic in nature. Its contact angle has been recorded at  $108^\circ$  [17–19]. This hydrophobicity is exemplified by poor wetting, poor adhesiveness and a lower surface free energy. In contrast, a hydrophilic surface represents better wetting, better adhesiveness, and a higher surface energy. Figure 2.3 is a comparison between the hydrophobic and hydrophilic nature of a surface. For any given solid/liquid

interaction, there exists a range of contact angles that can be found. Contact angle measurements generally define three major aspects [20], [21]:

1. The affinity of a liquid to a solid surface: if water is used to measure the contact angle, the hydrophobic or hydrophilic character of the surface can be deduced.
2. If several reference liquids are used, the surface energy of the solid can be calculated, discriminating between polar and dispersive components.
3. The measure of the hysteresis between advancing angle and receding angle give information on non-homogeneity of the surface.

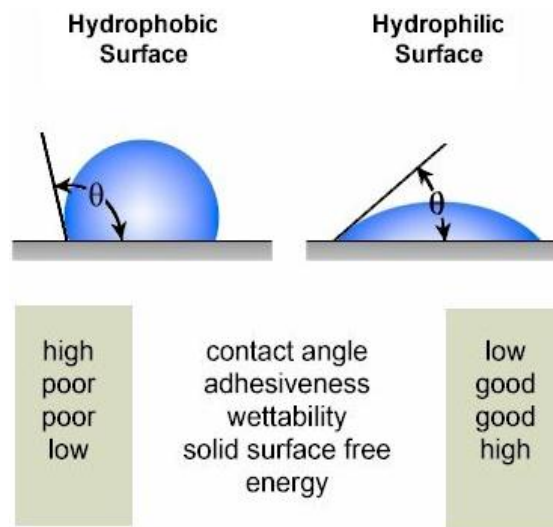


Figure 2.3: Characteristics of a hydrophobic surface vs. a hydrophilic surface

### 2.3 Hydrophobicity Loss and Recovery of PDMS

The surface properties of PDMS are best described by regarding the polymer side chains as the primary surface-active entities [22]. The methyl groups arranged around the silicon-oxygen backbone are responsible for the hydrophobic nature of the polymer. The

low surface free energy  $16\text{--}21 \text{ mN m}^{-1}$ , is due to closely packed methyl groups on the surface. The Pauling electronegativity difference of 1.7 between silicon and oxygen results in a 40–50% polar character of the siloxane bond. The polar nature of the siloxane bond makes PDMS susceptible to hydrolysis during acidic or basic conditions. The positively polarized silicon atom is electron withdrawing, thus polarizing the methyl group and making it less susceptible to radical attack. The methyl groups in PDMS have higher thermal and oxidative stability compared to methyl groups within other hydrocarbon polymers [23]. The methyl groups surrounding the flexible siloxane backbone are what render the polymer surface hydrophobic.

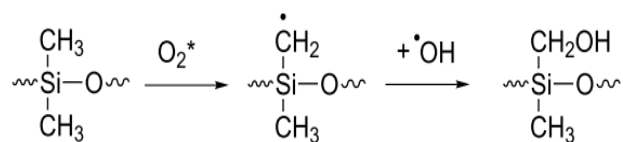
The hydrophobic surface properties of silicone rubber prevent the formation of continuous water films. Instead, water droplets are formed which simply bead off the surface. However, this hydrophobicity can be temporarily lost. An overview of the literature reveals that hydrophobicity can be lost by oxidation during exposure to corona discharge in air, radio frequency and microwave plasma treatments, wet chemical treatments, or by excimer or deep UV irradiation [22–24]. The resultant hydrophilic polymer promotes spreading of water on its surface. After exposure to ambient air that spans from minutes to days, hydrophobicity is regained. The change from a hydrophilic surface back to a hydrophobic surface is referred to as hydrophobic recovery. Differences in the recovery kinetics reported indicate that the phenomenon is a complex process. Variances in curing methods as well as the loss and the gain of hydrophobicity all affect the hydrophobic recovery kinetics. Owen and Smith proposed probable mechanisms for hydrophobic recovery of silicone rubbers after exposure to corona or plasma have been summarized [25], [26]:

- (1) Reorientation of polar hydrophilic groups at the surface back into the polymer bulk
- (2) Condensation of silanol groups at the surface.
- (3) External contamination of the surface.
- (4) Loss of volatile oxygen-rich species to the atmosphere
- (5) Migration of low molar mass species from the bulk to the surface.

The large segmental flexibility of unoxidized and lightly oxidized PDMS enables fast reorientation of polar groups. The driving force for this hydrophobic recovery is the thermodynamic requirement of minimizing the surface free energy. Reorientation of surface segments is a local process and is not believed to explain the full recovery of hydrophobicity of oxidized silicone rubber. Low molar mass PDMS is believed to migrate from the bulk to the silicone rubber surface resulting in a hydrophobic recovery [23], [27], [28].

## 2.4 Literature Review: Hydroxyl Group Formation

The formation of hydroxyl groups on a solid surface has been studied extensively [8], [9], [28]. A review of the literature shows that various applications are used in the formation of hydroxyl groups with PDMS. These modification techniques include electrical discharges (corona, plasma, and microwave treatments) and wet chemical solutions [8], [29–31]. In 1970, Hollahan and Carlson, reported on the effects of electrical discharges on the PDMS surface [9]. They proposed a reaction for the formation of hydroxyl groups based on infrared spectroscopy they observed. Scheme 2 shows the proposed reaction of PDMS after surface oxidation ( $\text{Si-CH}_2\text{-OH}$ ).



Scheme 3: Development of [Si-CH<sub>2</sub>-OH] structures [9]

#### 2.4.1 Effect of Plasma Discharges on PDMS

Exposing PDMS to plasma is a frequently used technique [8]. Treating PDMS with plasma modifies the surface and affects the chemical composition and topography [30]. Oxygen plasma treatments have become increasingly popular in the field of microfluidics [31]. Treatment with an oxygen plasma modifies the polymer surface by transferring energy to the polymer which catalyzes reactions that would not occur otherwise, and incorporating oxygen anions from the plasma into the polymer [7]. Oxygen plasma treatments are advantageous to PDMS because exposure leads to oxidation, chain scission, cross-linking, and the formation of a silica like surface [32]. A silica like surface (SiO<sub>x</sub>) contains silicon atoms bonded to more than two oxygen atoms. Unfortunately, plasma treating a surface requires equipment that is not often readily available due to high costs. Brent Ginn and Oliver Steinbock devised and tested an inexpensive method to generate hydroxyl groups on the surface of PDMS. In conjunction with a plasma cleaner, the researchers generated plasma in an 1100-W countertop microwave oven ( $\lambda = 2.45$  GHz) [30]. Contact angle measurements were used to characterize the modified polymer surface.

Contact angle measurements showed that the degree of the contact angle decreased with increasing exposure time. They reported an average contact angle for their native sample as  $112 \pm 2^\circ$ . PDMS was exposed to plasma over increments varying from 0

to 25 seconds. At 25 seconds, there is a drastic decrease in the contact angle and values less than  $15^\circ$  were reported. Generation of plasma proves to make the PDMS surface extremely hydrophilic. The value of the lowest contact angle seen here is comparable to a water droplet placed on a glass slide, which is a strongly wettable surface. Figure 2.4 presents the data found from both the microwave plasma treatment and the plasma treatment performed by Ginn and Steinbock.

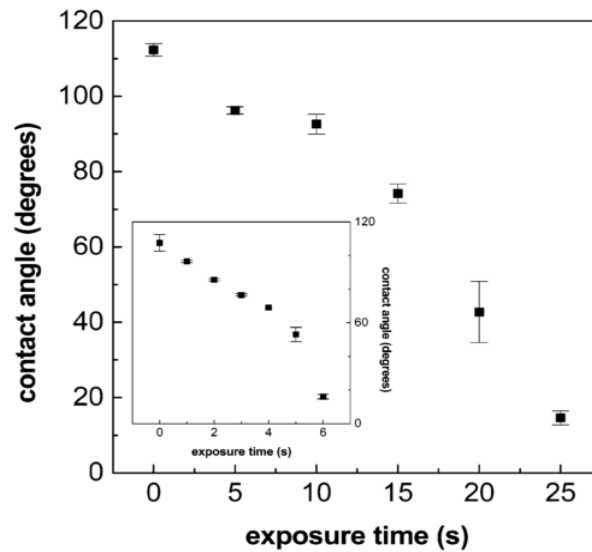


Figure 2.4 Contact angle measurements of PDMS and water as a function of exposure to plasma discharges for 25s. (The plot is of a microwave plasma treated surface, the inset is of a plasma cleaner treated surface) [30].

When the plasma-treated surfaces are allowed to react with ambient air, hydrophobicity is recovered. The researchers observed this rotation in the following way. A PDMS sample was exposed to oxygen plasma for 25s. The initial contact angle was observed at  $15 \pm 2^\circ$ . After three hours of exposure to ambient air, the contact angle readily increased to  $79^\circ$ . This gain of hydrophobicity can be attributed to passive transport of low-molar-mass PDMS species from the bulk state of the polymer. Studies

also suggest that possible rearrangement of the polar species plays a role as well. Figure 2.5 shows the recovery Ginn and Steinbock observed after exposure for 25s. The gain of hydrophobicity after modification is approximately 30° lower than the contact angle of native PDMS. Studies suggest that this is caused by the formation of the silica-like surface[30], [32].

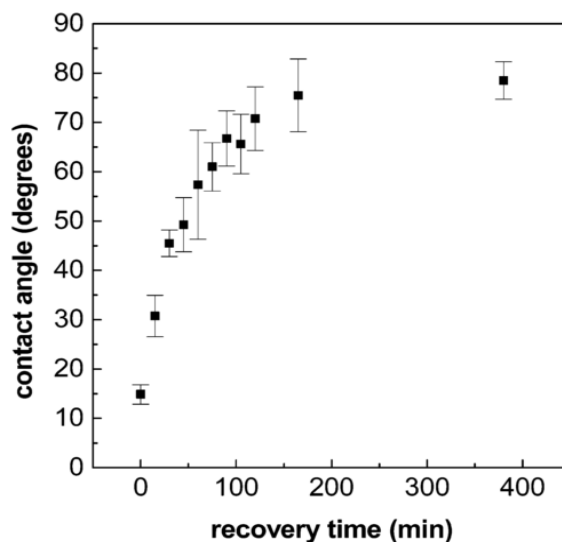


Figure 2.5 Reorientation of hydroxyl groups back into the polymer bulk as a function of contact angles versus recovery time after 25s plasma exposure [30].

#### 2.4.2 NaOH Wet Chemical Solution

In addition to plasma treating the surface of PDMS, a wet chemical solution may be used to form hydroxyl groups on the polymer surface. The chemical technique is beneficial because it does not require expensive laboratory equipment. Ren *et al.* [7] used sodium hydroxide (NaOH) to regenerate O<sub>2</sub> plasma treated PDMS microchannels after exposure to air. The researchers observed that the electroosmotic flow of the air-exposed channels dropped to 60% of its original value. Subsequently, the air-exposed channels were restored to the original electroosmotic flow after immersion in NaOH for three

hours. They concluded that the base led to the removal of low molar mass PDMS chains and reorientation of the hydroxyl groups onto the surface.

In a similar fashion, Hoek, Tho, and Arnold used aqueous NaOH as a surface treatment to control the electroosmotic flow in PDMS microchannels. The researchers placed PDMS microchannels in 1M NaOH for a maximum of twenty-four hours. Following treatment, the channels were washed with deionized water for thirty minutes to remove all NaOH. For comparison, they also studied the O<sub>2</sub> plasma effect on the PDMS surface. Contact angle measurements and ATR-FTIR were used to evaluate the modified PDMS samples. Through experimentation, it was concluded that treatment of PDMS microchannels with 1M NaOH for twenty-four hours increases the electroosmotic flow so that it equals the high flow rates achieved using the O<sub>2</sub> plasma treatment [31].

Contact angle measurements were used to obtain information of the changes in surface chemistry. After performing a plasma treatment, a contact angle of 8° was observed. This is more than 100° less than the native angle observed at 109°. This extreme decrease shows that the surface is hydrophilic and that silanol groups were formed on the surface. Compared to previous research, the plasma treated PDMS surface was unstable and within hours the surface reverts back and a contact angle of 96° was reported. The contact angle of PDMS treated with NaOH is similar to native PDMS and remains hydrophobic, exhibiting a value of 106°. This finding indicates that NaOH treated PDMS produces different surface modifications and different ionisable surface groups than those formed by a plasma treatment [31].

The ATR-FTIR spectra provided further information on the differences of plasma treated and NaOH treated surfaces. Figure 2.6 shows the absorption spectra for native,

plasma treated, and NaOH treated PDMS. For plasma treated PDMS, characteristic bands of  $\text{-OH}$  ( $3200\text{-}3400\text{ cm}^{-1}$ ),  $\text{Si-OH}$  ( $910\text{ cm}^{-1}$ ), and  $\text{Si-O-Si}$  ( $1012$  and  $1060\text{ cm}^{-1}$ ) stretches are seen [31]. For the NaOH treated PDMS samples there is an increase in the  $\text{-OH}$  band along with slightly different band intensities than those of plasma treated PDMS. The intensity of the absorption bands associated with the  $\text{Si-C}$  bond ( $760$  and  $845\text{ cm}^{-1}$ ) and the asymmetric  $\text{Si-O-Si}$  stretching vibrations decrease. At the same time, the absorption bands associated with the  $\text{-CH}_3$  groups increased. The finding that the contact angle is unaffected by the NaOH treatment can be further explained by ATR-FTIR spectra. The formation of an alcohol is possible. These  $\text{C-OH}$  groups are difficult to detect by ATR-FTIR analysis. They show absorptions in the  $1000\text{-}1200\text{ cm}^{-1}$  region which overlaps with the strong absorption bands of the  $\text{Si-O-Si}$  stretching.

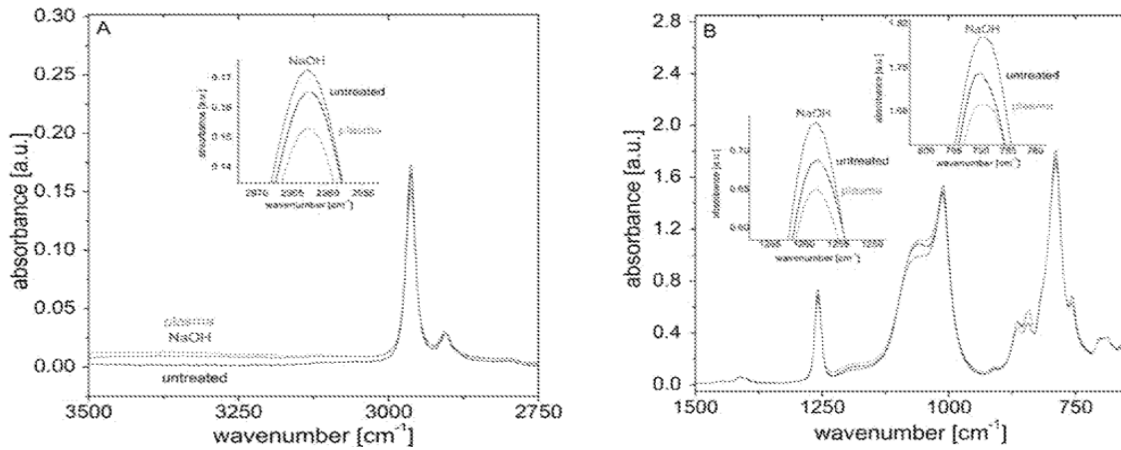
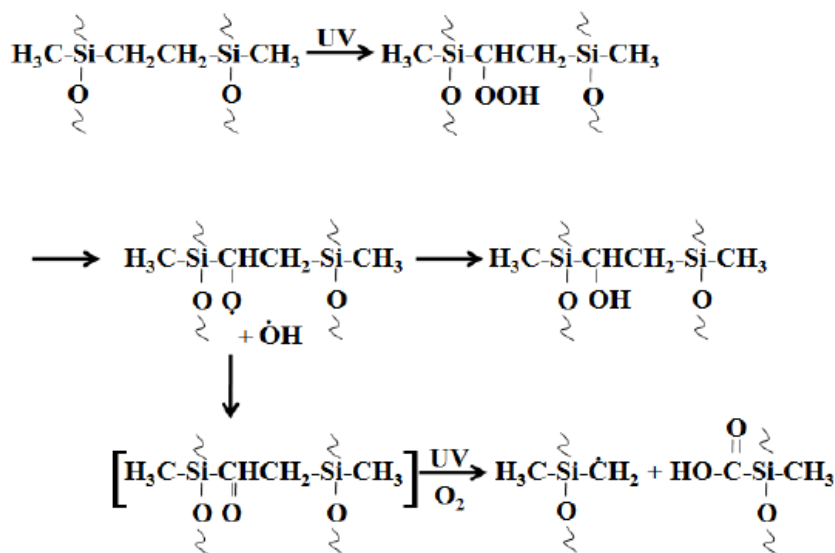


Figure 2.6: ATR-FTIR spectra of native, plasma treated, and NaOH treated PDMS at (A) high wavenumbers ( $3500\text{-}2750\text{ cm}^{-1}$ ) and (B) low wavenumbers ( $1500\text{-}600\text{ cm}^{-1}$ ). The inlets show the maximum absorbance peak associated with the  $\text{-CH}_3$  groups [31].

## 2.5 Literature Review: Carboxylic Group Formation

Extensive literature can be found on formation of hydroxyl groups on a polymer surface. An –OH group can be formed on a surface by electrical discharges, microwave irradiation, and UV/ozone irradiation to name a few. Most of the techniques associated with formation of hydroxyl groups involve multiple steps which increases time and difficulty. These methods can also be cost ineffective. Waddell and Shreeves devised a simple one step process to modify the surface of PDMS. The researchers exposed PDMS to 254 nm narrow band Hg radiation under a continuous purge of nitrogen. This technique is advantageous because it is inexpensive, accessible to most facilities, and does not require a high level skill set to operate. The researchers also found that exposure to 254 nm radiation leads to the formation of carboxylic groups [5]. Scheme 3 is a proposed reaction that shows the changes of PDMS after interaction with a UV source [8]. Contact angle measurements, ATR-IR spectroscopy, SEM, and AFM were used to characterize the polymer surface.



Scheme 4: Formation of carboxylic groups by UV irradiation [8]

Contact angle measurements showed that the hydrophobicity of the surface decreased with an increase of UV exposure time. Figure 2.7 illustrates the contact angle found with respect to irradiation time. It can be seen that the contact angle decreases gradually until 90° where the minimum contact angle is seen. A more detailed examination of the wettability data indicates following the initial increase in wettability there is a slight decrease followed by a plateau in the data. An exposure time greater than two hours has no additional change in wettability. At two hours and beyond, an increase in the contact angle can be observed. This increase can be attributed to the degradation of the polymer backbone which causes the surface to become glassy and brittle [5].

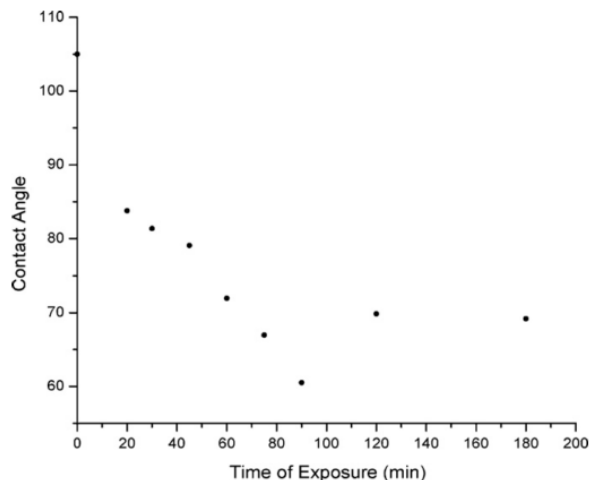


Figure 2.7 Change in contact angle with respect to irradiation time. The contact angle progressively decreases until the formation of cracks occur at 90 minutes [5].

ATR-IR spectra of native and irradiated PDMS showed an increase in the formation of hydroxyl groups in respect to irradiation time. The formation of hydroxyl groups on the surface increased with exposure time up to three hours, beyond which a slight decrease in band intensity was observed. In addition, a decrease is seen in the

siloxane bands in the compound. Figure 2.8 gives the IR spectra of native and irradiated PDMS. In the spectra, the  $\text{-OH}$  stretch can be observed at  $3400\text{ cm}^{-1}$  and the carbonyl stretch can be seen at  $1725\text{ cm}^{-1}$ . The occurrences of these two bands signify that carboxylic groups are formed on the polymer surface [5].

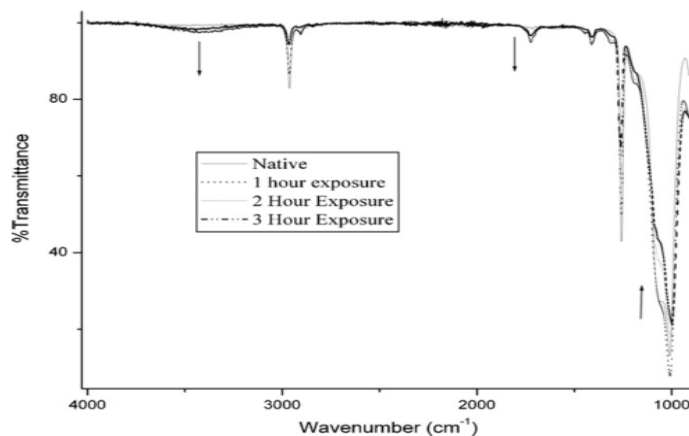


Figure 2.8: IR spectra of native and irradiated PDMS. Carboxylic groups can be detected by the formation of  $\text{-OH}$  stretch and the carbonyl stretch [5]

Padma Dharmarajan further investigated modification of PDMS by 254 nm narrow band irradiation. She studied the trend in the variation of surface energy of the modified surface with increasing UV exposure time. She also quantified the amount of carboxylic groups present on the surface. The characterization techniques she used included contact angle goniometry and ATR-IR. Contact angle measurements showed that increased exposure times led to a progressive decrease in contact angles. This indicated that the wettability of the PDMS surface increased with increasing exposure time as well. The contact angle results show that the surface has a peak surface energy at 75 minutes of UV exposure, after that the surface starts to recover its hydrophobicity. As the surface gradually becomes more hydrophilic upon exposure, the surface begins to

transform into a glassy layer. With prolonged exposure, this glassy layer leads to the formation of cracks. This cracking is the result of automatic relaxation of the surface from the induced stress. Migration of low molecular weight PDMS from the bulk to the surface facilitated by these cracks causes the surface to recover its hydrophobicity [33], [34].

The infrared spectra showed that carboxylic acid groups were formed on the surface by irradiation at 254 nm. The peak intensities varied for different exposure times. A measure of the carbonyl peak area showed that the samples irradiated for 75 minutes had the maximum area. The presence of carboxylic acids was quantified using a methylene blue staining dye and absorbance measurements were carried out. Again, the results revealed that the 75 minute irradiated sample contained the maximum number of polar hydrophilic carboxylic acid groups per unit area on the surface. Figure 2.9 shows the number of carboxylic acid groups found per square centimeter [33].

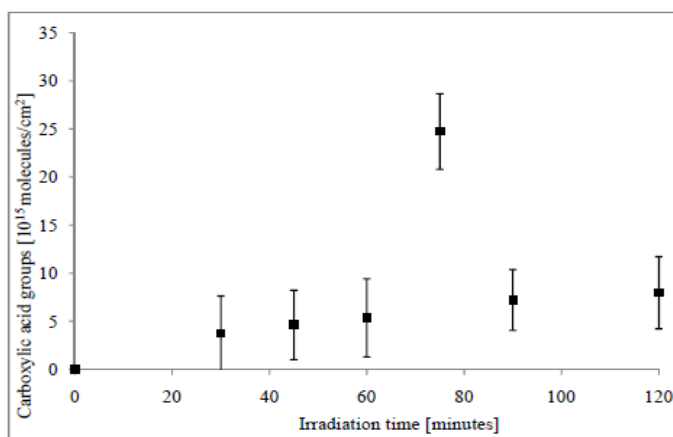


Figure 2.9: Quantification of carboxylic groups on irradiated PDMS surface.

Dharmarajan also explored the hydrophobic recovery of carboxylic groups on the PDMS surface. She studied the long term stability of modified surfaces in different storage environments. The investigated environments included air, water, ethanol, PBS, pH 10 NaOH solution, and 50:50 acetic acid/ water. Through ATR-IR analysis, it was found that all storage environments, excluding 50:50 acetic acid/ water, result in the loss of carbonyl groups. This was observed by a decrease in peak intensity of the carbonyl band seen at  $1725\text{ cm}^{-1}$ . Conversely, the 50% acetic acid solution environment assisted in stabilizing the carboxylic acid groups on the surface. To monitor the rotation of the carboxylic group bond back into the polymer bulk, Padma irradiated a PDMS sample at 45 minutes and stored the sample in air over a ten day period. Figure 2.10 represents the contact angle variation for the 45 minute irradiated sample stored in air. From the graph, it can be seen that the hydrophobicity starts recovering one day after irradiating the sample. The contact angle gradually increases and plateaus at day seven. The final contact angle reached is  $98^\circ \pm 1.3$ . Similar to hydroxyl groups, the polar carboxylic acid groups rotate back into the bulk state of PDMS [33].

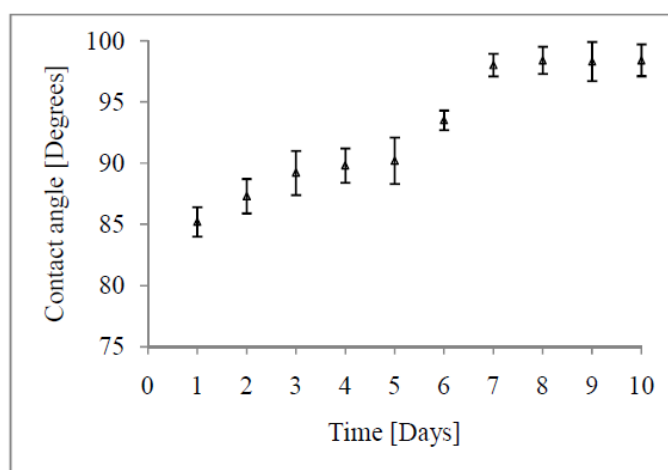


Figure 2.10: Rotation of the carboxylic bond of a 45 minute irradiated PDMS sample stored in air over a ten day period [33]

## 2.6 Pentafluorophenol

Pentafluorophenol (PFP) is an aromatic polyfluoro-terminated intermediated [35]. Figure 2.11 gives the chemical structure of PFP. Within the literature, PFP is used as a coupling agent to convert carboxyl groups present on the surface of a polymer [36], [37]. Patrino *et al.* coupled PFP with a water-soluble carbodiimide, 1-(3-dimethylaminopropyl)-3-ethyl carbodiimide hydrochloride (EDC), to show that poly(acrylic acid) grafted onto PDMS could direct surface chemistry. The researchers immersed the sample in an ethanol solution of PFP and EDC and used X-ray photoelectron spectroscopy (XPS) imaging to find intense maxima of fluorocarbon species on the grafted region [11].

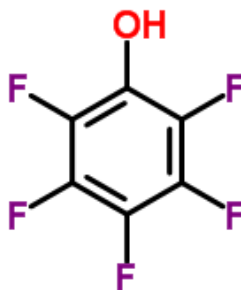
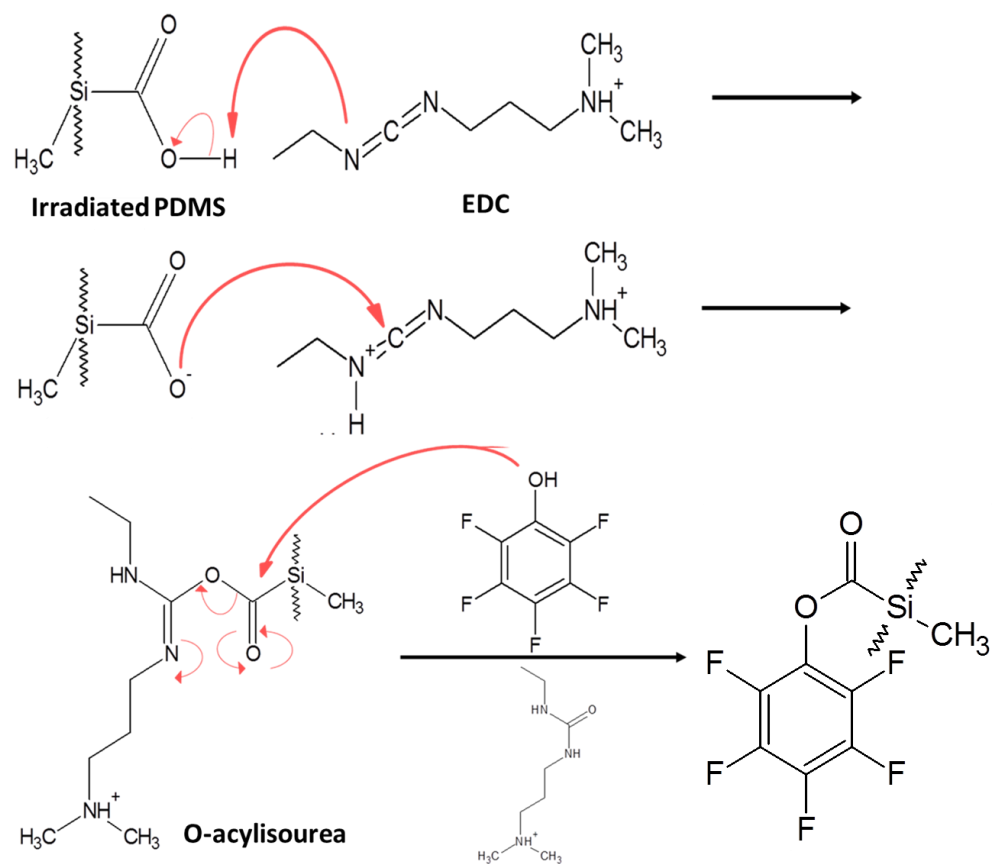


Figure 2.11: Structure of Pentafluorophenol

EDC is a carbonyl zero-length crosslinking agent that has the ability to form bonds with carboxyl groups. EDC reacts with a carboxyl group first and forms an amine-reactive *O*-acylisourea intermediate. The intermediate is unstable so PFP readily attaches and easily replaces the carboxyl group bond. Scheme 4 is a proposed reaction of the coupling of PFP/EDC to a modified PDMS surface (PDMS-PFP).



Scheme 5: Reaction mechanism for the coupling of PFP to PDMS induced by EDC [38]

# **CHAPTER THREE**

## **MODIFICATION AND CHARACTERIZATION**

### **TECHNIQUES OF PDMS**

#### **3.1 Plasma Treatment**

Plasma is produced and sustained by adding energy (heat) to gas, and is often referred to as the fourth state of matter [39]. Figure 3.1 is a representation of the four different states of matter. Plasma modification of a polymer surface utilizes the chemical reactions which occur at the polymer surface as a result of the interaction of the surface with reactive species created under the conditions of plasma [40]. Plasma is a gas that contains both charged and neutral species such as positive and negative ions, electrons, atoms, and molecules. Plasma is an electrically neutral gas because any imbalance of charge is removed by the generated electric fields. Consequently, the density of negative ions plus the density of electrons is equal to the density of positively charged ions. The degree of ionization is an important parameter of plasma. It is the fraction of the original neutral atoms or molecules which have been ionized. For fully ionized plasmas, the degree of ionization approaches unity, and neutral atoms or molecules play little to no role.

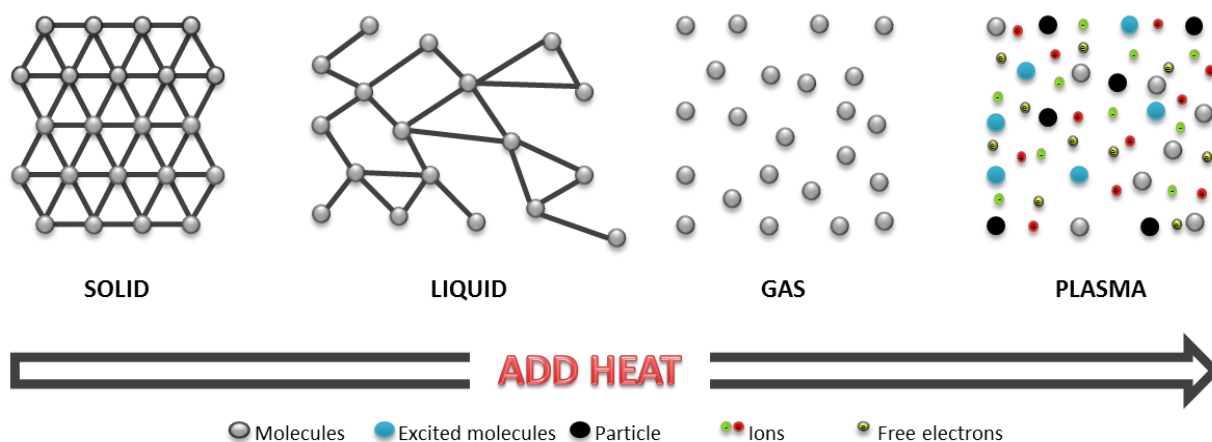


Figure 3.1: Plasma is the fourth state of matter

Advantages of plasma treatments include: (1) surface modification can be achieved with the minimum alteration of the bulk characteristics of the polymer because modification is limited to a thin layer at the surface, (2) nearly all polymers, regardless of chemical activity, can undergo surface modification by plasma treatments due to the energy generated by plasma, and (3) a variety of surface modifications such as cross-linking or change of surface energy can be achieved. These advantageous features are non-specific to polymers; therefore almost any polymer can be modified by plasma treatments.

A polymer surface can be modified by plasmas of a gas. A plasma treatment is a chemical modification that can be obtained by argon, hydrogen, oxygen, nitrogen, water, ammonia, carbon monoxide, and air, to name a few [40]. Owen and Smith reported on the effects of radio frequency (RF) plasma treatments of PDMS. They found that the effects were broadly similar for argon, helium, oxygen, and nitrogen. All of the treatments yielded a thin, brittle silica-like layer on the surface. The researchers also proposed that the migration of the untreated polymer chains from the bulk to the surface

through cracks in the silica-like layer was the primary cause of hydrophobic recovery. Van der Mei *et al.* hypothesized that a thick treated layer, opposed to a thin, brittle layer, might inhibit the migration of hydrophobic groups towards the surface. The research group reported that repeated oxygen plasma treatment of polyethylene, with a seven day interval in between, was more effective in creating a permanently hydrophilized surface than employing a higher RF power or a longer duration of the treatment [41]. Plasmas are initiated and sustained by electric fields which are produced by either direct current (DC) or alternating current (AC) power supplies. AC frequencies of excitation are 100 kHz at the low end of the spectrum, 13.56 MHz in the RF portion of the spectrum, and 2.45 GHz in the microwave region of the spectrum. These plasmas are often referred to as electric discharges, gaseous discharges, or glow discharges because they emit light [39]. Figure 3.2 is a representation of the reaction that occurs within a plasma chamber.

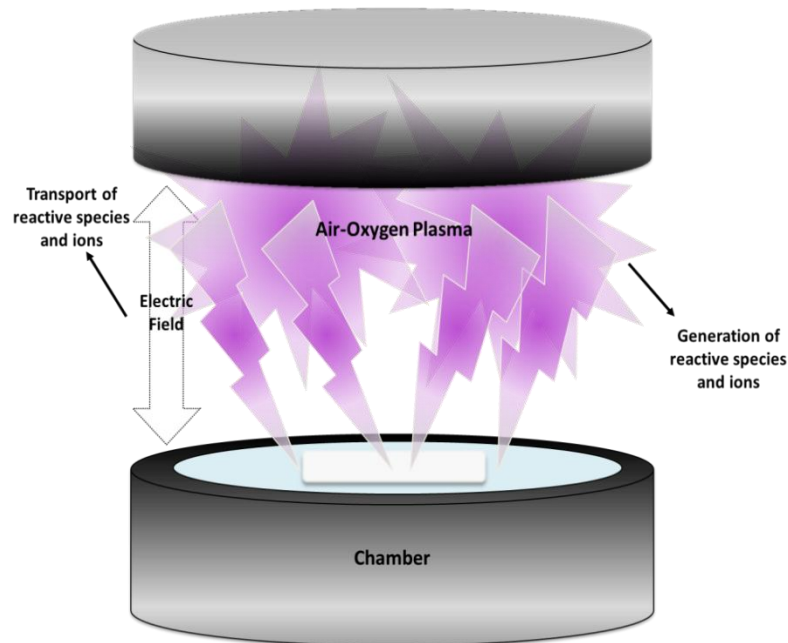


Figure 3.2: Concept of plasma processing. Energy is supplied to plasma discharges and produces reactive molecules and ions. The molecules and ions are transported to the polymer surface.

### 3.2 Wet Chemistry

The term wet chemistry refers to chemistry done in the liquid phase. A review of the literature shows that NaOH has been used previously to regenerate microchannels of microfluidic devices. Spehar *et al.* preconditioned PDMS/PDMS and glass/PDMS microchannels with NaOH before determining the electroosmotic flow in the channels [42]. Ren *et al.* observed that the electroosmotic flow of oxygen plasma treated PDMS microchannels dropped to 60% of its original value after exposure to ambient air. The researchers treated the channels with a 1M NaOH solution for approximately three hours and restored the electroosmotic flow. They proposed that treatment of the air exposed channels with a base removed low molar mass PDMS chains and reorientation of the hydroxyl groups onto the surface [7].

The effect of the NaOH treatment on the electrokinetic characteristics and properties were not clear in the studies performed by the aforementioned researchers [7], [42], [43]. Hoek, Tho, and Arnold attempted to explain these properties. They used a 1M NaOH solution and an O<sub>2</sub> plasma treatment to compare the electroosmotic flow of native, PDMS/PDMS, and PDMS/glass microchannels. They studied the effect of NaOH treatment time on the electroosmotic flow and found that at twenty-four hours the electroosmotic flow equaled the flow rates achieved when using a plasma treatment [31].

### 3.3 Ultraviolet Surface Modification

Modification of PDMS by narrow band 254 nm radiation has not been studied extensively. The 254 nm light source is readily available in the form of a mercury lamp that is easily accessible in most laboratories. One set of experimenters exposed PDMS at

a fluence of  $15 \text{ mJ/cm}^2$  to 254 nm of radiation for three hours. Analysis of the infrared spectra showed an increase in hydroxyl groups as well as a decrease in contact angle measurements [44]. Waddell *et al.* reported on the modification of PDMS by narrow band 254 nm radiation under a nitrogen atmosphere. ATR-IR results showed an increase in both the hydroxyl and carbonyl stretching region and the formation of carboxylic acids influenced the wettability of the surface [5]. Dharmarajan expounded on this research and investigated the surface characteristics and functionality after carboxylic acids were formed. Irradiation times at 254 nm excimer radiation were varied and the results were analyzed by contact angle measurements, infrared spectral analysis, and UV-Vis spectroscopy. A maximum for the concentration of carboxylic acids on the surface was seen at 75 minutes in all experiments [33].

### 3.4 Contact Angle Goniometry

A goniometer is an instrument that can measure contact angle as well as surface tension and interfacial tension [45]. Surface tension,  $\gamma$ , results from an imbalance of molecular forces in a liquid and is a measurement of the cohesive energy present at an interface. The magnitude of surface tension is determined by the internal forces in the liquid [3], [46]. Interfacial tension exists in the boundary region between two bulk phases and is used to describe the tension between two immiscible liquids, such as water and oil [46]. Measuring surface tension, interfacial tension, or contact angles provides information on material properties such as wettability, absorption, surface free energy, adsorption, and spreading.

Goniometry is an extremely versatile technique used for characterization of both liquids and solids. Application of contact angle goniometers range from developing engineered surfaces and liquids to controlling the purity of semiconductors [47]. A goniometer captures images of test liquid droplets on a surface. Software may be used to analyze the test droplet as a function of time. The test droplet is a function of surface tension of liquid, gravity, and of the difference in density between the test liquid and surrounding medium. On a solid surface, the liquid forms a drop with a contact angle that also depends on the solid's surface free energy. The test droplet on the surface is captured as an image and analyzed with a drop profile fitting method that determines contact angle and surface tension.

#### 3.4.1 Contact Angle Measuring: Static Sessile Drop Method

The measurement of a contact angle on a solid surface is the most practical way to obtain surface energetics. Among the various modern surface analytical tools available, contact angle and wetting techniques remain standard methods for benchmarking surface quality [48]. Contact angles describe the shape of a liquid droplet resting on a solid surface. When a tangent that originates at the liquid-solid-gas interface and is drawn along the liquid-vapor interface, the contact angle is the resulting angle formed between the tangent line and the surface. Figure 3.3 represents this tangent line. Due to simplicity, the sessile drop method is one of the most widely utilized procedures to measure contact angles. The contact angle of a sessile liquid drop can be obtained directly by measurement of the slope of the tangent line [49]. This method uses an optical subsystem to capture the profile of a pure liquid drop on a solid substrate [50]. This technique is

advantageous because only small quantities of liquid are used, it is applicable to liquid-vapor, liquid-liquid and liquid-solid interfaces, and it can be used under extreme conditions of temperature and pressure [51].

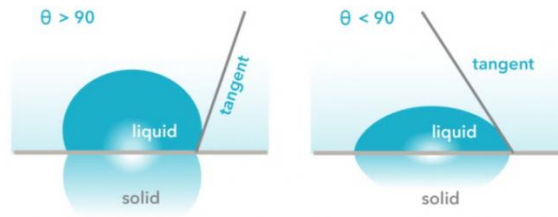


Figure 3.3: Tangent line that measures the contact angle.

#### 3.4.2 Hysteresis and Young's equation

Surface roughness amplifies hydrophobicity. Examples of this property include dew drops on a leaf, and liquids on stain resistant fabric. On both the leaves and stain resistant fabric, water droplets bead up to minimize its interaction with the surface. The water droplets formed on these superhydrophobic surfaces easily roll off, which indicates a low hysteresis of the contact angle. Figure 3.4 shows how a contact angle is observed; when looking at the angle, one observes a two dimensional projection of a three dimensional drop [14]. Contact angle hysteresis (CAH) is the difference between the maximum (advanced/advancing) and minimum (recede/receding) contact angle values [52]. CAH governs the wetting properties of the polymer surface and dictates a diversity of phenomena occurring at the solid/liquid interface, including the spreading and sliding of drops [53].

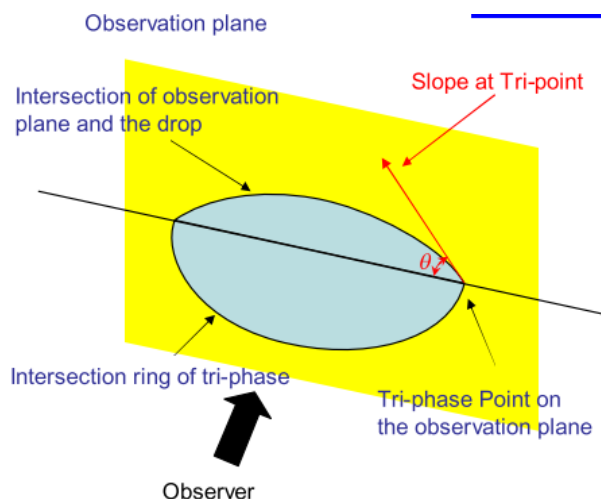


Figure 3.4 Representation of how contact angles are observed [14]

Along with CAH, Young's equation (equilibrium contact angle) is essential for understanding the wetting phenomenon. Measurement of contact angles on a given solid surface is the most practical way to obtain surface energetics. Young's equation is at the center of contact angle research and describes the nature of the contact angle [53], [54]. The equation treats the contact angle of a liquid as the result of the mechanical equilibrium of a drop resting on a plane solid surface under the action of the three interfacial tensions. This equation correlates the Young contact angle,  $\theta_Y$ , the interfacial force between the liquid drop and vapor phase,  $\gamma_{LV}$ , the interfacial force between the liquid drop and the test surface of the solid phase,  $\gamma_{SL}$ , and the interfacial force between the test surface of the solid phase and the vapor phase,  $\gamma_{SV}$ . Figure 3.5 is a graphical representation of how the three interfacial forces are balanced.

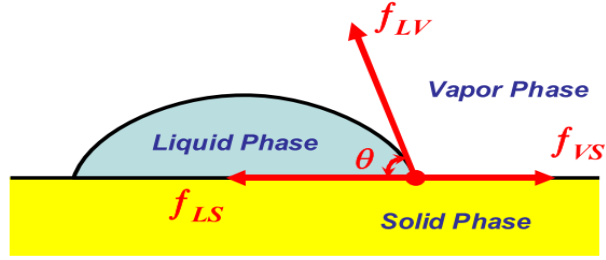


Figure 3.5: Diagram of the interfacial forces that forms the contact angle [14]

The correlation between the contact angle and the interfacial tensions is given in the following equation proposed by Thomas Young [47], [50], [52], [53], [55–59]:

$$\cos \theta = \frac{\gamma_{SV} - \gamma_{SL}}{\gamma_{LV}} \quad (3.1)$$

The concept of the contact angle and its equilibrium is advantageous because it gives a definition to the notion of wettability as well as indicates the surface parameters requiring measurements [58].

### 3.4.3 Surface Free Energy

Knowledge of the reactivity or energy of surfaces and their interaction with fluids is very important. The reactivity of a surface is measured in terms of surface free energy (SFE). SFE is defined as the work required to increase the area of a test drop on a solid surface by 1 cm<sup>2</sup>. SFE is determined by measuring the contact angle formed by a range of liquids on a given surface [60]. Figure 3.6 shows the correlation between drop surface tension and the surface energy of the test liquid. The figure shows that as the surface tension on the drop increases, hydrophobicity increases and the surface energy decreases.

Vice versa, as the surface energy of the test surface increases, hydrophobicity decreases and the surface energy increases.

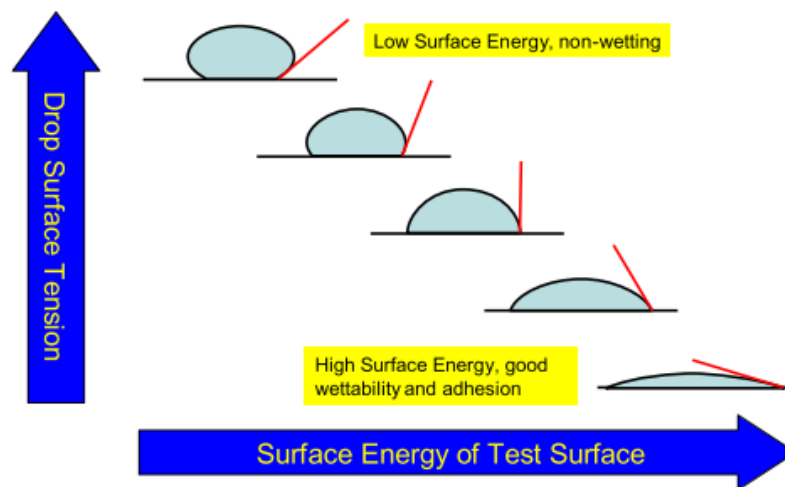


Figure 3.6: Relationship between surface energy of the solid and surface tension of the liquid [14]

The SFE of a solid consists of both polar and dispersive energies. The polar component accounts for the coulombic interactions of polar groups that include dipole-dipole interactions, hydrogen bonding interactions, dipole-induced interactions, and acid-base interactions. The dispersive component accounts for London type (van der Waals) forces, arises from non polar interactions. Dispersion energy exists between all molecules but polar energy exists only when polar groups are present [33], [60], [61]. SFE was first approached and studied by William Zisman [58]. He measured the contact angles of a surface with test liquids of differing surface tensions,  $\gamma$ , and plotted  $\cos \theta$  versus  $\gamma$ . This plot, known as a Zisman plot, is a determination of the dispersive component of the surface energy. SFE can be calculated by the following equations:

$$\gamma_S^{TOT} = \gamma_S^D + \gamma_S^P \quad (3.2)$$

$$\cos \theta = \frac{\gamma_S}{\gamma_L} \quad (3.3)$$

$$(1 + \cos \theta)\gamma_L = 2[(\gamma_S^D \gamma_L^D)^{0.5} + (\gamma_S^P \gamma_L^P)^{0.5}] \quad (3.4)$$

$$(1 + \cos \theta)\gamma_L = 4 \left[ \frac{\gamma_S^D \gamma_L^D}{\gamma_S^D + \gamma_L^D} + \frac{\gamma_S^P \gamma_L^P}{\gamma_S^P + \gamma_L^P} \right] \quad (3.5)$$

$$(1 + \cos \theta)\gamma_L = 2[(\gamma_S^D \gamma_L^D)^{0.5} + (\gamma_S^+ \gamma_L^-)^{0.5} + (\gamma_S^- \gamma_L^+)^{0.5}] \quad (3.6)$$

where

$\gamma$  is the surface energy (mN/m)

$\theta$  is the contact angle (°)

D is the dispersive component

P is the polar component

S is the solid surface

L is the liquid drop

(+) is the surface tension contributed by acid

(-) is the surface tension contributed by base

Equation 3.3 assumes that the interaction between the drop and the testing surface is greater than the internal force of the drop and is mainly used for testing surfaces with low contact angle. The distinction between the polar and dispersive components led to the development of the geometric and harmonic mean methods of SFE determination.

According to the Owens, Wendt, Rabel, and Kaelble method interfacial energy can be calculated by equation 3.4 using the geometric mean approach. This method is suitable

for testing surfaces with similar ionization potentials. Likewise in equation 3.5, the interfacial energy is equal to the harmonic mean of two separated phases and is suitable for non-polar low energy surface. Equation 3.6 gives the acid-base theory for calculation of SFE. This theory evaluates polar based on an energy interchange mode of the acid and base and it is applicable to materials with polar surfaces [14].

When researching contact angle relation to surface tension, Kabza, Gestwicki, and McGrath deduced that Zisman's method for obtaining the materials surface tension is based on the experimental finding that when a liquid spreads freely on an analyzed surface, its surface tension is lower than or equal to that of the surface upon which it is spreading [45]. Zisman called the value of the surface tension of the liquid that is equal to that of the analyzed material  $\gamma_c$ , the critical surface tension (CST). CST is obtained when a series of contact angles is measured using liquids with progressively smaller surface tensions. The surface tension of these liquids is then plotted against the cosine value of the corresponding contact angle. CST is defined by the intercept of the horizontal line when  $\cos \theta$  is extrapolated to one. CST is equal to the dispersive component of SFE. If CST is substituted into equations 3.2 and 3.4 the polar component of SFE can be calculated [58]. An illustration of the Zisman plot can be seen in figure 3.7.

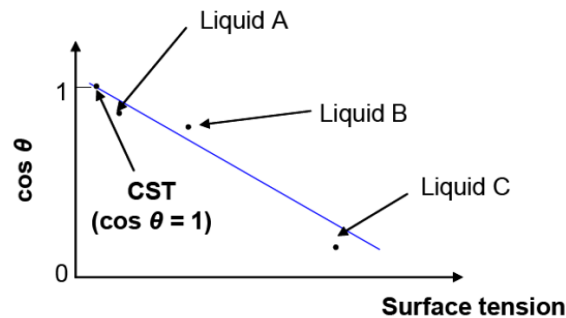


Figure 3.7: Representation of the Zisman plot [58]

### 3.5 Ultraviolet-Visible Spectroscopy

Molecular spectroscopy is a means of investigating molecules. It most often involves the absorption of electromagnetic radiation. Absorbed ultraviolet and visible radiation generally results in electronic transitions, which is defined as promotion of electrons from the ground state to a high energy state [62]. Ultraviolet -visible (UV-Vis) spectroscopy is one of the oldest methods in molecular spectroscopy. Within the UV-Vis region, electronic transitions occur when atomic or molecular orbitals of electrons within the material is irradiated with light [63]. The ultraviolet region falls in the range between 190-380 nm and the visible region falls between 380-750 nm. A compound absorbs light only if there is a minimum of five conjugated auxochromic or chromophoric groups present. Auxochromic groups ( $-\text{OH}$ ,  $\text{OR}$ ,  $-\text{NH}_2$ ,  $-\text{NHR}$ ,  $-\text{SH}$ ,  $-\text{SR}$ ,  $-\text{Hal}$ ) contain non-bonding electron pairs. Chromophoric groups are photosensitive and absorb light at a particular wavelength. When the two groups are attached, the absorption and wavelength are altered. Methylene blue is an example of this type of compound. Methylene blue is a cationic dye that has a maximum absorption of approximately 666 nm in the UV/Vis spectrum. Within the scope of this research, it is used to determine the concentration of a carboxylic acid on the surface of PDMS. Figure 3.8 is a structural representation of the methylene blue dye [64].

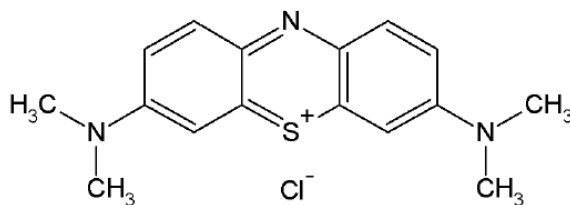


Figure 3.8: Chemical structure of methylene blue [64]

The Beer-Lambert law forms the mathematical-physical basis of light absorption measurements of solutions in the UV-Vis region and is the linear relationship between absorbance and concentration of absorbing species. It is expressed as follows [65]:

$$A = \varepsilon bc = -\log\left(\frac{I}{I_0}\right) \quad (3.7)$$

where

A is the absorbance

$\varepsilon$  is the molar absorptivity with units of  $\text{L mol}^{-1} \text{cm}^{-1}$

b is the path length of the sample with units of cm

c is the concentration of the compound in solution with units of mol/L

$I_0$  is the incident light intensity, and

I is the intensity of the light that exists in the cell.

A spectrophotometer is an instrument used to measure the amount of photons (the intensity of light) absorbed after it passes through a sample. The concentration of a colored solution can be determined with a spectrophotometer. A spectrophotometer consists of a light source, monochromator, cuvette compartment, detector and amplifier with an indicating device. Figure 3.9 is a diagram of a single beam spectrophotometer. In this instrument, light is dispersed into several basic wavelengths by a prism or grating monochromator and allows for the continuous wavelength measurement over the entire spectral region. In a single beam spectrophotometer, the reference sample is measured first and the colored solution is measured with respect to the reference [65].

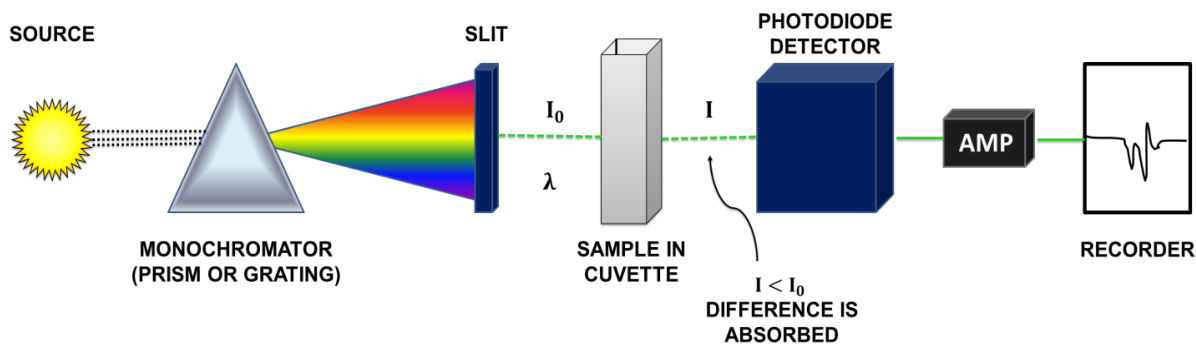


Figure 3.9: Diagram of a single beam spectrophotometer

### 3. 6 Attenuated Total Reflectance Infrared Spectroscopy

Infrared spectroscopy (IR) is one of the most important analytical techniques available [66]. IR is the absorption measurement of different IR frequencies by a sample positioned in the path of an IR beam [67]. Infrared spectroscopy can be described as the use of instrumentation in measuring a physical property of matter, and the relating of the data to chemical composition. Infrared analysis can be used for almost any type of sample as long as the material is composed of or contains molecules rather than pure elements. It is a nondestructive type of analysis (the sample can normally be recovered for other use), and is useful for microsamples [68]. Infrared spectroscopy is a technique based on the vibrations of the atoms of a molecule. An infrared spectrum is obtained by passing infrared radiation through a sample and determining what fraction of the incident radiation is absorbed at a particular energy. The energy at which any peak in an absorption spectrum appears corresponds to the frequency of a vibration of a part of the sample molecule [66].

The main goal of IR spectroscopic analysis is to determine the chemical functional groups in the sample. Different functional groups absorb characteristic frequencies of IR radiation. Using various sampling accessories allows IR spectrometers

to accept wide ranges of sample types such as gases, liquids, and solids. IR spectroscopy is important for compound identification [67]. One of the strengths of IR spectroscopy is its ability as an analytical technique to obtain spectra from a very wide range of materials. The instruments used are called infrared spectrophotometers, and the physical property measured is the ability of matter to absorb, transmit, or reflect infrared radiation. Traditionally, IR spectrometers have been used to analyze solids, liquids and gases by means of transmitting the infrared radiation directly through the sample [68].

Mid-infrared spectroscopy is an extremely reliable and well recognized fingerprinting method. Many substances can be characterized, identified and also quantized. The mid-infrared (MIR) region is divided into the group frequency region, 4000-1500  $\text{cm}^{-1}$ , and the fingerprint region, 1500-650  $\text{cm}^{-1}$ . In the group frequency region the principal absorption bands are assigned to vibration units consisting of only two atoms of a molecule, meaning that the units are more or less dependent on only the functional group that gives the absorption and not on the complete molecular structure. The group frequency region can be further subdivided and generalized as follows: the X—H stretching region (4000-2500  $\text{cm}^{-1}$ ), the triple-bond region (2500-2000  $\text{cm}^{-1}$ ), and the double-bond region (2000-1500  $\text{cm}^{-1}$ ). The major factors in the spectrum of the fingerprint region are single-bond stretching frequencies and bending vibrations of polyatomic systems that involve motions of bonds linking a substituent group to the remainder of the molecule. Multiplicity is too great for assured individual identification of the bands, but collectively the absorption bands aid in identifying the material [66], [69].

Attenuated total reflectance (ATR) spectroscopy utilizes the phenomenon of total internal reflection [66]. Total internal reflection occurs when light traveling in an optically dense medium (one having a high refractive index) impinges on an interface with a less dense medium [70]. Figure 3.10 is a scheme of a typical ATR cell. A beam of radiation entering a crystal will undergo total internal reflection when the angle of incidence at the interface between the sample and crystal is greater than the critical angle. The critical angle is a function of the refractive indices of the two surfaces. The beam penetrates a fraction of a wavelength beyond the reflecting surface and when a material that selectively absorbs radiation is in close contact with the reflecting surface, the beam loses energy at the wavelength where the material absorbs. The resultant attenuated radiation is measured and plotted as a function of wavelength by the spectrometer and gives rise to the absorption spectral characteristics of the sample [71].

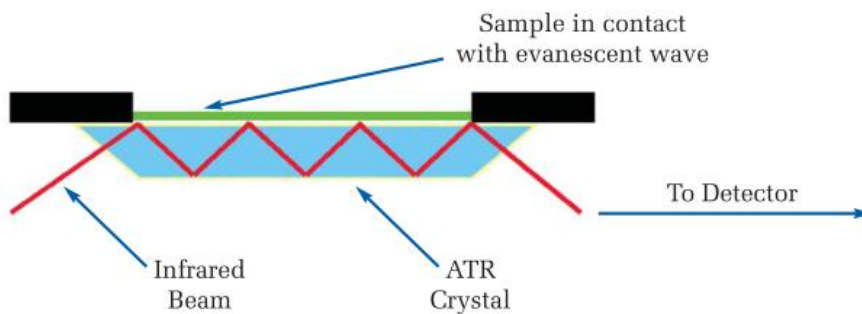


Figure 3.10: Schematic of an attenuated total reflectance system

The history of ATR, which belongs to the internal reflection spectroscopy methods, began more than two centuries ago. Newton observed that when a propagating wave of radiation undergoes total internal reflection at the interface between two media of different refractive indices, an evanescent field penetrates the interface into the

medium with the lower refractive index. The exploitation of this phenomenon for generating useful absorption spectra did not begin until the early 1960s, with the pioneering efforts of Harrick and Fahrenfort, followed by experimental work by Sharpe. Over the past thirty years, numerous applications of ATR have been reported and reviewed [70].

The depth of penetration in ATR spectroscopy is a function of the wavelength,  $\lambda$ , the refractive index of the crystal,  $n_2$ , and the angle of incident radiation,  $\theta$ . The depth of penetration,  $d_p$ , for a non-absorbing medium is given by the following:

$$d_p = \frac{\frac{\lambda}{n_1}}{\left\{ 2\pi \left[ \sin \theta - \left( \frac{n_1}{n_2} \right)^2 \right]^{\frac{1}{2}} \right\}} \quad (3.8)$$

where  $n_1$  is the refractive index of the sample. The crystals used in ATR cells are made from materials that have low solubility in water and are of a very high refractive index. Different designs of ATR cells allow both liquid and solid samples to be examined [72]. The materials most commonly used in ATR cells include, germanium, thallium bromoiodide (KRS-5), silicon, zinc selenide, and diamond. The physical and chemical properties of diamond place it among the best material for an ATR crystal. The hard scratch resistant properties make the diamond plate suitable for a wide range of application. It can withstand highly acidic and basic samples and does not react with strong oxidizing or complex agents. Diamond plated ATR crystals are useful in applications of both liquid and solid samples [73]. Table 3.1 summarizes the properties of the commonly used materials for ATR crystals.

Table 3.1: Physical properties of commonly used ATR crystals [66], [72], [73]

<b>Materials</b>	<b>Spectral range (cm<sup>-1</sup>)</b>	<b>Refractive Index</b>	<b>Depth of penetration (μm)</b>
<b>Diamond</b>	45,000-2,500 1,667-33	2.4	1.66
<b>Ge</b>	5,500	4	0.65
<b>KRS-5</b>	20,000-400	2.37	1.73
<b>Si</b>	8,300-1,500 360-70	2.37	1.73
<b>ZnSE</b>	20,000-650	2.4	1.66

An attenuated total reflection accessory operates by measuring the changes that occur in a totally internally reflected infrared beam when the beam comes in contact with a sample. An infrared beam is directed onto an optically dense crystal with a high refractive index at a certain angle. This internal reflectance creates an evanescent wave that extends beyond the surface of the crystal into the sample held in contact with the crystal. This evanescent wave protrudes only a few microns (0.5μm-5μm) beyond the crystal surface and into the sample. Consequently, there must be good contact between the sample and the crystal surface. In regions of the infrared spectrum where the sample absorbs energy, the evanescent wave will be attenuated or altered. The attenuated energy from each evanescent wave is passed back to the IR beam, which then exits the opposite end of the crystal and is passed to the detector in the IR spectrometer. The system then generates an infrared spectrum [71]. For the technique to be successful, the following two requirements must be met:

1. The sample must be in direct contact with the ATR crystal, because the evanescent wave only extends beyond the crystal 0.5μm-5μm

2. The refractive index of the crystal must be significantly greater than that of the sample or else internal reflectance will not occur. The light will be transmitted rather than internally reflected in the crystal

ATR surpasses other analytical methods because of its surface sensitivity. ATR spectroscopy can be distinguished from other techniques in two different ways: (1) the long-range frequency effect on sensitivity caused by the factor contained in the expression for the effective thickness,  $d_e$ , and (2) frequency shifts of the band maximum caused by dispersion of the refractive index spectra across the absorption band. Long-range frequency suggests that when normalizing ATR spectra, the normalization band should be relatively close to the band of interest because the depth of penetration is wavenumber-dependent. If such bands do overlap, one would expect band distortions and intensity changes. Attenuated total reflectance addresses the experimental issues most often encountered with transmission spectra [66], [70], [71]. Harrick and Graf *et al.* concluded that the frequency shifts, along with the sensitivity difference between high and low wavenumber regions and the spectral distortion at angles near the critical angle are the primary concerns in ATR quantitative analysis [70]. ATR-IR analysis is used extensively when determining surface changes of modified polymers [74–76]. Hu *et al.* used a simple-one step method to graft the surface of PDMS with different monomers. They used ATR-IR to observe the successful attachment of amino acids, acrylamide, hydroxyethyl acrylate and several other monomers to the PDMS surface [77].

### 3.7 Contact Angle Titration Curve

A contact angle titration curve was employed to further investigate the surface functionalization of the –OH, –COOH, and the fluoro-terminated –PFP functional groups on the modified polymer surface. The objective of the contact angle titration is to characterize the surface of PDMS when ionizable functional groups are present and to examine the surface ionization. This curve was based on contact angle measurements as a function of a 0.1M buffered solution prepared from pH 1 to pH 12. Homes-Farley *et al.* have previously shown that the contact angle of buffered drops of water is sensitive to the state of ionization of functional groups covalently bound at the surface of functionalized polyethylene. Low-density polyethylene films were oxidized with chromic acid solutions to produce a material containing carboxylic acid groups on the surface. The researchers used ATR-IR, contact angle measurements, and direct potentiometric titration to analyze the [PE-CO<sub>2</sub>H] surfaces. One of the relevant observations to this research is the relation of the measured contact angle of a small drop of aqueous solution at known pH to the extent of ionization of surface functional groups [78].

Young's equation, refer to equation (3.1), was used to relate the measured contact angle at known pH to the extent of ionization,  $\alpha_i$ , of surface carboxylic acid groups. With

$$\alpha_i = \frac{[\text{CO}_2^-]}{[\text{CO}_2^-] + [\text{CO}_2\text{H}]} \quad (3.9)$$

$$\alpha_i(\text{pH}) = \frac{\gamma_{\text{LS}}(\text{pH } 1) - \gamma_{\text{LS}}(\text{pH})}{\gamma_{\text{LS}}(\text{pH } 1) - \gamma_{\text{LS}}(\text{pH } 13)} \quad (3.10)$$

$$\alpha_i(\text{pH}) = \frac{\gamma_{\text{LS}}(\text{pH } 1) + \gamma_{\text{LV}} \cos \theta_{\text{pH}} - \gamma_{\text{SV}}}{\gamma_{\text{LS}}(\text{pH } 1) - \gamma_{\text{LS}}(\text{pH } 13)} \quad (3.11)$$

$$\alpha_i(\text{pH}) = \frac{\cos \theta_{\text{pH}} - \cos \theta_{\text{pH}1}}{\cos \theta_{\text{pH}12} - \cos \theta_{\text{pH}1}} \quad (3.12)$$

equation 3.9 relating the degree of ionization of the surface carboxylic acid groups to equation 3.10, which is the liquid/solid interfacial free energies at limiting values of pH for which the surface carboxylic groups are completely protonated (pH 1) or completely ionized (pH 12). Equation 3.10 assumes that the change in the liquid/solid interfacial free energy (with changes in pH as well) is dependent on the linear relationship between the number of carboxylic acid groups converted to carboxylate ions. Equations 3.11 and 3.12 are rearrangements that relate the extent of ionization to experimental values of the contact angle. Both equations assume that the liquid/solid interface is linearly related to the extent of ionization and that the solid/vapor and liquid/vapor interfaces are independent of pH [78].

Variation in the effective or apparent  $pK_a$ ,  $pK_a^{\text{eff}}$ , with relation to the extent of ionization is a useful alternative when determining the dependence of contact angle measurements on pH for surface functionalization. Equation 3.13 relates the extent of ionization at a particular value of pH to the effective  $pK_a$  of a simple monobasic acid. For a monobasic acid,  $pK_a^{\text{eff}}$  is independent of the extent of ionization. For a polybasic acid,  $pK_a^{\text{eff}}$  increases with  $\alpha_i$ , and reflects the decreasing acidity of the remaining COOH groups as COO<sup>-</sup> groups appear [78].

$$pK_a^{\text{eff}} = \text{pH} - \log\left(\frac{\alpha_i}{1-\alpha_i}\right) \quad (3.11)$$

## **CHAPTER FOUR**

### **EXPERIMENTAL**

#### 4.1 Chemicals, Reagents, and Sample Preparation

Sylgard® 184 silicone elastomer base and platinum based curing agent are products of Dow Corning Corporation, Midland, MI. ACS reagent grade acetic acid (glacial), 1-bromonaphthalene (96%), stabilized diiodomethane (99+%), ACS reagent grade formamide, methylene blue dye, and sodium chloride were obtained from Acros Organics (Geel, Belgium). A.C.S. certified monosodium phosphate, disodium phosphate, reagent grade ethylene glycol, and sodium hydroxide were obtained from Fisher Scientific (Waltham, MA). Crosslinking agent 1-ethyl-3-[3-dimethylaminopropyl] carbodiimide hydrochloride (EDC) was obtained from Thermo Scientific (Rockford, IL). Coupling reagent pentafluorophenol (99+%) was obtained from Acros Organics (Geel, Belgium) and Matrix Scientific (Columbia, SC). Sylgard® 184 elastomer base and platinum based curing agent was prepared in a 10:1 w/w ratio, combined in a disposable cup, and stirred five to six minutes until bubbles were distributed throughout the mixture indicating the two parts were mixed thoroughly. The PDMS was then placed into a petri dish, degassed in a vacuum chamber for ten to fifteen minutes, and either left overnight to cure or cured on a hot plate for approximately two hours at 65°C. The cured samples were cut out of the petri dish into pieces approximately 6 cm<sup>2</sup> in size.

## 4.2 Plasma Discharge

Native PDMS was treated with air-oxygen plasma to generate hydroxyl groups on the surface. An 115V PDC-32G plasma cleaner manufactured by Harrick Plasma, Ithaca, NY was used to create plasma. Figure 4.1 is a picture of the plasma cleaner used within the research. The plasma cleaner includes a 3" diameter x 6.5" length Pyrex chamber with a 2.75" x 6.5" quartz sample tray. The sample was placed in the plasma cleaner chamber and the vacuum pump was turned on to evacuate the excess air in the chamber. The plasma cleaner was then turned on and the RF level was turned to high. On a high setting, 720V DC, 25mA DC, and 18W are applied to the RF coil. Air-oxygen was bled into the chamber by slightly opening the 1/8" NPT 3-way valve and closing it back. Plasma is generated once a purplish glow is observed (see Figure 3.2). PDMS samples were exposed to plasma discharges for sixty seconds.



Figure 4.1: Harrick Plasma PDC-32G Plasma Cleaner

#### 4.3 NaOH Solution

A 1M sodium hydroxide (NaOH) solution was prepared from the readily available solid NaOH and deionized water. Native PDMS, approximately 6 cm<sup>2</sup> in size, was treated with a 1M solution of sodium hydroxide (NaOH). The PDMS sample was immersed in 10 mL of the NaOH solution and left in a covered petri dish to soak for twenty-four hours. Once twenty-four hours passed, the sample was removed from the petri dish, rinsed with ethanol, dried under a steady stream of nitrogen and observed using ATR-IR spectroscopy.

#### 4.4 Mercury Radiation Set-up

Sample irradiation was performed using a USHIO lamp manufactured by USHIO America Incorporated of Cypress, California. Samples were placed in a ~0.5L chamber under a continuous flow of ultra-high purity oxygen at a rate of 2.0 L/min. Figure 4.2 shows the set-up for irradiation. PDMS samples were placed facing the lamp with a distance of 5 mm between the top surface of the sample and the light source, and covered with a poly(vinyl chloride) cup. Before irradiation began, the chamber was purged for approximately fifteen minutes with the ultra-high purity oxygen which created an oxygen-rich environment. Nitrogen was delivered to the mercury lamp chamber to avoid oxidation of the bulb, and the lamp was turned on. The samples were exposed to 254 nm Hg radiation at a fluence of 13 mW/cm<sup>2</sup>. Individual samples were exposed for 30 minutes, 45 minutes, 60 minutes, 75 minutes, 90 minutes, and 120 minutes.



Figure 4.2: USHIO excimer lamp and irradiation set-up

#### 4.5 PFP Bond Formation

Fresh PDMS samples were irradiated at both 30 minutes and 75 minutes. After irradiation, the samples were immersed in cold ethanol, cold 50:50 acetic acid/water, cold acetone, and cold phosphate buffer solutions of PFP (0.2M) and EDC (0.1M). Each solution was 10 mL and the PDMS sample was allowed to soak for 24 hrs. Once removed from the solution, the samples were rinsed with ethanol, dried with a stream of nitrogen, and analyzed using both contact angle goniometry and ATR-IR spectroscopy.

#### 4.6 Contact Angle Measurements

Contact angle measurements were captured using a Rame' Hart goniometer, model 50-00/100-00, fitted with a Sony XCD-X700-1.05 camera. Figure 4.4 shows a photograph of the goniometer set-up. The sessile drop technique was used for contact angle measurements and Fire I software for image capture. A microsyringe was used to dispense deionized, ultra-filtered water with a specific conductance of less than  $2 \mu\Omega/\text{cm}$ . 40- $\mu\text{L}$  drops of test liquid were placed at six separate points on the polymer surface. All

measurements were evaluated using the DropSnake plug-in found in the National Institute of Health ImageJ software package. The DropSnake method unifies the global form of a drop and the locality of its contact angle. A snake is linked by elasticity constraints whose forces are of limited range. The snaked curve reveals contact angle while keeping trace of the global form of a drop. This method also allows for finding symmetry in the image which enhances detection of the drop's baseline and tilt angle [50], [79]. Figure 4.3 shows a representation of the contact angle goniometer used within this research.

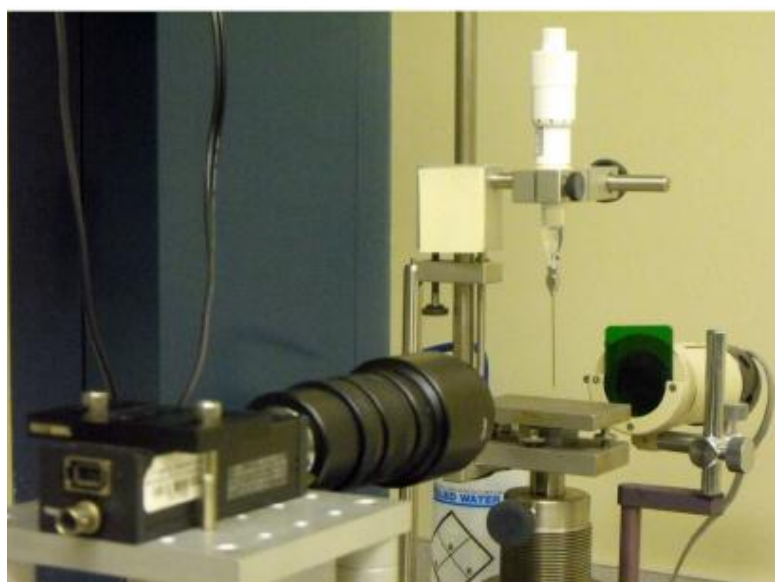


Figure 4.3 Rame' Hart Contact Angle Goniometer

#### 4.7 Absorbance Measurements

A spectrophotometer was used to determine the concentration of carboxylic groups present in the methylene blue dye solution used to stain the surface of the polymer. Figure 4.4 shows a picture of the 8452A Hewlett Packard Diode Array

spectrophotometer used. Diode array spectrophotometers are capable of acquiring complete UV-Vis absorbance spectra. A photodiode array has detectors that are all integrated on a single silicon chip. The HP8452A is a single beam instrument that has 512 detectors and uses a single deuterium discharge lamp for the full UV and visible range. Since the instrument is single beam, a reference scan is ran first to determine the intensity of the lamp at each wavelength,  $I_o(\lambda)$ , and then the sample scan is ran second. The absorbance is calculated from the ration of the two spectra:

$$A(\lambda) = \log \frac{I_o(\lambda)}{I(\lambda)} \quad (4.1)$$

where

$I(\lambda)$  is the intensity of the light that exists in the cell

The plot of  $A(\lambda)$  versus  $\lambda$  is the spectrum of the solution.



Figure 4.4: HP 8452A Diode Array Spectrophotometer

## 4.8 Infrared Spectroscopy

A Perkin Elmer Spectrum One Infrared Spectrometer equipped with a single bounce universal ATR accessory was used to evaluate the native and modified surface of PDMS containing  $\text{-OH}$ ,  $\text{-COOH}$ , and  $\text{-PFP}$  bonds. This instrument correlates bands found in the IR spectra to functional groups found within the molecule. The ATR-IR instrument can be seen in Figure 4.5. Infrared radiation absorbs the vibrational frequencies of molecules in a sample that are equal to its own frequency. The absorption of infrared radiation reveals this vibration and appears as peaks in a spectrum that plots absorbance versus wavenumber.



Figure 4.5: Perkin Elmer Spectrum One Infrared Spectrometer with ATR accessory

## **CHAPTER FIVE**

### **RESULTS AND DISCUSSION**

#### **5.1 Hydroxyl Groups**

Experimentation through plasma treatments and sodium hydroxide treatments show results that are complimentary to one another. After a piece of native PDMS is exposed to either treatment, hydroxyl groups are formed on the polymer surface. Each treatment presents a different modified surface, but both conclusively show that the newly formed hydroxyl groups rotate back into the bulk state of the polymer only minutes after exposure.

##### **5.1.1 Plasma Treatment**

Contact angle measurements were used to characterize the modified PDMS surface. The contact angle measurements were taken over a time period of six hours. The increments within each hour varied. In the first hour, each contact angle was taken in ten minute increments. During the second hour, the contact angle was taken in fifteen minute increments. The third hour was twenty minute increments. The fourth hour was thirty minute increments. Lastly, one contact angle was taken at each of the fifth and sixth hours. Native (untreated) PDMS is very hydrophobic and shows a contact angle of  $108 \pm$

4.0°. Immediately after exposure to the air-oxygen plasma, the modified PDMS surface turns hydrophilic and a contact angle of  $21.3 \pm 3.9^\circ$  is observed. The change in hydrophobicity is attributed to the formation of silanol groups of the surface [30].

#### 5.1.2 NaOH Treatment

Contact angle measurements were unaffected by the NaOH treatment. The contact angle is shown at  $96.6 \pm 2.0^\circ$  which is comparable to native PDMS. Hoek, Tho, and Arnold studied the effects of NaOH on electroosmotic flow in microfluidic devices. In their research, they used contact angles and ATR-FTIR as means of analysis. Similarly, they observed a hydrophobic contact angle from the NaOH treated surface. The trio theorized that the inability of NaOH to form hydrophilic surfaces is a further indication that different ionisable surface groups are formed on the NaOH modified surface in contrast to the surface of PDMS treated with plasma. They concluded that the effect of NaOH leads to the formation of alcohol groups. However, the C—OH absorption band seen around the  $1000\text{--}1200\text{ cm}^{-1}$  region is undetectable in ATR-IR due to overlap with the strong Si—O—Si stretching absorption band in the same region [31].

After treating the polymer, the newly formed hydroxyl groups were placed on the diamond plated surface of the ATR-IR and exposed to ambient air. The ATR-IR analysis of the NaOH treated PDMS surfaces was studied to decipher the functional groups formed on the modified polymer surface. Figure 5.1 shows the infrared spectra of the peaks seen on the treated PDMS surface. Table 5.1 gives an assignment of the major peaks seen in the IR spectra. Comparable to the results seen by Hoek, Tho, and Arnold, the ATR-IR analysis shows an increase in the —OH stretching region and a decrease in

the intensities of the Si—O—Si and Si—CH<sub>3</sub> absorption bands. This indicates breaking of the polymer chain at the Si—O or Si—C bonds took place [31].

Table 5.1: Assignment of spectral peaks with –OH presence [80].

Wavenumber (cm <sup>-1</sup> )	Description of Peaks
<b>3015-3625</b>	-OH stretch
<b>2963</b>	Asymmetric –CH <sub>3</sub> stretch in ≡Si-CH <sub>3</sub>
<b>1258</b>	Symmetric –CH <sub>3</sub> stretch in ≡Si-CH <sub>3</sub>
<b>1010</b>	-(CH <sub>2</sub> )- vibration in ≡Si-(CH <sub>2</sub> ) <sub>2</sub> -Si≡
<b>843</b>	≡Si-O stretching in ≡Si-OH
<b>788</b>	-CH <sub>3</sub> rocking ; ≡Si-C≡ stretching in ≡Si-CH <sub>3</sub>

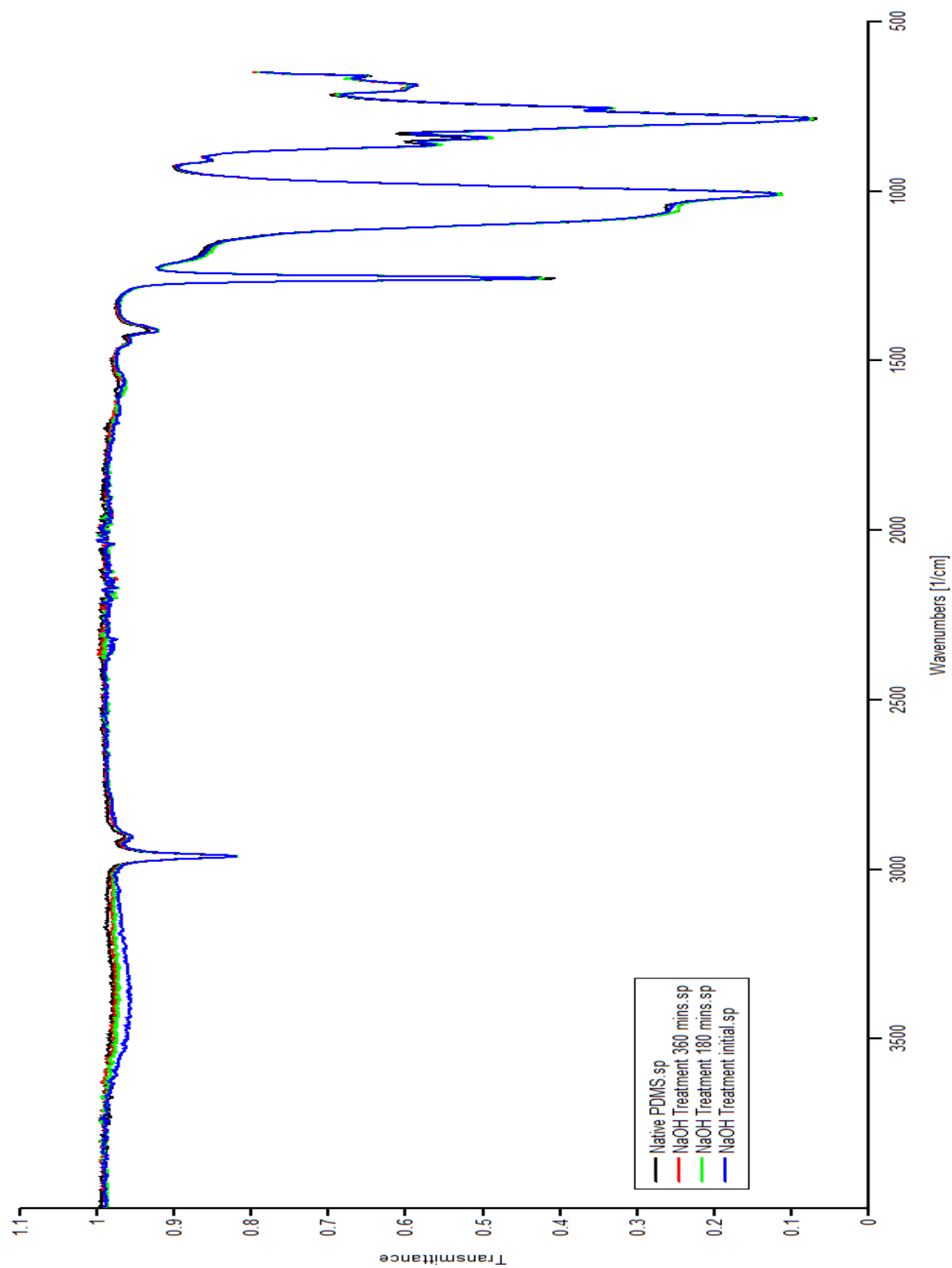


**Figure 5.1: ATR-IR spectra of PDMS treated with NaOH.**

### 5.1.3 Surface Tension

Zisman's method for obtaining the surface tension of a material is shown below in Figure 5.2. The value of  $\gamma_c$ , the critical surface tension, on the surface of plasma treated PDMS was obtained after a series of test liquids with progressively smaller surface tension was plotted against the cosine value of the corresponding contact angles. The test liquids included water, 1-bromonaphthalene, diiodomethane, ethylene glycol, and formamide. At the intersection of  $\cos \theta = 1$ ,  $\gamma_c \approx 45$  mN/m.

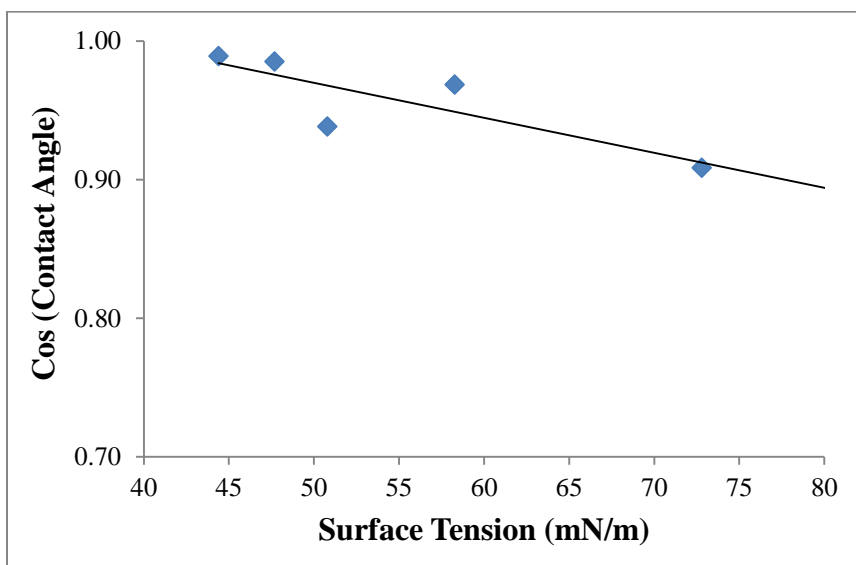


Figure 5.2: Zisman Plot of plasma treated PDMS

### 5.1.4 Recovery of Hydroxyl Group

As previously mentioned, the (-OH) modified surface is not a stable hydrophilic surface. Upon exposure to ambient air, the bond recedes and rotates back into the bulk polymer. Results show that within minutes of the plasma treatment, the bond begins to rotate back into the polymer bulk. After only ten minutes, the contact angle increases to

65°. Within six hours, the contact angle reverts to 92° which is comparable to native PDMS. Figure 5.3 representative contact angle observations for the air-oxygen plasma treatment. Each drop image represents a time increment during six hour time span.

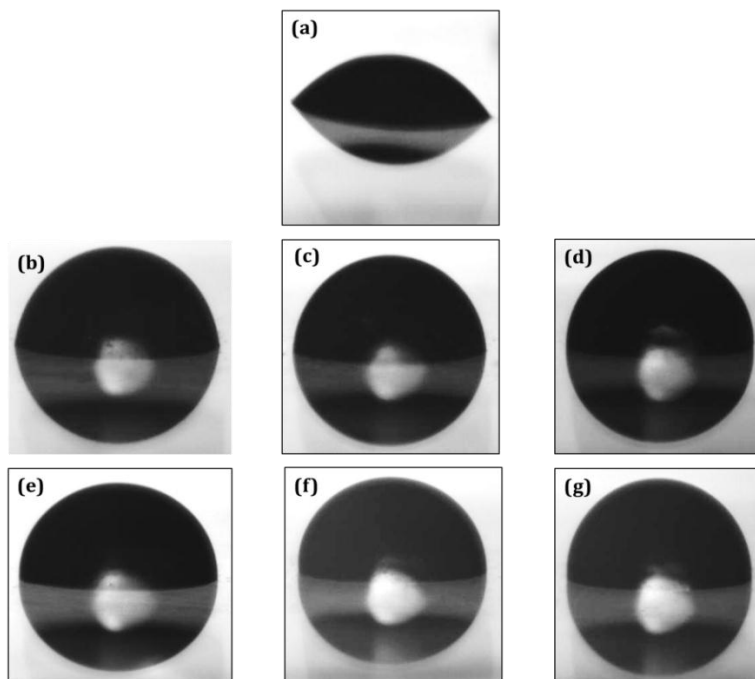


Figure 5.3: Contact angle test drops on Air-oxygen plasma treated PDMS at (a) initial, (b) after one hour, (c) after two hours, (d) after three hours, (e) after four hours, (f) after five hours, and (g) after six hours.

Figure 5.4 shows the contact angle as a function of elapsed recovery time after air-oxygen plasma exposure. As previously mentioned it is observed that the modified surface becomes hydrophilic but loses this property after a short period of time. Recent studies suggest that this rotation of the bond back into the bulk is due to passive transport of low-molar-mass PDMS species from the bulk to the surface and possibly a reorientation of the polar species. However, the polymer never fully regains its initial hydrophobicity. The saturation limit (difference in native PDMS contact angle and the

final contact angle observed after surface modification) is approximately 15° lower than the measured contact angle of native PDMS. This can be attributed to the formation of a silica-like layer on the modified surface [30].

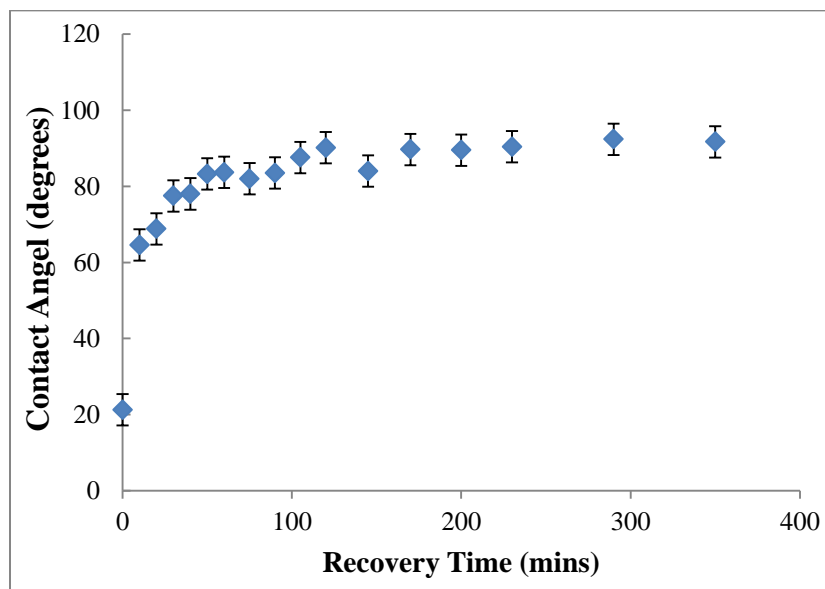


Figure 5.4: Contact angle as a function of elapsed recovery time after exposure to air oxygen plasma.

An increase in the presence of  $\text{-OH}$  groups on the polymer surface is seen in the region of  $3015\text{-}3625\text{ cm}^{-1}$ . Further analysis of the area under the curve within this region displays the rotation of the  $\text{-OH}$  group back into the polymer bulk and can be seen in Figure 5.5. The same time increments from the contact angle analysis were used to monitor the rotation of the hydroxyl bond back into the polymer bulk. Similar to the plasma treatment, the presence of hydroxyl groups begins to recede back in the bulk state of the polymer. However, this rotation is seen after two to three hours as opposed to ten minutes. This difference in rotation is explained by the absence of silanol on the NaOH treated surface [31].

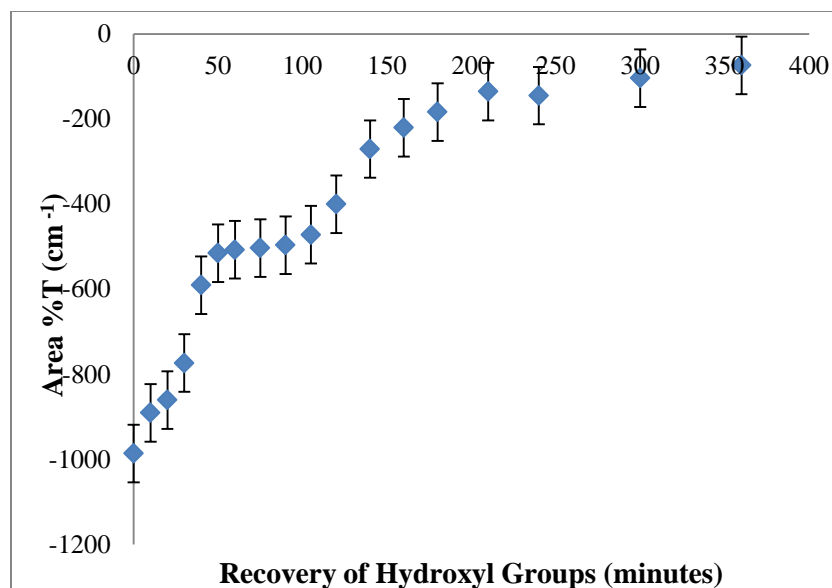


Figure 5.5: Observation of hydroxyl group rotation by area under the curve analysis of IR spectra taken during NaOH ambient air experiment

Chen and Linder, researchers at the University of Memphis, studied the stability of radio-frequency plasma treated PDMS surfaces [29]. They used contact angles and FTIR-ATR to analyze the surface of the plasma treated polymer. They found analogous results in the loss of hydrophilicity as well. They looked at the material properties of PDMS for further explanation of this phenomenon. PDMS is an amorphous elastomer with a glass transition temperature around  $-130^{\circ}\text{C}$ . At room temperature, the polymer terminals, loops, and segments have some level of freedom for movement. Following a physical or chemical change, the elastomers move to a new equilibrium. The change of the hydrophilicity of PDMS after the plasma treatment is considered a relaxation process. Throughout this process, the hydrophilic groups generated on the PDMS surface and the siloxane chains orient toward the PDMS bulk, which is a more hydrophilic environment. The rate of this process is influenced by the difference in the dielectric constants of PDMS and air. A dielectric constant is the ratio of the [permittivity](#) of a substance to the

permittivity of free space. PDMS has a dielectric constant of 2.65 and ambient air has a dielectric constant of 1.00. The team found that when the PDMS specimens are exposed to ambient air, the difference seen in the dielectric constants aids in speeding up the relaxation process [29].

## 5.2 Carboxylic Groups

The results obtained from the PDMS surface modified with carboxylic acid groups are very comparable to the results obtained by Padma Dharmarajan. Again, a native piece of PDMS is modified and the newly formed surface is characterized by contact angle measurements, UV/Vis spectrometry, and ATR-IR spectroscopy.

### 5.2.1 Contact Angle Measurements

PDMS pieces were exposed to 245nm Hg radiation at varying irradiation times. The different irradiation times were 30 minutes, 45 minutes, 60 minutes, 75 minutes, 90 minutes, and a final increment of 120 minutes. Contact angle measurements show that as the exposure time increases, the contact angle gradually decreases. This decrease in contact angle indicates that the hydrophilicity and wettability of the modified PDMS surface increases. Native PDMS is extremely hydrophobic in character and the contact angle is observed at  $109.4 \pm 3.2^\circ$ . Analysis of the contact angle measurements show that the contact angle progressively decreases until 75 minutes of exposure. Beyond this point, an increase in the contact angle is seen at 90 minutes and 120 minutes. The lowest contact angle was detected at  $65.2 \pm 5.1^\circ$  and occurred when the surface was irradiated for 75 minutes. Irradiation of PDMS led to a surface that became glassy and smooth,

forming a silica like layer. Increased irradiation exposure after 75 minutes led to a tough, brittle like surface where cracking ensued. Previous research theorized that the PDMS surface becomes strained by increased UV exposure and the cracks are a result of a relaxation of the polymer surface [5]. The migration of low molar mass PDMS from the bulk to the surface through these cracks resulted in the slight increase in the observed contact angle [33]. Figure 5.6 represents the observed contact angle with respect to increased irradiation times. Figure 5.7 shows the images of the contact angle of the modified PDMS surface.

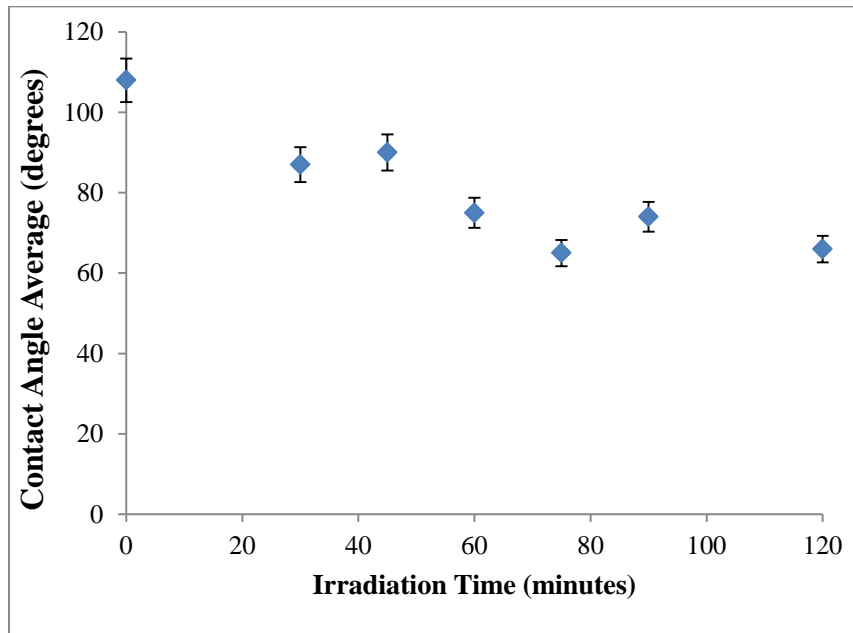


Figure 5.6: Contact angle versus increased irradiation time.

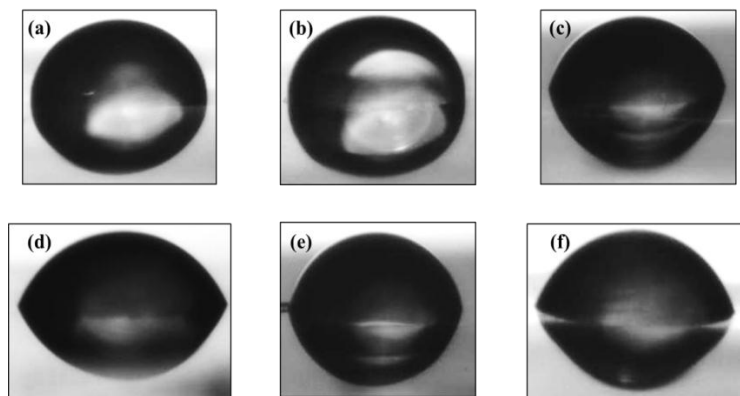
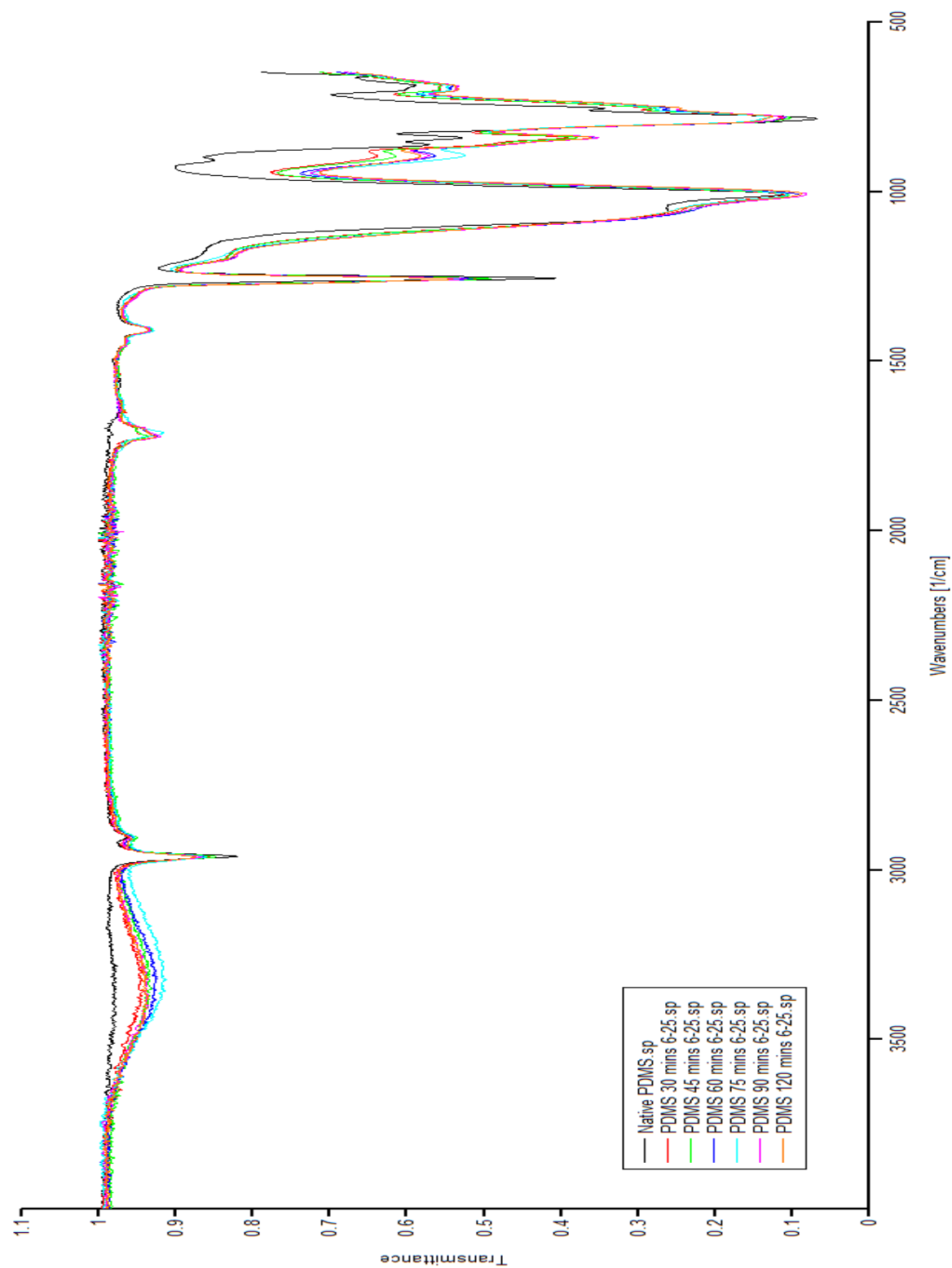


Figure 5.7: Contact angle drops on PDMS after COOH formation on (a) 30 minutes, (b) 45 minutes, (c) 60 minutes, (d) 75 minutes, (e) 90 minutes, and (f) 120 minutes irradiated samples.

### 5.2.2 ATR-IR spectra Results

Infrared spectra of the modified PDMS samples were studied and reviewed to determine the functional groups on the surface. The infrared spectra show similar trends to that of the contact angle. An increased presence of carboxylic groups is seen until the 75 minutes irradiation in the  $-OH$  region ranging from  $3015-3690\text{ cm}^{-1}$ . After this time, the presence of the carboxylic group in that region begins to diminish. At 75 minutes of irradiation time, maximum band intensities are seen in both regions. The higher shift in the carbonyl peak indicates that an inorganic silica like layer has begun to form.

Existence of the carboxylic group is further indicated by the presence of the small carbonyl band seen at  $1714\text{ cm}^{-1}$ . Both the hydroxyl stretch and the carbonyl stretch are absent in the IR spectra of native PDMS. Figure 5.8 shows the spectra gathered from PDMS samples after UV exposure in the six time increments ranging from 30 minutes to 120 minutes. Table 5.2 gives the assignment of the functional groups found in the spectra



**Figure 5.8: ATR-IR spectra of PDMS after UV exposure to form -COOH groups.**

Table 5.2: Assignment of spectral peaks with –COOH presence [80]

Wavenumber (cm <sup>-1</sup> )	Description of Peaks
<b>3015-3690</b>	-OH stretch in –COOH
<b>2964</b>	Asymmetric –CH <sub>3</sub> stretch in ≡Si-CH <sub>3</sub>
<b>1714</b>	C=O stretch in –COOH
<b>1259</b>	Symmetric –CH <sub>3</sub> stretch in ≡Si-CH <sub>3</sub>
<b>1012</b>	-(CH <sub>2</sub> )- vibration in ≡Si-(CH <sub>2</sub> ) <sub>2</sub> -Si≡
<b>843</b>	≡Si-O stretching in ≡Si-OH
<b>784</b>	-CH <sub>3</sub> rocking ; ≡Si-C≡ stretching in ≡Si-CH <sub>3</sub>

### 5.2.3 UV-Vis Experimentation

In order to determine the number of carboxylic acid groups formed on the surface of the irradiated PDMS, a staining dye, methylene blue was used. Methylene blue attaches only to the carboxylic groups that are formed on the PDMS surface. From this, it is concluded that a surface with a higher absorbance value would contain a higher concentration of carboxylic groups on the surface. Figure 5.9 shows the absorbance values obtained versus the irradiation time. It is seen that at 75 minutes of exposure, the absorbance is the highest. The graph also shows that the absorbance steadily increases until 75 minutes and at 90 minutes and 120 minutes the absorbance decreases abruptly. This indicates that the maximum concentration of carboxylic groups is reached at 75 minutes of exposure time. The absorbance values of irradiated PDMS after a methylene blue experiment show an inverse proportional relationship to irradiated PDMS.

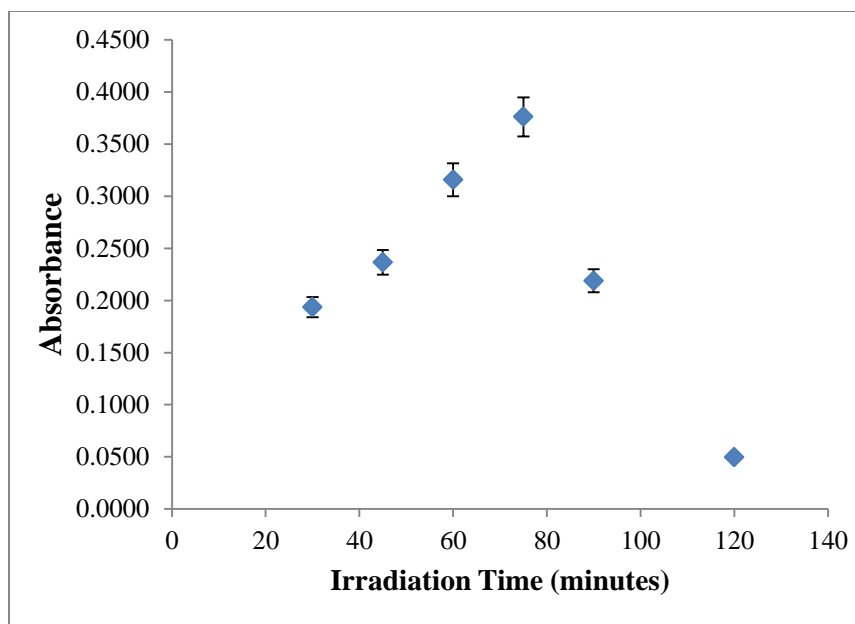


Figure 5.9: Difference in absorbance of PDMS samples stained with methylene blue with respect to exposure time

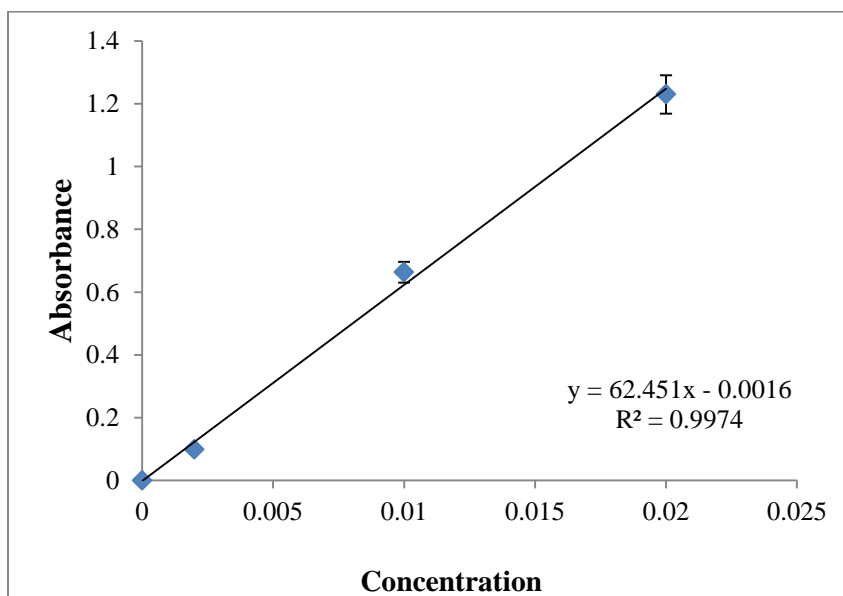


Figure 5.10: Calibration graph used to determine concentration of carboxylic groups

Figure 5.10 is a graph of the calibration curve that was used to determine the concentration of the carboxylic groups on the modified PDMS surfaces. Similar to the research of Padma Dharmarajan, a ratio of 1:1 was assumed for the concentration of the methylene blue dye to the concentration of carboxylic acid groups. The surface area of PDMS was used to then convert to the exact number of molecules of carboxylic groups per unit area on the sample surface. Figure 5.11 is a graphical representation of the amount of carboxylic groups found of the surface at varying irradiation times. The experimentation with methylene blue showed that the number of carboxylic groups on the surface is greatest at 75 minutes of exposure. At this time, there are approximately  $2.42 \times 10^{15}$  molecules/cm<sup>2</sup>. Dharmarajan reported that she found the concentration to be  $2.5 \times 10^{16}$  molecules/cm<sup>2</sup>. She compared this value to that found by Homes-Farley et al. This group of researchers studied the behavior of carboxylic groups covalently attached to the surface of polyethylene. Through experimentation, they found and reported that the surface density of carboxylic groups was  $1.6 \times 10^{13}$  molecules/cm<sup>2</sup> [33]. Figure 5.12 shows the solutions used to measure the absorbance, the color of the solution is an indication of how many carboxylic groups are present on the modified polymer surface.

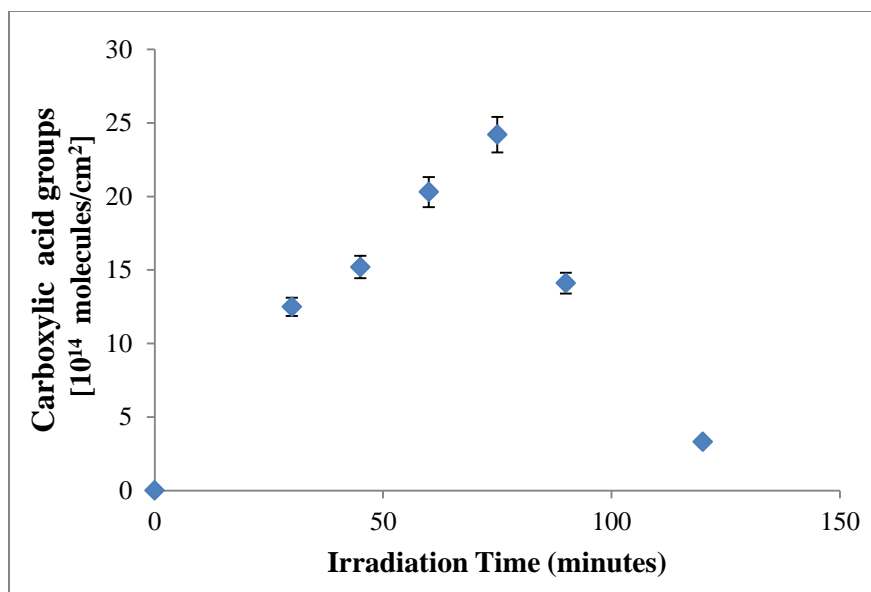


Figure 5.11: Number of carboxylic groups per cm<sup>2</sup> on the surface of irradiated PDMS as a function of exposure time.

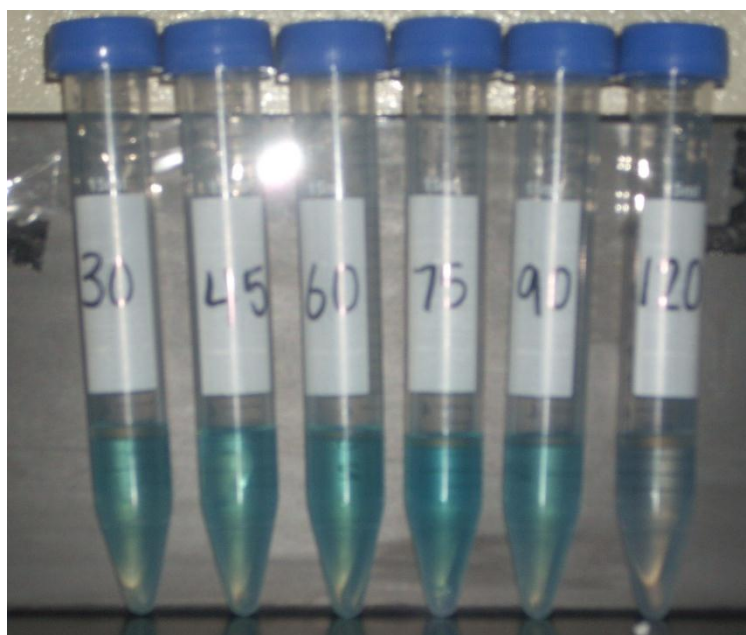


Figure 5.12: Methylene blue experiment used to measure absorbance

#### 5.2.4 Surface Tension of Irradiated PDMS

Figure 5.13 shows the different contact angles observed when five different test liquids are placed on the surface of irradiated PDMS at varying time intervals. The test liquids used include water, 1-bromonaphthalene, diiodomethane, ethylene glycol, and formamide. At 75 minutes, each test liquid exhibits its lowest contact angle value on the surface of the irradiated PDMS. These low contact angle values denote that PDMS irradiated for 75 minutes has a higher surface energy and good wettability characteristics. Figure 5.14 gives the Zisman plots of each test liquid. The results show that at 75 minutes of irradiation the surface energy is the highest. The critical surface tension of the five test liquids was calculated using Young's equation (equation 3.1) and,  $\gamma_c \approx 45$  mN/m.

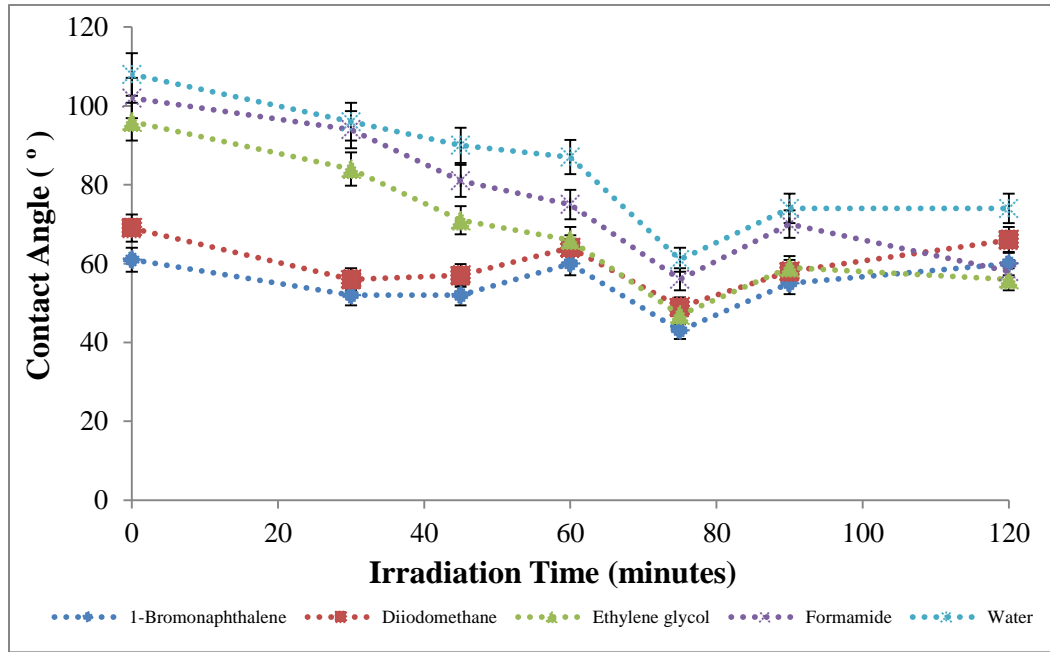


Figure 5.13: Contact angle variations of test liquids on PDMS surfaces of varying irradiation times.

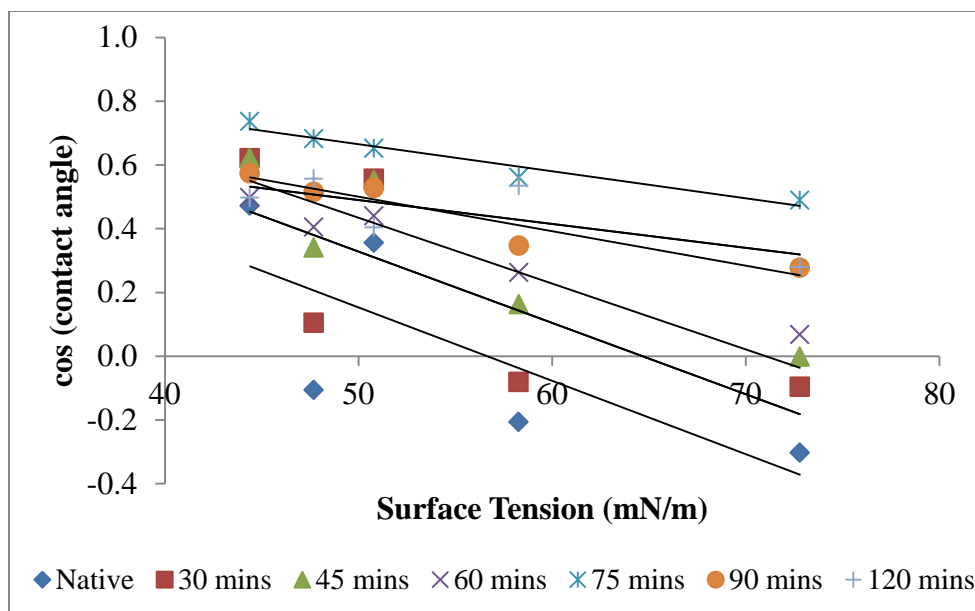


Figure 5.14: Zisman plots of irradiated PDMS

### 5.2.5 Recovery of Carboxylic Groups

Similar to the plasma oxidized surface that creates hydroxyl groups, the carboxylic group formed after UV exposure rotates back into the polymer bulk. As seen previously, plasma oxidized surfaces rotate back rapidly after being exposed to ambient air. For a method of comparison, the rotation of carboxylic groups back into the polymer bulk was monitored as well. Figure 5.15 represents the recovery of samples irradiated at both 30 minutes and 75 minutes. The samples were exposed to air over a ten day period and the average contact angle from each day was recorded. Initially after UV exposure, the surface loses some of its hydrophobicity with the contact angles seen at  $89.5 \pm 3.8^\circ$  and at  $65.3 \pm 4.1^\circ$  for 30 and 75 minutes respectively. At 30 minutes, after six days the contact angle increases to  $99.2 \pm 3.8^\circ$  and plateaus from days 7 to 10. At 75 minutes, the contact angle increases gradually each day and begins to plateau at day nine reaching a maximum of  $92.6 \pm 2.3^\circ$ .

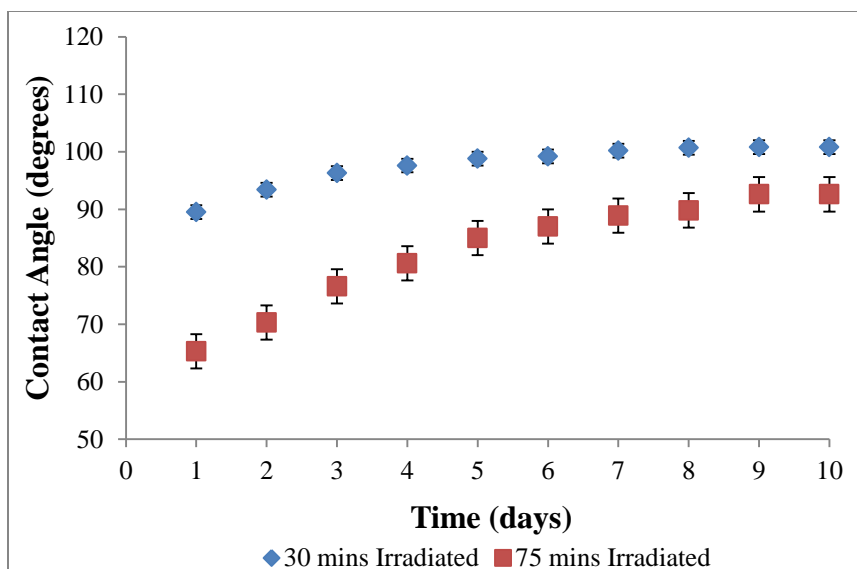


Figure 5.15: Rotation of carboxylic groups back into the PDMS bulk

The results and data found through experimentation agree with the results and data found by Dharmarajan and Homes-Farley *et al.* [33], [78]. The increased contact angle, the increased presence of the  $\text{--OH}$  stretch of  $\text{COOH}$  in the infrared spectra, and the high absorbance value in the UV-Vis spectrum visibly show that at 75 minutes the concentration of carboxylic groups on the UV modified PDMS surface is at its maximum. The trends seen in the above graphs and figures are very comparable to those seen previously. Beyond 75 minutes of UV exposure, the polymer backbone degrades. This can be attributed to the increased contact angle seen after 75 minutes and the decay in band intensities in the infrared spectra. PDMS surfaces that are exposed to irradiation longer than 75 minutes began to retreat back to the hydrophobic nature of the native polymer. The cracks that occur after the 75 minute mark facilitates the migration of low molecular weight PDMS from the bulk to the surface. This is the primary cause of the recovery of hydrophobicity.

### 5.3 Fluoro-Terminated Groups

For the purpose of this research, PFP was linked to the surface of UV modified PDMS. PFP has a higher molecular weight than both hydroxyl and carboxylic groups. We hypothesized that the larger molecular weight of PFP should sustain the functional group formed. Contact angle measurements, ATR-IR spectra, and a contact angle titration curve were employed to characterize the surface of PDMS with PFP.

#### 5.3.1 Contact Angle Measurements

Contact angle measurements for a 75 minute irradiated PDMS-PFP sample exhibited the most change. A more hydrophobic contact angle is seen. Compared to an irradiated PDMS sample ( $CA=65.2 \pm 5.1^\circ$ ), the observed contact angle of PFP modified PDMS in each respective solution is  $10\text{-}30^\circ$  higher. Perhaps this change in the contact angle is an indication that PFP successfully attached to the UV modified polymer surface. Alternatively, the change in contact angle can be attributed to a physio-adsorption of the PFP to the surface. In an acetic acid-water solution, the contact angle is observed at  $92.8 \pm 2.4^\circ$ . For an acetone solution, the contact angle is detected at  $74.1 \pm 4.6^\circ$ . The ethanol solution has a contact angle of  $75.9 \pm 2.7^\circ$ . In a PBS solution, the contact angle is seen at  $86.5 \pm 2.0^\circ$ . The 30 minutes PDMS-PFP sample for all solutions show similar results to irradiated PDMS and no significant change in contact angle was seen. For all solutions, the contact angle was observed between  $85^\circ - 90^\circ$  with an average standard deviation of  $\pm 3.2$ . Table 5.3 represents the contact angle measurements of both the 30 minute and 75 minute UV modified PDMS-PFP samples. Figure 5.16 shows a pictorial representation of the contact angles observed at 75 minutes.

Table 5.3: Contact angle measurements of native and irradiated PDMS samples after immersion in PFP solutions

<b>Solutions</b> (0.2M PFP, 0.1M EDC)	<b>Contact Angle Measurements</b>		
	<b>Native</b>	<b>30 min Irradiated</b>	<b>75 min Irradiated</b>
<b>Acetic acid-water</b>	103.9 ± 2.3°	94.3 ± 1.7°	92.8 ± 2.4°
<b>Acetone</b>	103.9 ± 2.9°	90.3 ± 5.1°	74.1 ± 4.6°
<b>Ethanol</b>	103.9 ± 2.4°	98.8 ± 2.4°	75.9 ± 2.7°
<b>PBS</b>	105.8 ± 2.2°	85.5 ± 3.6°	86.5 ± 2.0°

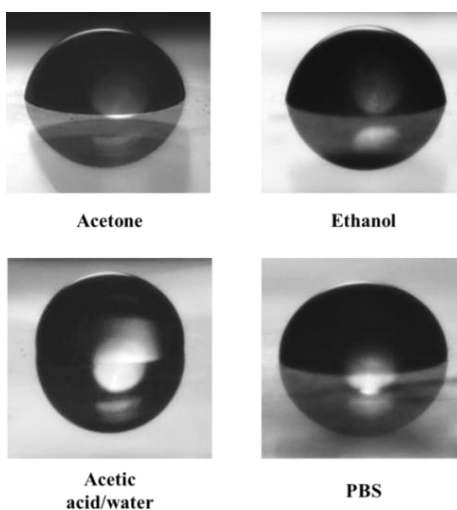


Figure 5.16: Contact angle droplets for PDMS-PFP in varying solutions

### 5.3.2 ATR-IR spectra Analysis

An infrared spectrum of pentafluorophenol was analyzed and studied to determine the major peaks that should be observed when PFP is placed in a solution. Figure 5.17 shows an IR spectrum of PFP. One of the most prominent ways to detect PFP in an IR spectrum is by the presence of the carbon-fluorine bond. The carbon-fluorine bond is the strongest bond in organic chemistry. The bond strength increases with the addition of

more fluorine's. For this reason carbon-fluorine bond stretching appears as a strong peak between 1000 and 1400  $\text{cm}^{-1}$ . In the IR spectrum of PFP, this bond can be seen at 1312  $\text{cm}^{-1}$  as a triple peak. Table 5.3 gives the peaks found in the pentafluorophenol compound.

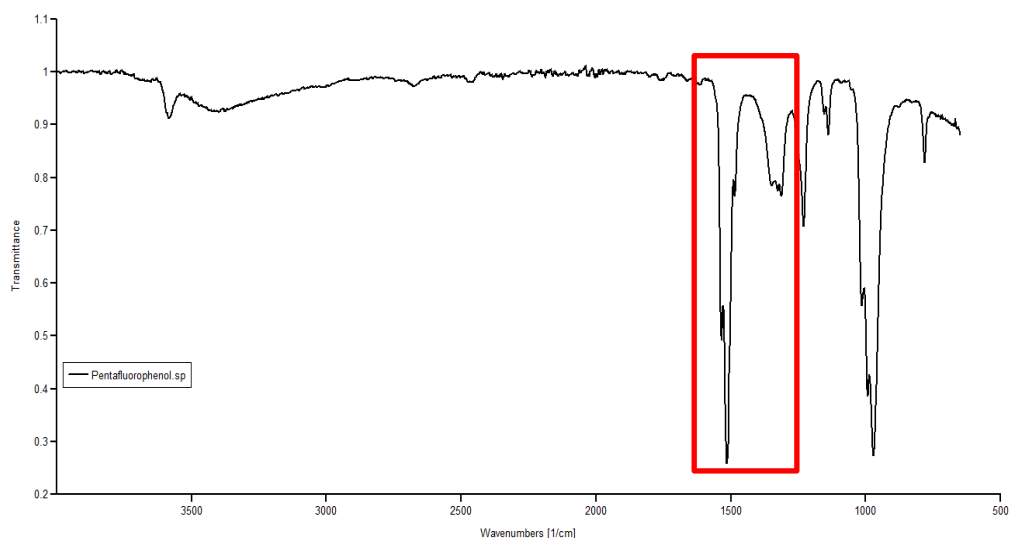


Figure 5.17: Pentafluorophenol IR spectrum

Table 5.4: Spectral assignment of Pentafluorophenol IR spectrum

Wavenumber ( $\text{cm}^{-1}$ )	Description of Peaks
<b>3536-3024</b>	-OH stretch
<b>3584</b>	Intramolecular hydrogen bonding
<b>1514</b>	Ring stretch
<b>1312</b>	C-F stretch
<b>1138, 1014, 971, 871, 781, 737, 722</b>	Ring breathing

The ATR-IR spectra of various solutions containing PFP linked to PDMS by EDC were recorded. Multiple samples were irradiated at both 30 minutes and 75 minutes,

soaked in 10mL acetic acid/water, acetone, ethanol, and PBS solutions with PFP (0.2M) and EDC (0.1M) for twenty-four hours, rinsed in ethanol, and dried under a steady stream of nitrogen. The prominent C-F band ( $1000\text{--}1400\text{ cm}^{-1}$ ) observed in PFP could not be seen. However, there are several other factors that indicate that PFP is present on the carbonyl surface for both 30 minute and 75 minute modified samples. The carbonyl peak formed when PDMS is irradiated significantly decreases in both the ethanol and PBS solutions. The neighboring double band observed in the ethanol solution is attributed to  $\text{CH}_3$  and  $\text{CH}_2$  bending. The carbonyl peak does not decrease in the acetone,  $[(\text{CH}_3)_2\text{CO}]$ , due to the carbonyl bond found in the compound. Dharmarajan found that 50:50 acetic acid-water solution assists in stabilizing the carboxylic acid group on the surface of PDMS, and this explains why the carboxyl group band is still found in the spectrum of the acetic acid solution [33]. The proposed reaction for the coupling of PFP to the surface of PDMS (see Scheme 5) shows the formation of an ester as the final product. The IR spectra of the modified PDMS samples do not support the formation of an ester (seen at  $1755\text{--}1650\text{ cm}^{-1}$ , C=O stretch, and  $1300\text{--}1000\text{ cm}^{-1}$ , C—O stretch). The missing ester stretches can be attributed to the strong carbonyl peaks and to the strong PDMS backbone stretches seen in the respective spectra. Infrared spectra of irradiated PDMS, acetic acid-water/PFP, acetone/PFP, ethanol/PFP, and PBS/PFP solutions at 30 minutes and 75 minutes, respectively, are shown in Figures 5.18 and 5.19. The inset seen in each figure is an enlarged picture of the carboxyl and ring stretching regions. The ring stretching region observed at  $1514\text{--}1524\text{ cm}^{-1}$  is an indication that PFP is present on the irradiated PDMS surface. IR spectra of 30 minute and 75 minute irradiated only PDMS does not contain this stretch. This is due to the fact that UV modified PDMS does not form ring structures.

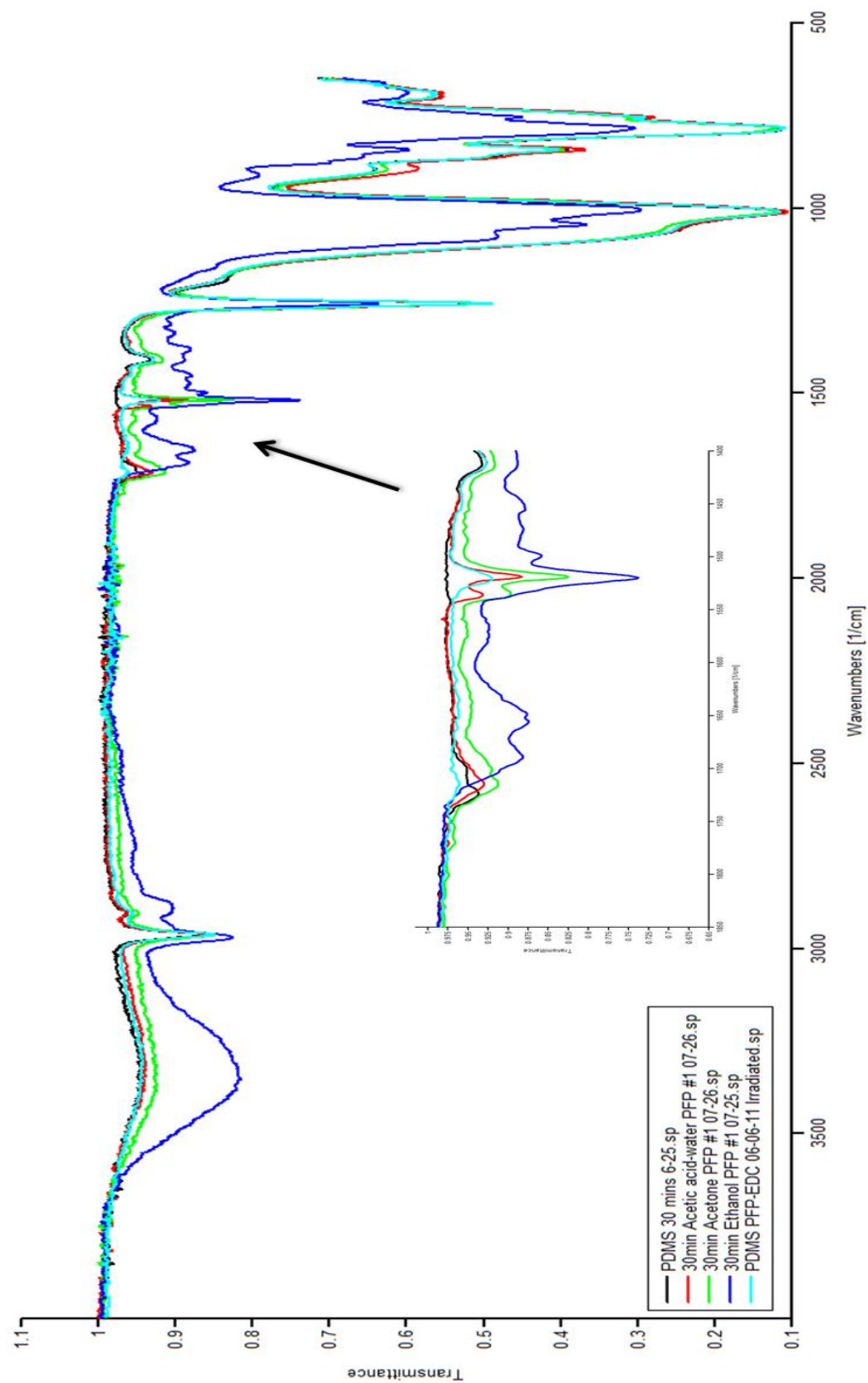


Figure 5.18: 30 minutes irradiated samples in varying solutions containing PFP.

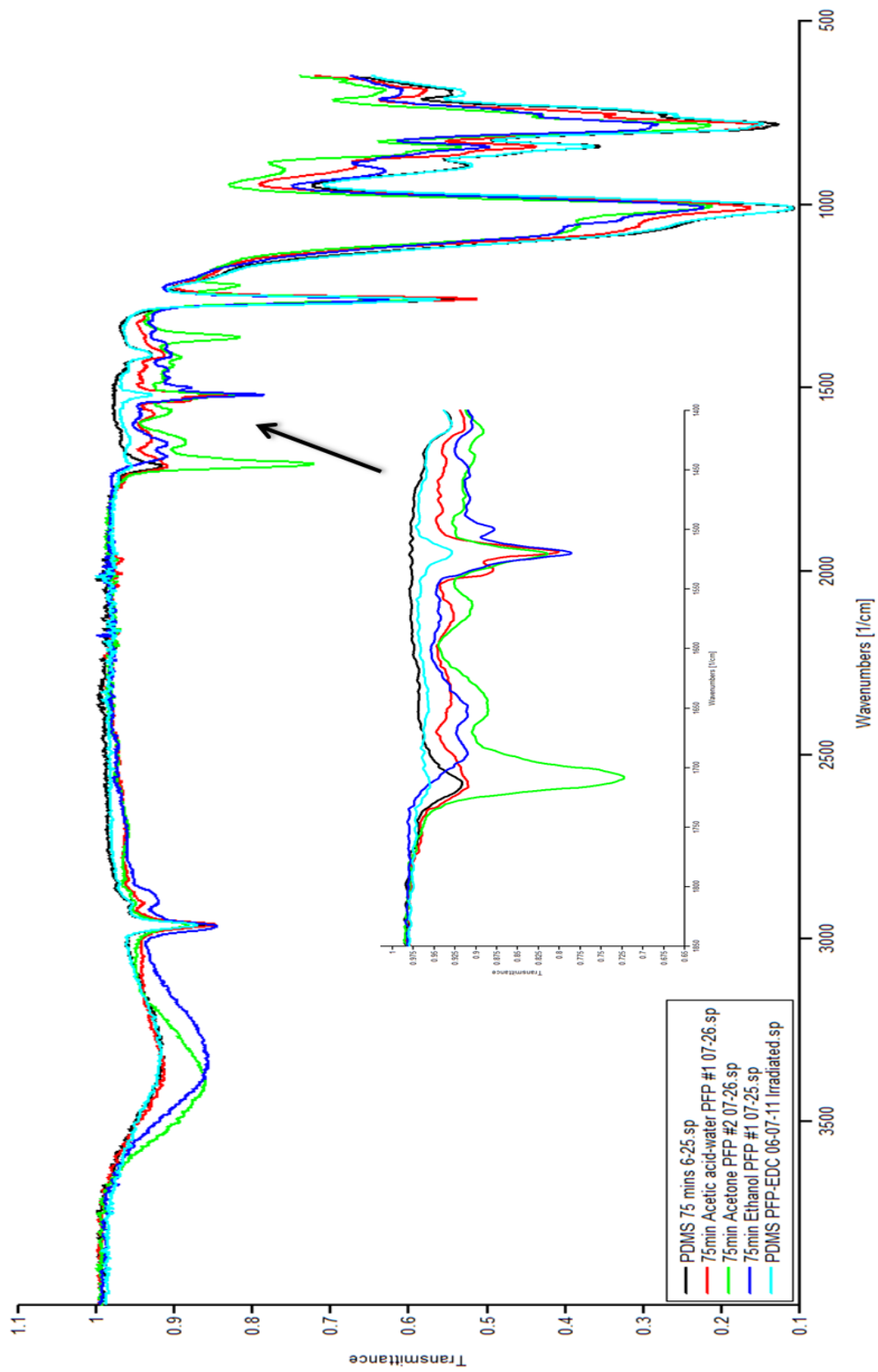


Figure 5.19: 75 minutes irradiated samples in varying solutions containing PFP.

### 5.3.3 UV-Vis Methylene Blue Experiment

In order to quantify the presence of pentafluorophenol on the PDMS surface, an experiment similar to the methylene blue experiment for carboxylic groups was performed. PDMS samples, 1.2 cm in diameter, were irradiated at six various time increments ranging from 30 minutes to 120 minutes. Following irradiation, the samples were each placed in 10 mL of a solution of 50:50 acetic acid/water, EDC (0.1 M), and PFP (0.2 M). Each sample remained in the solution for twenty-four hours. After being removed from the solution the samples were rinsed with DI water and placed in a conical tube that contained 3 mL of a basic solution of methylene blue (0.5mM, pH 10) for six hours. Finally, the samples were removed from the methylene blue, rinsed with DI water to remove the loosely bound methylene blue, immersed in 50:50 acetic-acid and water solution for twenty-four hours, and analyzed in the spectrophotometer.

Figure 5.20 is a graph of the data obtained from the methylene blue treatment performed. As mentioned previously, methylene blue only attaches to carboxylic acids present on the modified surface. From the graph, it can be seen that the concentration of carboxylic acids on the surface of the PFP modified PDMS is significantly less than regular irradiated PDMS. Quantitatively, PDMS that has only been irradiated shows the highest concentration at 75 minutes and is approximately  $2.5 \times 10^{15}$  molecules/cm<sup>2</sup>. At the same irradiation time, PDMS that has also been soaked in the PFP solution only shows a concentration of  $2.5 \times 10^{14}$  molecules/cm<sup>2</sup>. These results indicate that PFP is present on the surface of UV-modified PDMS surface. Figure 5.21 shows a pictorial representation of the solutions used to measure the absorbance.

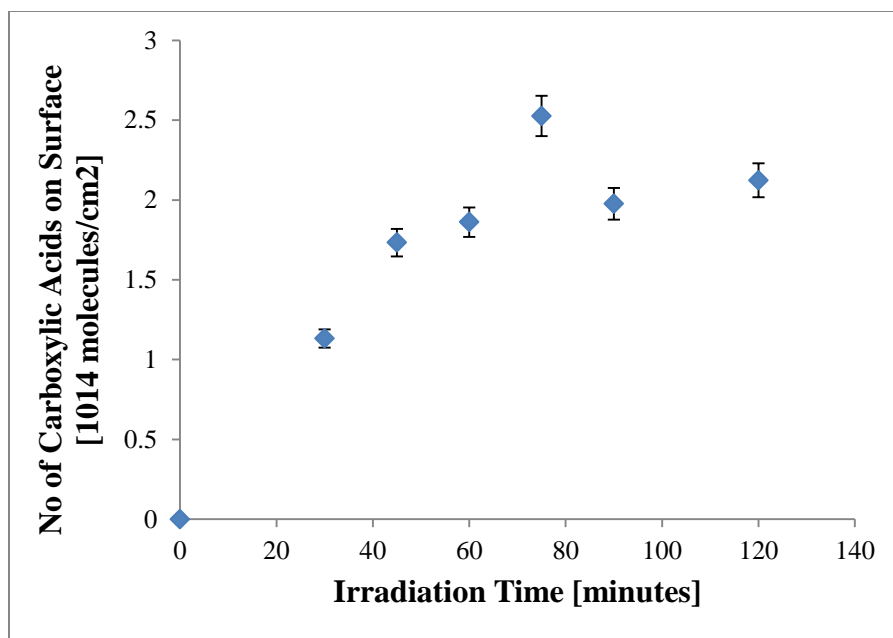


Figure 5.20: Methylene blue treatment to determine concentration carboxylic acids remaining on the surface PDMS after immersion in an acetic-acid/water PFP solution

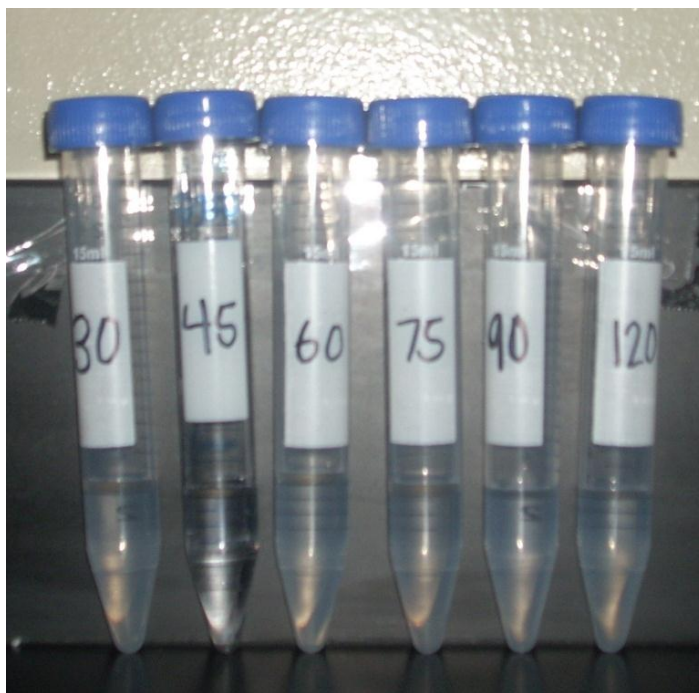


Figure 5.21: Methylene blue experiment indicates no change in color of the PFP based solution

#### 5.3.4 Recovery of Fluoro-terminated Group

Irradiated samples of PDMS were immersed in the four PFP containing solutions of acetic acid-water, acetone, ethanol, and PBS (each solution was 10 mL) and stored in ambient conditions over a period of ten days. Figures 5.22 thru 5.25 represent the contact angle variation for 30 minute and 75 minute irradiated samples stored in air. Water was used as the test liquid. Contact angle measurements show that at 30 minutes the angle is sustained over 10 days for all solutions. From the initial day to the final day, the contact angles averaged in a range of  $94^{\circ} \pm 2$  (acetic acid-water),  $90^{\circ} \pm 5$  (acetone),  $99^{\circ} \pm 1$  (ethanol), and  $85^{\circ} \pm 3$  (PBS). Contact angle measurements of PDMS irradiated at 30 minutes and stored in ambient conditions displays rotation of the PDMS-COOH bond back into the bulk state after only one day and there was a gradual increase in contact angle seen each day thereafter. No rotation of the PDMS-PFP bond in all solutions is an indication that PFP attached to the polymer surface and replaced the COOH bond formed from UV exposure. At 75 minutes, contact angle measurements indicate that acetic acid-water and acetone solutions maintain the PDMS-PFP bond and do not rotate back into the bulk state of the polymer. From the initial day to the final day, the contact angles averaged in a range of  $93^{\circ} \pm 3$  (acetic acid-water),  $86^{\circ} \pm 3$  (PBS). These two solutions indicate a strong presence of PFP on the polymer surface. The ethanol and PBS solutions exhibited minimal rotation of the PDMS-PFP bond back into the bulk state. Contact angle measurements indicate that the modified surface was stable for a few days and gradually increased for the next eight days. For both solutions the total measured rotation of the bond was approximately  $15^{\circ}$ . Compared to the rotation seen in COOH groups, initial contact angle was  $65^{\circ}$  and final contact angle was  $92^{\circ}$ , the rotation pattern is not the

same. This also indicates that the presence of PFP can be found on these modified surfaces.

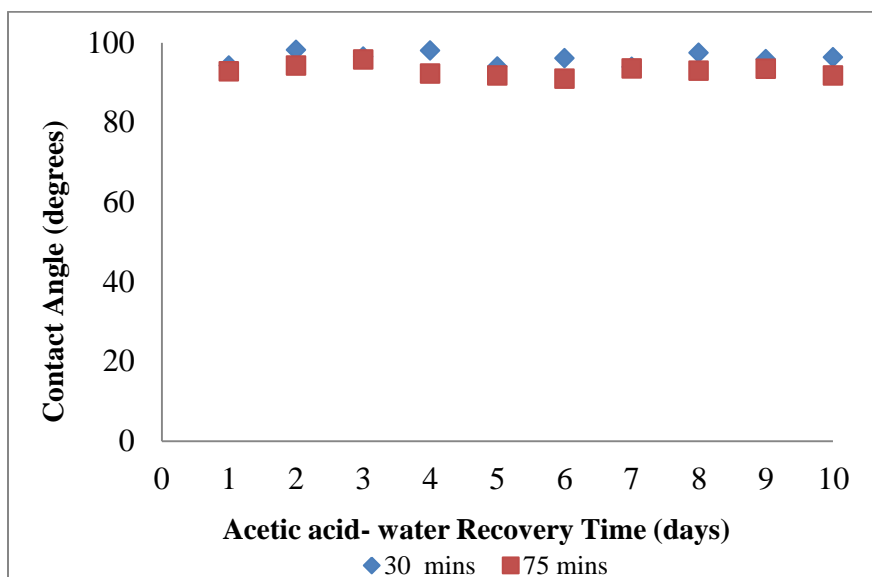


Figure 5.22: Recovery of PDMS surface after immersion in an acetic acid-water pentafluorophenol solution

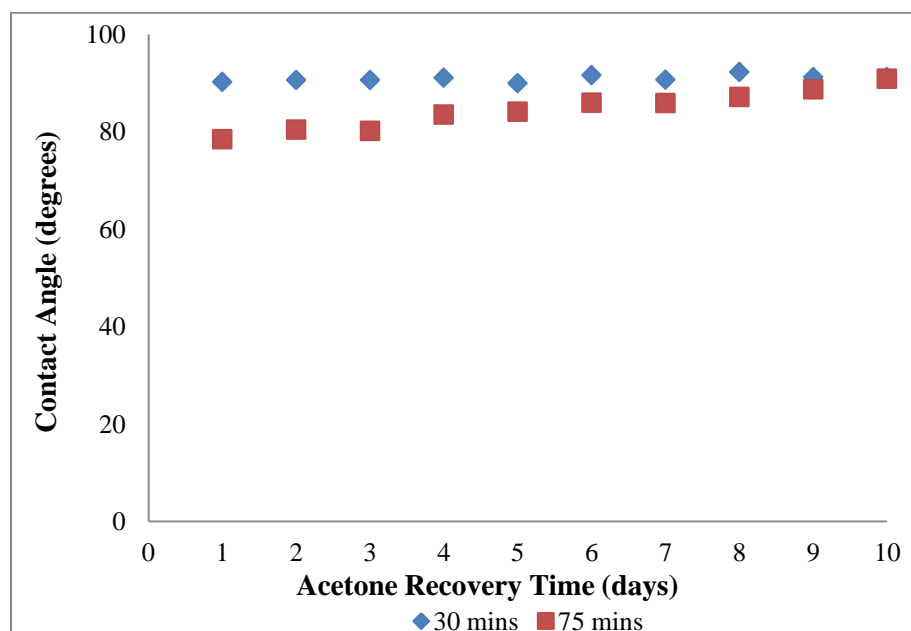


Figure 5.23: Recovery of PDMS surface after immersion in solution an acetone pentafluorophenol solution

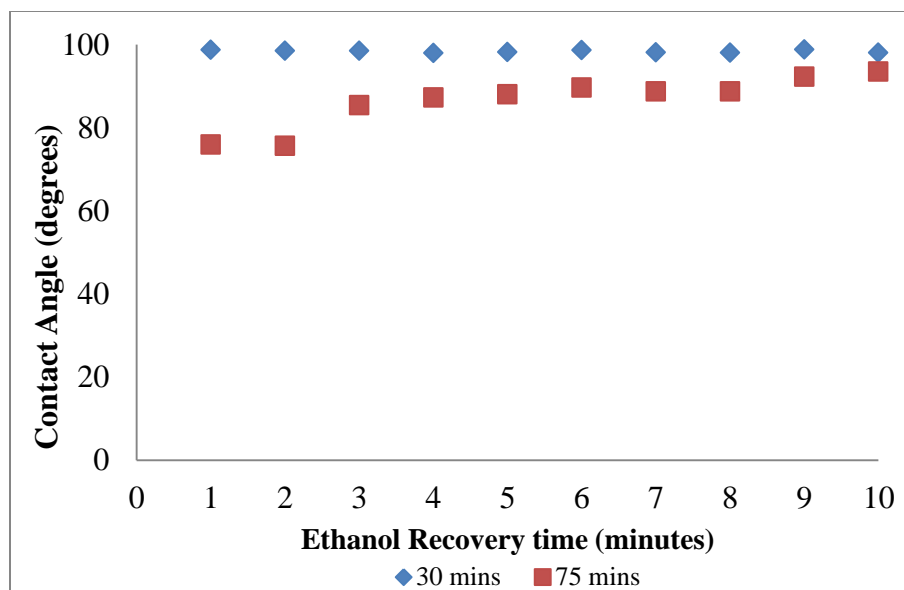


Figure 5.24: Recovery of PDMS surface after immersion in an ethanol pentafluorophenol solution

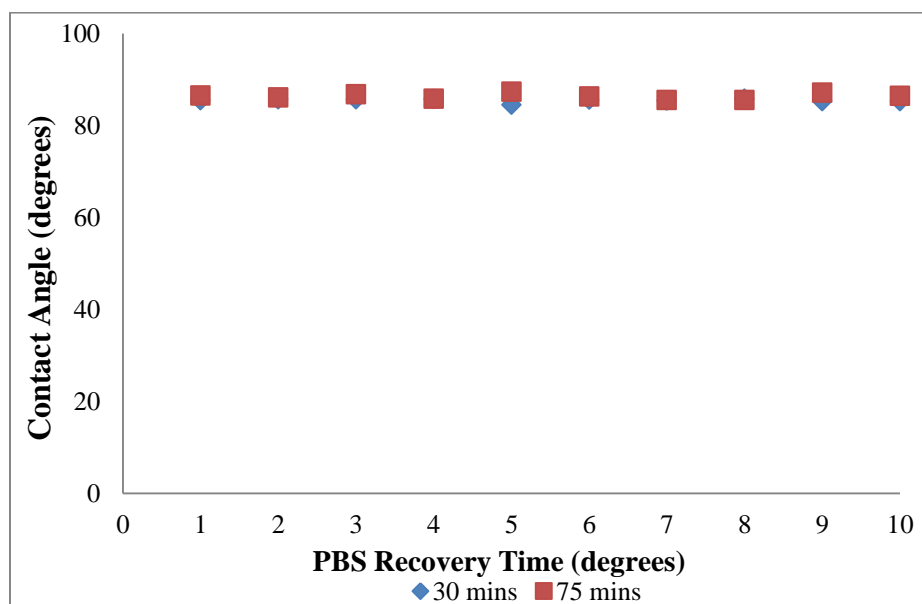


Figure 5.25: Recovery of PDMS surface after immersion in a PBS pentafluorophenol solution

### 5.3.5 Contact Angle Titration Curve

Figure 5.26 shows the dependence of contact angle measurements of a buffered aqueous solution on native, irradiated PDMS, and PDMS-PFP. No change in contact angle is seen in native or PDMS-PFP because these two surface do not have an acidic hydrogen to deprotonate. The contact angle titration curve further indicates the presence of PFP on UV modified PDMS via the EDC linker. The UV modified PDMS containing  $\text{-COOH}$  groups are transformed to carboxylate anion groups upon exposure to the buffered solution, rendering the surface more hydrophilic, and resulting in a decrease of the contact angle of irradiated PDMS as the pH of the buffered solution increases.

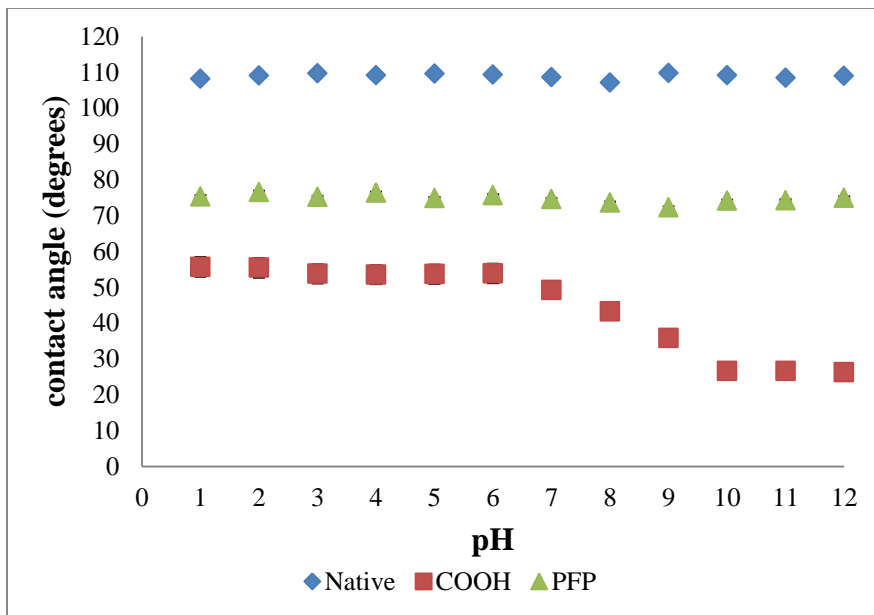


Figure 5.26: Contact angle titration curve of native, PDMS-COOH, and PDMS-PFP

The dependence of the contact angle on pH for surface-functionalized irradiated PDMS can be seen in Figure 5.27. The extent of ionization,  $\alpha_i$ , represents the strength of an acid. Young's equation gives the relation between the interfacial free energies. This

equation can be rearranged to relate to the degree of ionization of the surface carboxylic acids to the liquid/solid interfacial free energies at values of the pH for which the surface carboxylic acids are entirely protonated (pH 1) or completely ionized (pH 12) [78].

Figure 5.28 shows the variation in  $\text{pK}_a^{\text{eff}}$  plotted against the extent of ionization. The figure shows that the extent of ionization increases as the buffered solution becomes more basic. Irradiated PDMS exhibits characteristics of a polybasic acid. This proportional increase reflects either a change in the ease of ionization as carboxylic groups are converted to carboxyl groups or heterogeneity in the population of carboxylic acid groups being examined [78].

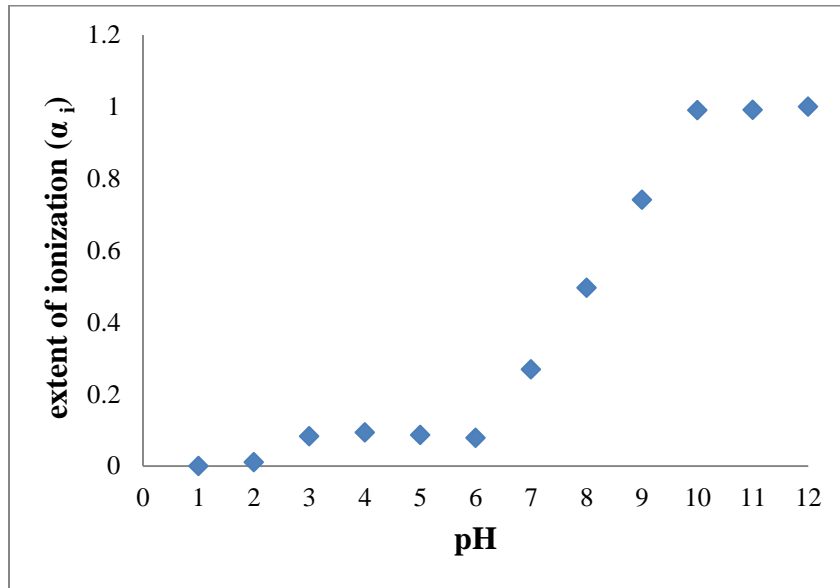


Figure 5.27: Extent of ionization as a function of pH

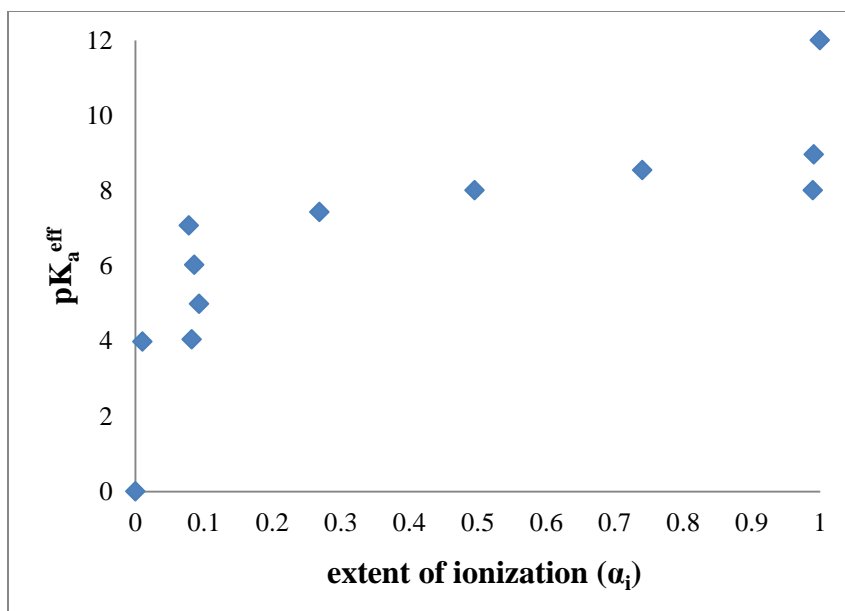


Figure 5.28: Variation in the effective  $pK_a$

## **CHAPTER SIX**

### **SUMMARY, FUTURE WORK, AND CONCLUSION**

#### **6.1 Summary**

The objective of this work was to compare and experimentally investigate poly(dimethylsiloxane) surfaces modified with hydroxyl, carboxylic, and fluoro-terminated groups. PDMS was modified using a plasma cleaner and NaOH solution to form hydroxyl groups, 254 nm UV irradiation to generate carboxylic groups, and a coupling reaction to link pentafluorophenol to the polymer surface via EDC. The surface properties of the modified PDMS were evaluated using contact angle measurements, contact angle titration curve, infrared spectral analysis, and UV-Vis spectroscopy.

Untreated PDMS surfaces were modified using four different techniques including a plasma treatment, a NaOH treatment, UV modification, and by a coupling reaction to attach PFP to the surface. A plasma cleaner along with air-oxygen gas was used to characterize the surface of PDMS. The energy created from the reaction of species and ions found in plasma with PDMS generated hydroxyl groups on the surface of PDMS. The newly formed hydroxyl groups were characterized by contact angle measurements. Results show that the presence of hydroxyl groups increased surface wettability of PDMS drastically. The once hydrophobic material became extremely hydrophilic. Results also show the hydroxyl groups formed lasted for only six hours once

the modified polymer was exposed to ambient air conditions. This gain of hydrophobicity can be attributed to passive transport of low-molar-mass PDMS species from the bulk state of the polymer and to the rearrangement of polar species.

A solution of NaOH was also used to form hydroxyl groups on the polymer surface. Untreated PDMS was immersed in a 1M solution of NaOH for twenty four hours and the surface was characterized by ATR-IR spectroscopy. IR spectrum of native PDMS shows no stretching in the –OH region ( $3000\text{--}360\text{ cm}^{-1}$ ). After soaking in the NaOH solution, an intense broad –OH peak was seen ranging from  $3015\text{--}3625\text{ cm}^{-1}$  in the group's stretching region. Contact angles show no change due to the formation of different ionisable surface groups. When the NaOH treated surfaces were left exposed to ambient air, the hydroxyl group rotated back into the polymer bulk. Although this observed rotation was slower than the rotation observed for hydroxyl groups from the plasma cleaner, the modified surface was not retained.

UV radiation was used to form carboxylic groups on the surface of untreated PDMS. Samples were exposed to varying irradiation times. Contact angle measurements, ATR-IR spectral analysis, and UV-Vis spectroscopy were used to characterize the newly formed carboxylic groups. Contact angle measurements showed that increased exposure times led to a progressive decrease in the contact angle. This indicated that the hydrophilicity of the PDMS surface increased with exposure time as well. ATR-IR spectra indicated the presence of carboxylic groups by the formation of the –OH stretch at  $3015\text{--}3690\text{ cm}^{-1}$  and by the presence of the carbonyl stretch at  $1714\text{ cm}^{-1}$ . A maximum presence of carboxylic groups was established at 75 minutes for both contact angle measurements and infrared spectra. The staining dye, methylene blue was used in

conjunction with UV-Vis spectroscopy to quantify the concentration of carboxylic groups on the polymer surface. Exposing irradiated PDMS to ambient air conditions over a ten day time period, at 30 minutes and 75 minutes of irradiation time, showed that the carboxylic group is not sustained. After day one, the group begins to rotate back into the polymer surface. Around days 5-7 the contact angle of the UV modified surface plateaus out and is an indication that the carboxylic group rotates back into the polymer's bulk state.

Untreated PDMS samples were irradiated and immersed in acetic acid-water, acetone, ethanol, and PBS solutions of PFP and EDC. The modified polymer surface was characterized using contact angle goniometry, ATR-IR spectral analysis, UV-Vis spectroscopy, and a contact angle titration curve. Results show that PFP attaches to the irradiated PDMS surface via a C—O bond. At 75 minutes of irradiation, contact angles show that the PFP modified surface of PDMS is more hydrophobic than the surface of irradiated PDMS. Infrared spectra show that a ring stretch can be observed in the region of  $1514\text{-}1524\text{ cm}^{-1}$ . This stretch is not seen in native or irradiated PDMS and is an indication that PFP successfully attached to the polymer surface. UV-Vis absorbance measurements were used in an anti-methylene blue experiment to determine if any carboxylic groups were left on the polymer surface. Results show that the concentration was of one magnitude lower than irradiated PDMS. The contact angle titration curve was employed to determine surface functionalization. Results showed that buffered solution used was unable to attach to any hydrogen atom and a straight-line graph seen. This further indicates that PFP is bound to the surface of irradiated PDMS. An ambient air experiment was performed over a ten day period with all four solutions of PFP. Little

change was seen in the rotation of the PFP group back into the bulk state of the polymer.

Table 6.1 summarizes the points of comparison for hydroxyl, carboxylic, and pentafluorophenol.

Table 6.1: Comparison of Hydroxyl, Carboxylic, and Pentafluorophenol groups

Functional Group	Molecular Weight (g/mol)	Formation Method	Lowest contact angle observed	IR peak of conformation (cm <sup>-1</sup> )	Recovery Time
<b>Hydroxyl</b>	17.02	Plasma and NaOH Treatment	21°	3015-3625	6 hours
<b>Carboxylic</b>	45.02	254 nm Hg radiation	65°	3015-3690 1714	5-7 days
<b>Pentafluorophenol</b>	184.07	Coupling reaction with EDC	85° - 95°	1514-1524	Sustained over 10 days

## 6.2 Conclusion and Future Work

The research data presented in this thesis provides additional insight towards the surface modification and characterization techniques of PDMS. By comparing the hydroxyl, carboxylic, and fluoro-terminated modified PDMS surfaces, we were able to conclude that a functional group with a higher molecular weight has an influence on the surface functionality after modification occurs. The advantage of this thesis work is that all experiments are reproducible and can be expounded upon to characterize other materials.

Storage of the modified polymer in air proves that hydroxyl groups rotate back within minutes; carboxylic groups rotate back within days, and the fluoro-terminated group PFP does not rotate back over the observed ten day period. The retention of the PDMS-PFP modified surface begins to answer the theorized hypothesis. This factor along

with the results seen from contact angle analysis, ATR-IR spectral analysis, UV-Vis spectroscopy absorbance measurements, and the contact angle titration curve, infers that pentafluorophenol was indeed attached to the PDMS surface.

Recommendations for future work include exploration of X-ray photoelectron spectroscopy (XPS) and Atomic Force Microscopy (AFM), the investigation of the long-term stability of PDMS-PFP surfaces, and the effect of PDMS-PFP on electroosmotic flow. XPS is a quantitative spectroscopic technique. XPS would give more insight into the empirical formula, elemental composition, electronic state and chemical state of PFP on the surface of PDMS. When XPS is used in conjunction with contact angle measurements, C—O ratios of the modified PDMS surfaces can be used to investigate the individual contribution of functional groups to the wettability of the surface. AFM is a form of high resolution scanning probe microscopy and it would provide resolution of the surface features on the sub-nanometer scale. AFM can be used to investigate the surface topography of the PDMS-PFP. Previous work proved that carboxylic bonds were sustained in an acidic solution of 50:50 acetic acid-water. Exploring the effect of the same or similar acidic solutions on PDMS-PFP could aid in computationally characterizing the electroosmotic flow of PFP modified microfluidic channels.

## REFERENCES

- [1] G. Ertl, "Surface Science," *Nature Materials*, 2007.
- [2] M. Prutton, *Introduction to Surface Physics*. New York: Oxford University Press Inc., 1994.
- [3] J. B. Hudson, *Surface Science: An Introduction*. Stoneham, MA: Butterworth-Heinemann, 1992.
- [4] B. Schnyder, T. Lippert, R. Kötz, A. Wokaun, V.-M. Graubner, and O. Nuyken, "UV-irradiation induced modification of PDMS films investigated by XPS and spectroscopic ellipsometry," *Surface Science*, vol. 532–535, pp. 1067–1071, Jun. 2003.
- [5] E. A. Waddell, S. Shreeves, H. Carrell, C. Perry, B. A. Reid, and J. McKee, "Surface modification of Sylgard 184 polydimethylsiloxane by 254nm excimer radiation and characterization by contact angle goniometry, infrared spectroscopy, atomic force and scanning electron microscopy," *Applied Surface Science*, vol. 254, no. 17, pp. 5314–5318, Jun. 2008.
- [6] S. Bhattacharya, A. Datta, J. M. Berg, and S. Gangopadhyay, "Studies on Surface Wettability of Poly ( Dimethyl ) Siloxane ( PDMS ) and Glass Under Oxygen-Plasma Treatment and Correlation With Bond Strength," *Glass*, vol. 14, no. 3, pp. 590–597, 2005.
- [7] X. Ren, M. Bachman, C. Sims, G. P. Li, and N. Allbritton, "Electroosmotic properties of microfluidic channels composed of poly(dimethylsiloxane)," *Journal of chromatography. B, Biomedical sciences and applications*, vol. 762, no. 2, pp. 117–25, Oct. 2001.
- [8] H. Hillborg and U. W. Gedde, "Hydrophobicity Changes in Silicone Rubbers," *IEEE Transactions on Dielectrics and Electrical Insulation*, vol. 6, no. 5, 1999.
- [9] J. R. Hollahan and G. L. Carlson, "Hydroxulation of Polymethylsiloxane Surfaces by Oxidizing Plasmas," *Journal of Applied Polymer Science*, vol. 14, pp. 2499–2508, 1970.
- [10] J. Lahann, M. Balcels, H. Lu, T. Rodon, K. F. Jensen, and R. Langer, "Reactive polymer coatings: a first step toward surface engineering of microfluidic devices.," *Analytical chemistry*, vol. 75, no. 9, pp. 2117–22, May 2003.
- [11] N. Patrito, C. McCague, S. Chiang, P. R. Norton, and N. O. Petersen, "Photolithographically patterned surface modification of poly(dimethylsiloxane) via UV-initiated graft polymerization of acrylates.," *Langmuir : the ACS journal of surfaces and colloids*, vol. 22, no. 8, pp. 3453–5, Apr. 2006.

- [12] R. R. LeVier, M. C. Harrison, R. R. Cook, and T. H. Lane, "What is silicone?," *Plastic and reconstructive surgery*, vol. 92, no. 1, pp. 163–7, Jul. 1993.
- [13] D. J. Campbell, K. J. Beckman, C. E. Calderon, P. W. Doolan, R. M. Ottosen, A. B. Ellis, and G. C. Lisensky, "Replication and Compression of Bulk and Surface Structures with Polydimethylsiloxane Elastomer," *Journal of Chemical Education*, vol. 75, no. 4, pp. 537–541, 1999.
- [14] A. S. T. Products, "Principles of Video Contact Angle Analysis What is Contact Angle Analysis ? To Determine surface energy indirectly," no. 978.
- [15] M. J. Jaycock and G. D. Parfitt, *Chemistry of Interfaces*. Chichester, England: Ellis Horwood Limited, 1981, pp. 234–272.
- [16] J. C. Berg, "Wettability," in *Surfactant Science Series Vol 49*, New York: Marcel, Dekker, 1993.
- [17] B. Kim, E. T. K. K Peterson, and I. Papautsky, "Long-term stability of plasma oxidized PDMS surfaces.," *Conference proceedings : ... Annual International Conference of the IEEE Engineering in Medicine and Biology Society. IEEE Engineering in Medicine and Biology Society. Conference*, vol. 7, pp. 5013–6, Jan. 2004.
- [18] M. Schneemilch and N. Quirke, "Effect of oxidation on the wettability of poly(dimethylsiloxane) surfaces.," *The Journal of chemical physics*, vol. 127, no. 11, p. 114701, Sep. 2007.
- [19] D. C. Duffy, J. C. McDonald, O. J. Schueller, and G. M. Whitesides, "Rapid Prototyping of Microfluidic Systems in Poly(dimethylsiloxane).," *Analytical chemistry*, vol. 70, no. 23, pp. 4974–84, Dec. 1998.
- [20] P. Glover, "Chapter 7 : Wettability," pp. 76–83, 1805.
- [21] R. Lipowsky, P. Lenz, and P. S. Swain, "Wetting and dewetting of structured and imprinted surfaces," *Colloids and Surfaces A: Physicochemical and Engineering Aspects*, vol. 161, no. 1, pp. 3–22, Jan. 2000.
- [22] M. J. Owen, "Siloxane Surface Activity," *Silicon Based Polymer Science: A Comprehensive Resource*, vol. 224, pp. 705–739, 1990.
- [23] H. C. Hillborg, "Loss and Recovery of Hydrophobicity of Polydimethylsiloxane after Exposure to Electrical Discharges of Polydimethylsiloxane after Exposure to Electrical Discharges," Royal Institute of Technolog, 2001.

- [24] J. Kim, "Hydrophobic Recovery of Polydimethylsiloxane Elastomer Exposed to Partial Electrical Discharge," *Journal of Colloid and Interface Science*, vol. 226, no. 2, pp. 231–236, Jun. 2000.
- [25] M. J. Owen and P. J. Smith, "Plasma Treatment of Polydimethylsiloxane," *Journal of Adhesion Science and Technology*, vol. 8, no. 10, pp. 1063–1075, 1994.
- [26] E. P. Everaert, H. C. Van Der Mei, J. De Vries, and H. J. Busscher, "Hydrophobic recovery of repeatedly plasma-treated silicone rubber. Part 1. Storage in air," in *Polymer Surface Modification: Relevance to Adhesion*, K. L. Mittal, Ed. Utrecht, The Netherlands: VSP, 1996, pp. 33–48.
- [27] J. Kim, "The Mechanisms of Hydrophobic Recovery of Polydimethylsiloxane Elastomers Exposed to Partial Electrical Discharges," *Journal of Colloid and Interface Science*, vol. 244, no. 1, pp. 200–207, Dec. 2001.
- [28] H. Hillborg and U. W. Gedde, "Hydrophobicity recovery of polydimethylsiloxane after exposure to corona discharges," *Polymer*, vol. 39, no. 10, pp. 1991–1998, 1998.
- [29] I.-J. Chen and E. Lindner, "The stability of radio-frequency plasma-treated polydimethylsiloxane surfaces.," *Langmuir : the ACS journal of surfaces and colloids*, vol. 23, no. 6, pp. 3118–22, Mar. 2007.
- [30] B. T. Ginn, O. Steinbock, and F. Distillers, "Polymer Surface Modification Using Microwave-Oven-Generated Plasma," *Notes*, vol. 19, pp. 8117–8118, 2003.
- [31] I. Hoek, F. Tho, and W. M. Arnold, "Sodium hydroxide treatment of PDMS based microfluidic devices.," *Lab on a chip*, vol. 10, no. 17, pp. 2283–5, Sep. 2010.
- [32] H. Hillborg, J. F. Ankner, U. W. Gedde, G. D. Smith, H. K. Yasuda, and K. Wikstro, "Crosslinked polydimethylsiloxane exposed to oxygen plasma studied by neutron reflectometry and other surface specific techniques," vol. 41, pp. 6851–6863, 2000.
- [33] P. Dharmarajan, "Surface Modification of Polydimethylsiloxane by Irradiation at 254 nm and Effects on Electroosmotic Flow," University of Alabama in Huntsville, 2010.
- [34] J. K. West, "Theoretical analysis of hydrolysis of polydimethylsiloxane (PDMS).," *Journal of biomedical materials research*, vol. 35, no. 4, pp. 505–11, Jun. 1997.
- [35] E. J. Forbes, R. D. Richardson, M. Stacey, and J. C. Tatlow, "Aromatic Polyfluoro-compounds Part II. Pentafluorophenol," *Journal of the Chemical Society*, pp. 2019–2021, 1959.

- [36] M. Ali, V. Bayer, B. Schiedt, R. Neumann, and W. Ensinger, "Fabrication and functionalization of single asymmetric nanochannels for electrostatic/hydrophobic association of protein molecules.," *Nanotechnology*, vol. 19, no. 48, p. 485711, Dec. 2008.
- [37] A. R. Katritzky, K. Suzuki, and S. K. Singh, "N-Acylation in combinatorial chemistry," vol. 2004, no. i, pp. 12–35, 2004.
- [38] D. Kloos, R. J. E. Derks, M. Wijtmans, H. Lingeman, O. a Mayboroda, a M. Deelder, W. M. a Niessen, and M. Giera, "Derivatization of the tricarboxylic acid cycle intermediates and analysis by online solid-phase extraction-liquid chromatography-mass spectrometry with positive-ion electrospray ionization.," *Journal of chromatography. A*, vol. 1232, pp. 19–26, Apr. 2012.
- [39] J. L. Cecchi, "Introduction to Plasma Concepts and Discharge Configuration," in *Handbook of Plasma Processing Technology: Fundamentals, Etching, Deposition, and Surface Interactions*, S. M. Rossnagel, J. J. Cuomo, and W. D. Westwood, Eds. Norwich, New York: Noyes Publications, 1990, pp. 14–66.
- [40] H. K. Yasuda, D. L. Cho, and Y.-S. Yeh, "Plasma-surface Interactions in the Plasma Modification of Polymer Surfaces," in *Polymer Surfaces and Interfaces*, W. J. Feast and H. S. Munro, Eds. Chichester, England: John Wiley & Sons, 1987, pp. 149–162.
- [41] H. C. Van Der Mei, I. Stokroos, J. M. Schakenraad, and H. J. Busscher, "Aging effects of repeatedly glow-discharged polyethylene: influence on contact angle, infrared absorption, elemental surface composition, and surface topography," *Journal of Adhesion Science and Technology*, vol. 5, no. 9, pp. 757–769, Jan. 1991.
- [42] A.-M. Spehar, S. Koster, V. Linder, S. Kulmala, N. F. de Rooij, E. Verpoorte, H. Sigrist, and W. Thormann, "Electrokinetic characterization of poly(dimethylsiloxane) microchannels.," *Electrophoresis*, vol. 24, no. 21, pp. 3674–8, Dec. 2003.
- [43] Y. Mourzina, A. Steffen, D. Kalyagin, R. Carius, and A. Offenhäusser, "Capillary zone electrophoresis of amino acids on a hybrid poly(dimethylsiloxane)-glass chip.," *Electrophoresis*, vol. 26, no. 9, pp. 1849–60, May 2005.
- [44] L. Chen, J. Ren, R. Bi, and D. Chen, "Ultraviolet sealing and poly(dimethylacrylamide) modification for poly(dimethylsiloxane)/glass microchips.," *Electrophoresis*, vol. 25, no. 6, pp. 914–21, Mar. 2004.
- [45] K. Kabza, J. E. Gestwicki, and J. L. Mcgrath, "Contact Angle Goniometry as a Tool for Surface Tension Measurements of Solids , Using Zisman Plot Method A

- Physical Chemistry Experiment,” *Journal of Chemical Education*, vol. 77, no. 1, pp. 63–65, 2000.
- [46] K. S. Birdi and H. Y. Erbil, *Handbook of Surface and Colloid Chemistry*. Boca Raton: CRC Press, 1997, pp. 1–118.
  - [47] D. Y. Kwok, T. Gietzelt, K. Grundke, H. Jacobasch, and A. W. Neumann, “Contact Angle Measurements and Contact Angle Interpretation . 1 . Contact Angle Measurements by Axisymmetric Drop Shape Analysis and a Goniometer Sessile Drop Technique,” *Interface*, vol. 7463, no. 9, pp. 2880–2894, 1997.
  - [48] L. M. Lander, L. M. Siewierski, W. J. Brittain, and E. A. Vogler, “A Systematic Comparison of Contact Angle Methods,” *Langmuir*, vol. 9, no. 8, pp. 2237–2239, 1993.
  - [49] L. R. Fisher, “Measurement of Small Contact Angles for Sessile Drops,” *Journal of Colloid and Interface Science*, vol. 75, no. 2, pp. 200–205, 1979.
  - [50] A. F. Stalder, T. Melchior, M. Müller, D. Sage, T. Blu, and M. Unser, “Low-bond axisymmetric drop shape analysis for surface tension and contact angle measurements of sessile drops,” *Colloids and Surfaces A: Physicochemical and Engineering Aspects*, vol. 364, no. 1–3, pp. 72–81, Jul. 2010.
  - [51] C. Atae-Allah, M. Cabrerizo-Vilchez, J. F. Gomez-Lopera, J. A. Holgado-Terriza, R. Roman-Roldan, and P. . Luque-scammilla, “Measurement of surface tension and contact angle using entropic edge detection,” *Measurement Science and Technology*, vol. 12, pp. 288–298, 2001.
  - [52] B. He, J. Lee, and N. a. Patankar, “Contact angle hysteresis on rough hydrophobic surfaces,” *Colloids and Surfaces A: Physicochemical and Engineering Aspects*, vol. 248, no. 1–3, pp. 101–104, Nov. 2004.
  - [53] E. Bormashenko, Y. Bormashenko, G. Whyman, R. Pogreb, A. Musin, R. Jager, and Z. Barkay, “Contact angle hysteresis on polymer substrates established with various experimental techniques, its interpretation, and quantitative characterization.,” *Langmuir : the ACS journal of surfaces and colloids*, vol. 24, no. 8, pp. 4020–5, Apr. 2008.
  - [54] A. W. Adamson, *Physical Chemistry of Surfaces*. Canada: John Wiley & Sons, 1990.
  - [55] A. Marmur, “Soft contact: measurement and interpretation of contact angles,” *Soft Matter*, vol. 2, no. 1, p. 12, 2006.
  - [56] M. a. Rodríguez-Valverde, F. J. Montes Ruiz-Cabello, P. M. Gea-Jódar, H. Kamusewitz, and M. a. Cabrerizo-Vílchez, “A new model to estimate the Young

- contact angle from contact angle hysteresis measurements,” *Colloids and Surfaces A: Physicochemical and Engineering Aspects*, vol. 365, no. 1–3, pp. 21–27, Aug. 2010.
- [57] M. Morra, E. Occhiello, and F. Garbassi, “Contact angle hysteresis in oxygen plasma treated poly(tetrafluoroethylene),” *Langmuir*, vol. 5, no. 3, pp. 872–876, May 1989.
  - [58] W. A. Zisman, “Relation of the Equilibrium Contact Angle to Liquid and Solid Constitution,” in *Contact Angle, Wettability, and Adhesion*, F. Fowkes, Ed. Washington, DC: American Chemical Society, 1964, pp. 1–51.
  - [59] H. Dobbs, “The modified Young’s equation for the contact angle of a small sessile droplet from an interface displacement model,” *International Journal of Modern Physics B*, vol. 13, no. 27, pp. 3255–3259, 1999.
  - [60] E. C. Combe, B. A. Owen, and J. S. Hodges, “A protocol for determining the surface free energy of dental materials,” *Journal of Adhesion Science and Technology*, vol. 5641, pp. 262–268, 2004.
  - [61] V.-M. Graubner, R. Jordan, O. Nuyken, B. Schnyder, T. Lippert, R. Kötz, and A. Wokaun, “Photochemical Modification of Cross-Linked Poly(dimethylsiloxane) by Irradiation at 172 nm,” *Macromolecules*, vol. 37, no. 16, pp. 5936–5943, Aug. 2004.
  - [62] M. R. Mueller, *Fundamentals of Quantum Chemistry: Molecular Spectroscopy and Modern Electronic Structure Computations*. Ipswich, MA: Kluwer Academic/plenum Publishers, 2001.
  - [63] B. M. Weckhuysen, “Ultraviolet-Visible Spectroscopy,” in *In-situ Spectroscopy of Catalysis*, The Netherlands: American Scientific Publishers, 2004, pp. 255–270.
  - [64] M. Wainwright, “Phenothiazinium photosensitisers: choices in synthesis and application,” *Dyes and Pigments*, vol. 57, no. 3, pp. 245–257, Jun. 2003.
  - [65] H.-H. Perkampus, *UV-VIS Spectroscopy and Its Applications*. Germany: Springer-Verlag, 1992.
  - [66] B. Stuart, *Infrared Spectroscopy: Fundamentals and Applications*. UK: John Wiley & Sons, 2004.
  - [67] C. P. Hsu, “Infrared Spectroscopy,” in *Handbook of Techniques for Analytical Chemistry*, Prentice Hall, 1997.
  - [68] N. L. Alpert, *IR: Theory and Practice of Infrared Spectroscopy*. Plenum Press, 1970.

- [69] H. . Willard, L. . Merritt, J. A. Dean, and F. A. Settle, *Instrumental Methods of Analysis*. Belmont, CA: Wadsworth Publishing.
- [70] M. W. Urban, *Attenuated Total Reflectance Spectroscopy of Polymers: Theory and Practice*. Washington, DC: American Chemical Society, 1996.
- [71] N. J. Harrick, *Internal Reflection Spectroscopy*. John Wiley & Sons, 1967.
- [72] F. Lewiner, J. P. Klein, F. Puel, and G. Fe, “On-line ATR FTIR measurement of supersaturation during solution crystallization processes . Calibration and applications on three solute / solvent systems,” *Chemical Engineering Science*, vol. 56, pp. 2069–2084, 2001.
- [73] T. Scherzer, “Depth profiling of the conversion during the photopolymerization of acrylates using real-time FTIR-ATR spectroscopy,” *Vibrational Spectroscopy*, vol. 29, pp. 139–145, 2002.
- [74] E. Goormaghtigh, V. Raussens, and J. Ruyschaert, “Attenuated total reflection infrared spectroscopy of proteins and lipids in biological membranes,” vol. 1422, 1999.
- [75] C. de Menezes Atayde and I. Doi, “Highly stable hydrophilic surfaces of PDMS thin layer obtained by UV radiation and oxygen plasma treatments,” *Physica Status Solidi (C)*, vol. 7, no. 2, pp. 189–192, Feb. 2010.
- [76] L. Zhang, L. Ren, and S. Hartland, “Detailed Analysis of Determination of Contact Angle Using Sphere Tensiometry,” *Journal of Colloid and Interface Science*, vol. 318, no. 192, pp. 306–318, 1997.
- [77] S. Hu, X. Ren, M. Bachman, C. E. Sims, G. P. Li, and N. Allbritton, “Surface modification of poly(dimethylsiloxane) microfluidic devices by ultraviolet polymer grafting,” *Analytical chemistry*, vol. 74, no. 16, pp. 4117–23, Aug. 2002.
- [78] S. R. Holmes-Farley, R. H. Reamey, T. J. McCarthy, J. Deutch, and G. M. Whitesides, “Acid-base behavior of carboxylic acid groups covalently attached at the surface of polyethylene: The usefulness of contact angle in following the ionization of surface functionality,” *Langmuir*, vol. 1, no. 6, pp. 725–740, Nov. 1985.
- [79] A. F. Stalder, G. Kulik, D. Sage, L. Barbieri, and P. Hoffmann, “A snake-based approach to accurate determination of both contact points and contact angles,” *Colloids and Surfaces A: Physicochemical and Engineering Aspects*, vol. 286, no. 1–3, pp. 92–103, Sep. 2006.

- [80] K. Efimenko, "Surface Modification of Sylgard-184 Poly(dimethyl siloxane) Networks by Ultraviolet and Ultraviolet/Ozone Treatment," *Journal of Colloid and Interface Science*, vol. 254, no. 2, pp. 306–315, Oct. 2002.